

國立交通大學

機械工程學系

碩士論文

新 Duffing-Van der Pol 系統的渾沌現象，實用渾沌廣
義同步，辛同步，應用 GYC 部分區域穩定理論的渾沌
同步及控制



**Chaos, Pragmatical Chaotic Generalized
Synchronization, Symplectic Synchronization, and
Chaos Synchronization and Control by GYC Partial
Region Stability Theory of a New Duffing-Van der Pol
System**

研究生：許凱銘

指導教授：戈正銘 教授

中華民國九十七年六月

新 Duffing-Van der Pol 系統的渾沌現象，實用渾沌廣義同步，
辛同步，應用 GYC 部分區域穩定理論的渾沌同步及控制

**Chaos, Pragmatical Chaotic Generalized Synchronization,
Symplectic Synchronization, and Chaos Synchronization
and Control by GYC Partial Region Stability Theory of a
New Duffing-Van der Pol System**

研究生：許凱銘

Student: Kai-Ming Hsu

指導教授：戈正銘

Advisor: Zheng-Ming Ge



國立交通大學

機械工程研究所

碩士論文

A Thesis

Submitted to Institute of Mechanical Engineering

College of Engineering

National Chiao Tung University

In Partial Fulfillment of the Requirement

For the Degree of master of science

In

Mechanical Engineering

November 2008

Hsinchu, Taiwan, Republic of China

中華民國九十七年六月

國立交通大學

論文口試委員會審定書

本校 機械工程 學系碩士班 許凱銘 君

所提論文(中文)新 Duffing-Van der Pol 系統的渾沌現象，實用渾沌廣義
同步，辛同步，應用 GYC 部分區域穩定理論的渾沌同步及控制
(英文)Chaos, Pragmatical Chaotic Generalized Synchronization,
Symplectic Synchronization, and Chaos Synchronization and
Control by GYC Partial Region Stability Theory of a New
Duffing-Van der Pol System

合於碩士資格水準、業經本委員會評審認可。

口試委員：

李青一

陳獻度

林宗南

指導教授：

文正銘

系主任：

周永

教授

中華民國 97 年 6 月 12 日

新 Duffing-Van der Pol 系統的渾沌現象，實用渾沌廣義同步，辛同步，

應用 GYC 部分區域穩定理論的渾沌同步及控制

學生：許凱銘

指導教授：戈正銘

摘要

本篇論文以相圖、龐卡萊映射圖、Lyapunov 指數、分歧圖以及參數圖等數值方法研究新 Duffing-Van der Pol 系統的渾沌現象。對此系統研究應用實用漸進穩定性理論和適應性控制法則來達成實用正反投影渾沌廣義同步；應用新動態表面控制和實用漸進穩定理論來獲得不同階系統之實用渾沌交織同步。更進一步使用 GYC 部分區域穩定理論來研究系統的廣義渾沌同步、渾沌控制和渾沌反控制。此外，將探討新 Duffing-Van der Pol 系統以 Legendre function 為參數的渾沌行為及同步。在以上研究中，皆可由相圖和時間歷程圖得到驗證。

Chaos, Pragmatical Chaotic Generalized Synchronization, Symplectic
Synchronization, and Chaos Synchronization and Control by GYC Partial
Region Stability Theory of a New Duffing-Van der Pol System

Student : Kai-Ming Hsu

Advisor : Zheng-Ming Ge

Abstract

In this thesis, the chaotic behavior in new Duffing-van der Pol system is studied by phase portraits, time history, Poincaré maps, Lyapunov exponent, bifurcation diagrams, and parametric diagram. A new kind of chaotic generalized synchronization system, *pragmatical hybrid projective chaotic generalized synchronization* (PHPCGS), is obtained by pragmatical asymptotical stability theorem and adaptive control law. Second new type for chaotic synchronization, *pragmatical chaotic symplectic synchronization* (PCSS), is obtained by new dynamic surface control and pragmatical asymptotical stability theorem. A new method, using GYC partial region stability theory, is studied for chaos synchronization, chaos control, and chaos anti-control. Moreover, the new Duffing-van der Pol system with Legendre function parameters is studied for chaos and synchronization. Numerical analyses, such as phase portraits and time histories can be provided to verify the effectiveness in all above studies.

誌 謝

此篇論文及碩士學業之完成，首先必須感謝指導教授 戈正銘老師的耐心指導與教誨。老師專業領域上的成就以及對於文學和史學上的熱情，都令學生印象深刻且受益匪淺。這兩年的相處，在學術研究之餘也體會到古典文學的美，這都開拓了學生不一樣的視野。

這研究的日子中，承蒙張晉銘、李任宇、李乾豪、李式中、吳宗訓學長和翁郁婷學姐的熱心指導，同時也感謝彥賢、俊諺、峻宇、聰文、瑜韓、志銘、育銘同學的相互勉勵和幫忙，使得本篇論文能夠順利的完成。

最後感謝我的家人，讓我可以不必擔心課業以外的事物，無後顧之憂的完成學業。最後，僅以此論文獻給你們。



CONTENTS

CHINESE ABSTRACT.....	i
ABSTRACT.....	ii
ACKNOWLEDGMENT	iii
CONTENTS.....	iv
LIST OF FIGURES	vi
Chapter 1 Introduction.....	1
Chapter 2 Chaos of a New Duffing-Van der Pol System.....	3
2.1 Description of New Duffing-Van der Pol System.....	3
2.2 Computational Analysis of a New Duffing-Van der Pol System.....	4
Chapter 3 Pragmatical Hybrid Projective Chaotic Generalized	
Synchronization of Chaotic System with Uncertain Parameters	
by Adaptive Control.....	10
3.1 The PHPCGS Scheme of Chaotic Systems by Adaptive Control....	10
3.2 Description of Two New Chaotic 4D Systems, a New Duffing-Van der Pol System and a New Mathieu-Duffing System.....	12
3.3 Numerical Results for PHPCGS of Two New Duffing-Van der Pol Systems.....	14
Chapter 4 Pragmatical Chaotic Symplectic Synchronization with Different	
Order System by New Dynamic Surface Control.....	19
4.1 Pragmatical Chaotic Symplectic Synchronization Scheme.....	20
4.2 Numerical Results for the PCSS by New Dynamic Surface Control	23
Chapter 5 Chaos Generalized Synchronization of New Duffing-Van der Pol	
Systems by GYC Partial Region Stability	
Theory.....	31
5.1 Chaos Generalized Synchronization Strategy.....	31

5.2	Numerical Simulations.....	32
Chapter 6	Chaos Control and Anti-control of a New Duffing-Van der Pol System by GYC Partial Region Stability Theory.....	43
6.1	Chaos Control Scheme.....	43
6.2	Numerical Simulations for Chaos Control.....	44
6.3	Numerical Simulations for Chaos Anti-control.....	48
Chapter 7	Hybrid Projective Symplectic Synchronization of a New Duffing-Van der Pol System with Legendre function Parameters by GYC Partial Region Stability Theory.....	57
7.1	Hybrid Projective Symplectic Synchronization Scheme.....	57
7.2	Chaos of a New Duffing-Van der Pol System with Legendre Function Parameters.....	58
7.3	Numerical Results.....	60
Chapter 8	Conclusions.....	67
Appendix I	GYC Pragmatical Asymptotical Theorem [29].....	69
Appendix II	GYC Partial Region Stability Theory [42].....	72
References.....		80

LIST OF FIGURES

Fig. 2.1	The bifurcation diagram for new Duffing-van der Pol system.	5
Fig. 2.2	The Lyapunov exponents for new Duffing-van der Pol system.	5
Fig. 2.3	Phase portrait, Poincaré maps, and time histories for new Duffing-van der Pol system with $a=0.012$ (period 2).	6
Fig. 2.4	Phase portrait, Poincaré maps, and time histories for new Duffing-van der Pol system with $a=0.01$ (chaos).	7
Fig. 2.5	Phase portrait, Poincaré maps, and time histories for new Duffing-van der Pol system with $a=0.0006$ (chaos).	8
Fig. 2.6	The parametric diagram for new Duffing-van der Pol system with $b=1, c=5, f=0.05$.	9
Fig. 3.1	Phase portrait and time histories of chaotic Mathieu-Duffing system.	16
Fig. 3.2	Time histories of errors.	17
Fig. 3.3	Time histories of the differences of uncertain parameters and estimated parameters.	18
Fig. 4.1	Time histories of errors.	27
Fig. 4.2	Time histories of the differences of uncertain parameters and estimated parameters.	28
Fig. 4.3	Time histories of boundary layer errors.	29
Fig. 4.4	Time histories of m which is a bounded function of time and approaches to zero.	30
Fig. 5.1	Phase portraits of error dynamics for Case I.	39
Fig. 5.2	Time histories of errors for Case I.	39

Fig. 5.3	Time histories of x_i, y_i for Case I.	39
Fig. 5.4	Phase portrait of error dynamics for Case II.	40
Fig. 5.5	Time histories of errors for Case II.	40
Fig. 5.6	Time histories of $x_i - y_i + 50$ and $-F \sin \omega t \cos \omega t$ for Case II.	40
Fig. 5.7	Phase portraits of error dynamics for Case III.	41
Fig. 5.8	Time histories of errors for Case III.	41
Fig. 5.9	Time histories of $\frac{x_i^3}{10} + 80$ and y_i for Case III.	41
Fig. 5.10	Phase portrait of error dynamics for Case IV.	42
Fig. 5.11	Time histories of errors for Case IV.	42
Fig. 5.12	Time histories of $x_i - y_i + 150$ and $-\frac{z_i}{2}$ for Case IV.	42
Fig. 6.1	Chaotic phase portraits for a new Duffing-Van der Pol system in the first quadrant.	52
Fig. 6.2	Phase portrait of error dynamics for Case I.	52
Fig. 6.3	Time histories of errors for Case I.	53
Fig. 6.4	Phase portrait of error dynamics for Case II.	53
Fig. 6.5	Time histories of errors for Case II.	54
Fig. 6.6	Time histories of x_i for Case II.	54
Fig. 6.7	Phase portrait of error dynamics for Case III.	54
Fig. 6.8	Time histories of errors for Case III.	55
Fig. 6.9	Time histories of x_i for Case III.	55
Fig. 6.10	Periodic phase portraits for a translated new Duffing-Van der Pol system in the first quadrant.	55
Fig. 6.11	Phase portraits of error dynamic.	56

Fig. 6.12	Time histories of errors.	56
Fig. 6.13	Time histories of x_i .	56
Fig. 7.1	Time histories of L_1 , L_1 , and L_1 .	63
Fig. 7.2	The bifurcation diagram for new Duffing-Van der Pol system with Legendre function parameters.	63
Fig. 7.3	The Lyapunov exponents for new Duffing-Van der Pol system with Legendre function parameters.	64
Fig. 7.4	Phase portrait, Poincaré maps, and time histories for new Duffing-Van der Pol system with Legendre function parameters when $k=0.35$ (period 1).	64
Fig. 7.5	Phase portrait, Poincaré maps, and time histories for new Duffing-Van der Pol system with Legendre function parameters when $k=0$ (chaos).	65
Fig. 7.6	Phase portraits of error dynamics.	65
Fig. 7.7	Time histories of errors.	66
Fig. A2.1	Partial regions Ω and Ω_1 .	79

Chapter 1

Introduction

In the phenomenon of chaos, the chaotic state is very sensitive to its initial condition and chaos causes often irregular behavior in practical systems. Slight errors occurring in initial states of two identical oscillators will lead to completely different trajectories after enough time. Research efforts have studied control and synchronization of chaos in many chaotic systems [1-4].

Many methods have been applied theoretically and experimentally to synchronize chaotic system [5-7]. Chaos synchronization has been widely investigated in a variety of fields such as secure communication [8], biological science [9], chemical reaction [10], physical science [11], and many other fields. So far, there exist many types of synchronization such as complete synchronization [4,12,13], phase synchronization [14,15], lag synchronization [16,17], projective synchronization [18-22], and generalized synchronization [23], etc. Complete synchronizations and antisynchronizations are the special cases of generalized projective synchronization where the scaling factor $\alpha = 1$ and $\alpha = -1$, respectively.

Many approaches for the synchronization of chaotic systems are based on the exact knowledge of the system structure and parameters. But in practice, almost all parameters of the system are uncertain. In current study, the traditional Lyapunov stability theorem and Babalat lemma are used to prove that the error vector approaches zero in adaptive synchronization [24-28]. But the question of that why the estimated parameters also approach uncertain parameters remains unanswered. By the pragmatism asymptotical stability theorem, the question can be answered strictly [29-31].

In symplectic synchronization, there exists a functional relationship between

“master” system and “slave” system. The final state y of “slave” system not only depends upon the state x of “master” system but also depends upon itself. In other words, the “slave” system does not completely obey the “master” system but plays a role to determine the final state y of “slave” system [32]. The generalized synchronization is a special case of the symplectic synchronization. Besides, the state variables of another different order system as a constituent of functional relation between “master” and “slave” are used.

Chaos control has attracted a great deal of attention from various fields. There are many control techniques for chaos control, such as active control [33], observer-based control [34], feedback and non-feedback control [35-38], inverse optimal control [39], adaptive control [40,41], etc. A new chaos synchronization and chaos control strategy by GYC partial region stability theory are proposed [42,43]. By using the GYC partial region stability theory, the controllers are of lower degree than that of controllers by using traditional Lyapunov asymptotical stability theorem [21-28]. The simple linear homogeneous Lyapunov function of error states makes the controllers introducing less simulation error.

This thesis is organized as follows. Chapter 2 gives the dynamic equation of new Duffing-Van der Pol system. The chaotic behaviors are studied. In Chapter 3 and Chapter 4, numerical simulations of generalized and symplectic synchronization scheme based on the pragmatical asymptotical stability theorem with adaptive control and new dynamic surface control are presented. In Chapter 5, numerical simulations of chaos synchronization scheme based on GYC partial region stability theory are presented. In Chapter 6, numerical simulations of chaos control and anti-control scheme based on GYC partial region stability theory are presented. In Chapter 7, numerical simulations of chaos synchronization scheme using chaotic system with Legendre function parameters are presented. In Chapter 8, conclusions are drawn.

Chapter 2

Chaos of a New Duffing-Van der Pol System

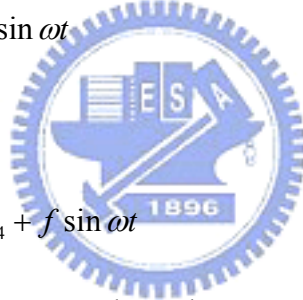
In this Chapter, the chaotic behaviors of a new Duffing-Van der Pol system is studied numerically by phase portraits, time histories, Poincaré maps, Lyapunov exponents, bifurcation diagrams, and parametric diagram.

2.1 Description of New Duffing-Van der Pol System

Duffing equation and Van der Pol equation are two typical nonlinear nonautonomous systems:

$$\begin{cases} \frac{dx_1}{dt} = x_2 \\ \frac{dx_2}{dt} = -x_1 - x_1^3 - ax_2 + d \sin \omega t \end{cases} \quad (2.1)$$

$$\begin{cases} \frac{dx_3}{dt} = x_4 \\ \frac{dx_4}{dt} = -bx_3 + c(1 - x_3^2)x_4 + f \sin \omega t \end{cases} \quad (2.2)$$



A new autonomous Duffing-Van der Pol system is proposed by coupling of these two typical nonautonomous systems. Exchanging $\sin \omega t$ in Eq. (2.1) with x_3 and $\sin \omega t$ in Eq. (2.2) with x_1 , we obtain the new autonomous Duffing-van der Pol system:

$$\begin{cases} \frac{dx_1}{dt} = x_2 \\ \frac{dx_2}{dt} = -x_1 - x_1^3 - ax_2 + dx_3 \\ \frac{dx_3}{dt} = x_4 \\ \frac{dx_4}{dt} = -bx_3 + c(1 - x_3^2)x_4 + fx_1 \end{cases} \quad (2.3)$$

where a, b, c, d, f are parameters. Computational analysis of Eq. (2.3) is studied as

follows.

2.2 Computational Analysis of a New Duffing-Van der Pol System

For numerical analysis of computation, this system exhibits chaos when the parameters of system are $a = 0.01, b = 1, c = 5, d = 0.67, f = 0.05$ and the initial states of system are $x_1(0) = 2, x_2(0) = 2.4, x_3(0) = 5, x_4(0) = 6$. The bifurcation diagram by changing damping parameter a is shown in Fig. 2.1. Its corresponding Lyapunov exponents are shown in Fig. 2.2. The phase portraits, time histories, and Poincaré maps of the systems are showed in Fig. 2.3~Fig. 2.5. When $a=0.012$, period 2 phenomena are shown in Fig. 2.3. When $a=0.01$ and $a=0.0006$, the chaotic behaviors are given in Fig. 2.4 and Fig. 2.5, respectively. In addition, the parametric diagram is obtained in Fig. 2.6.



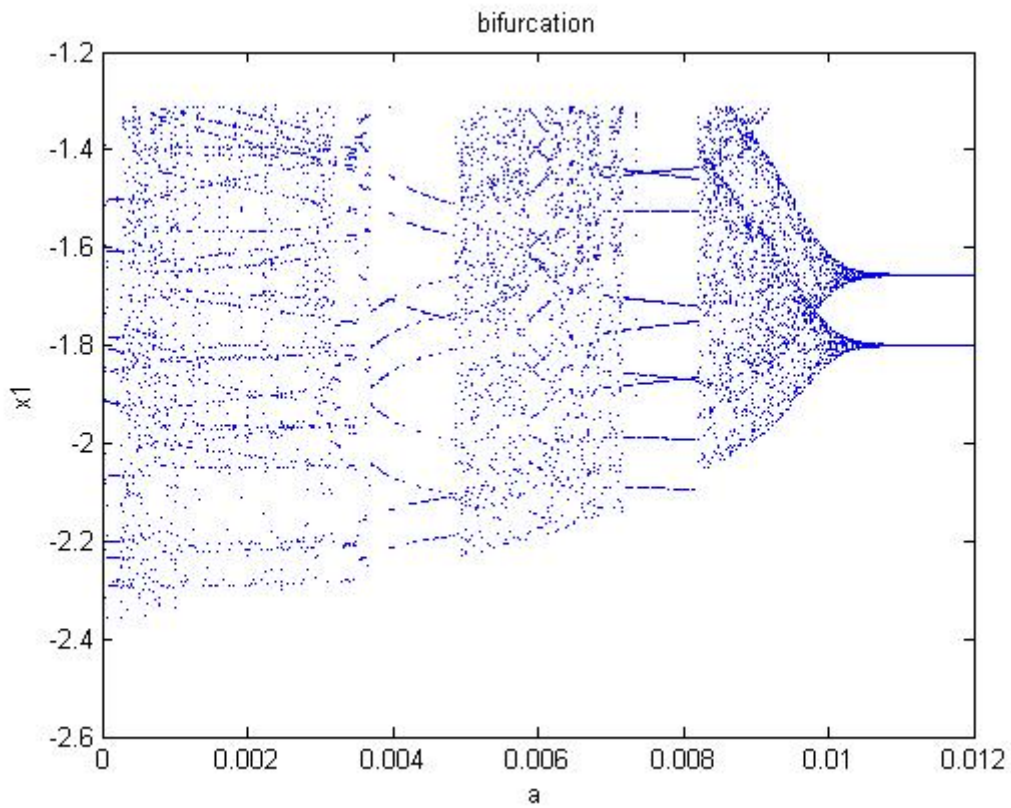


Fig. 2.1 The bifurcation diagram for new Duffing-Van der Pol system.

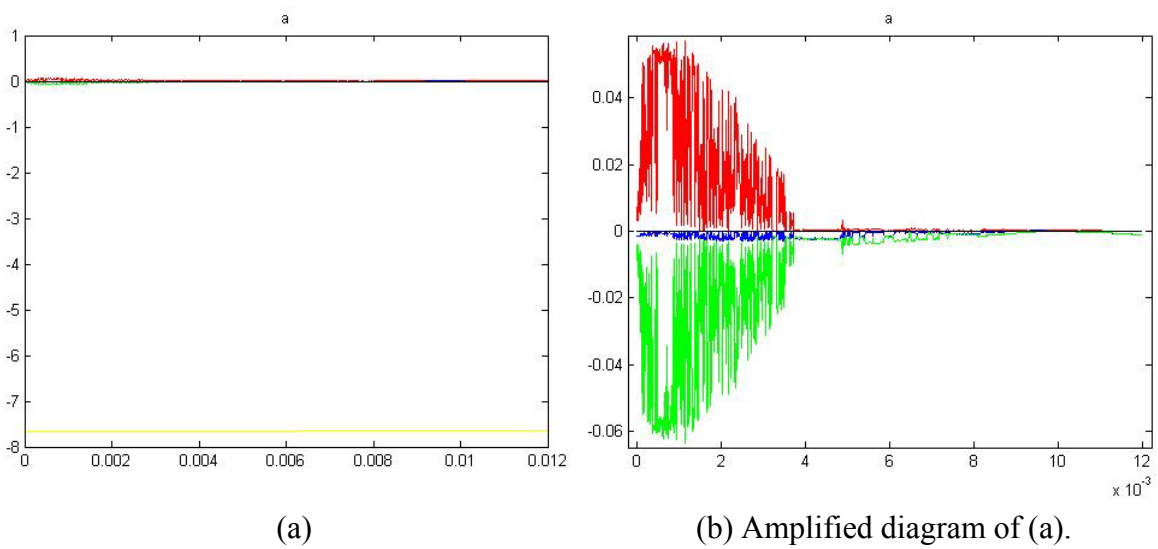


Fig. 2.2 The Lyapunov exponents for new Duffing-Van der Pol system.

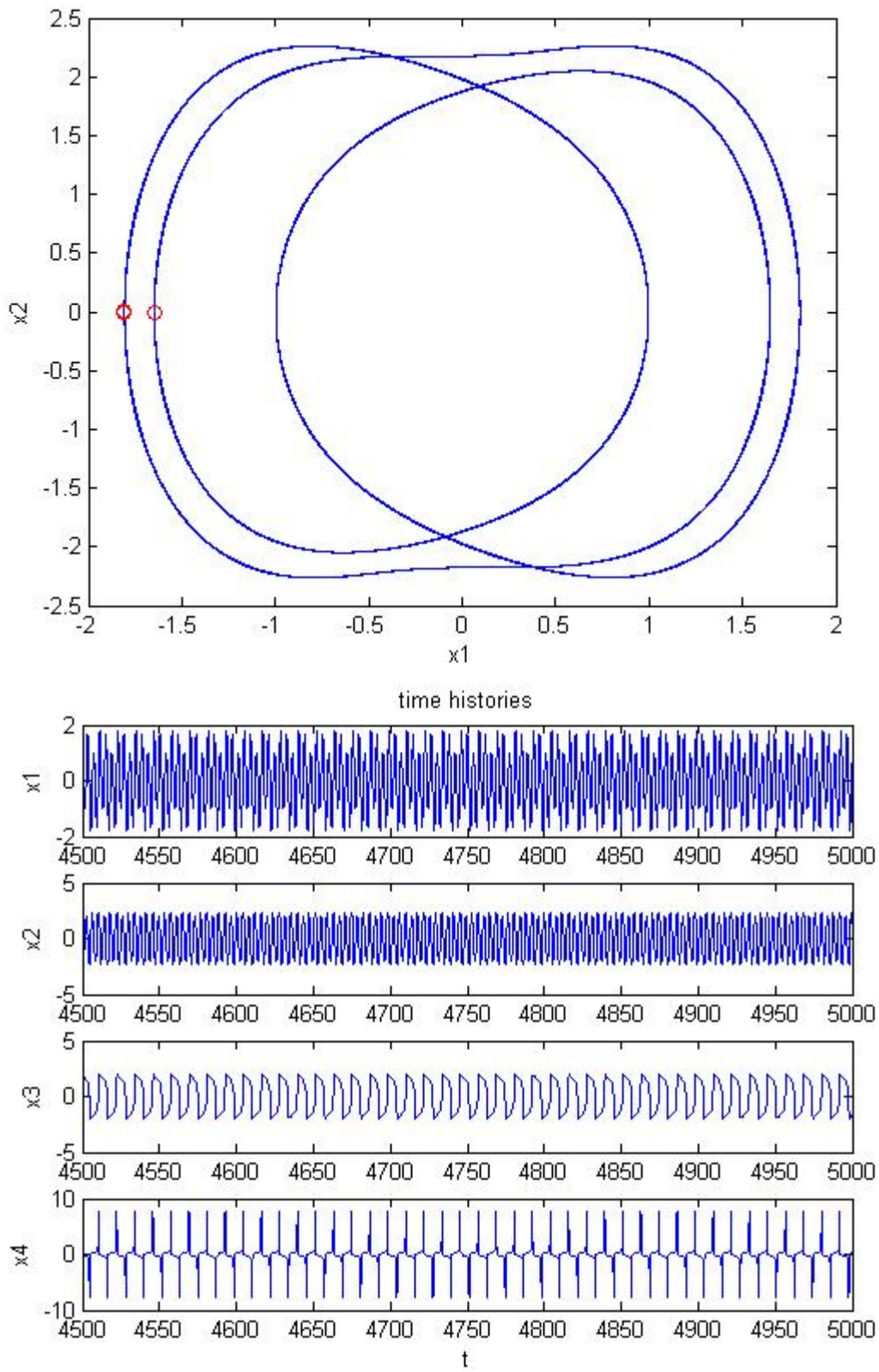


Fig. 2.3 Phase portrait, Poincaré maps, and time histories for new Duffing-Vander Pol system with $a=0.012$ (period 2).

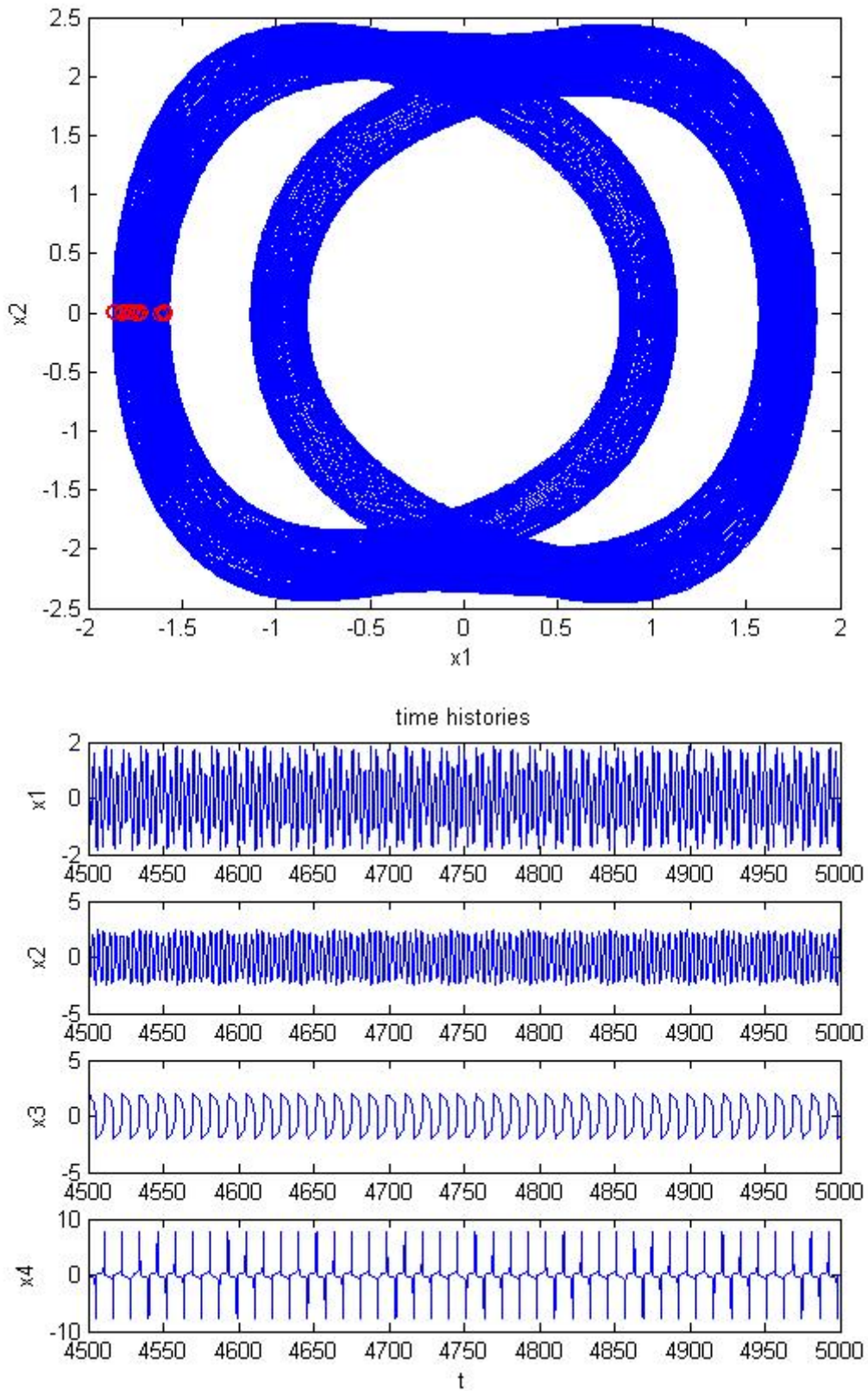


Fig. 2.4 Phase portrait, Poincaré maps, and time histories for new Duffing-Vander Pol system with $a=0.01$ (chaos).

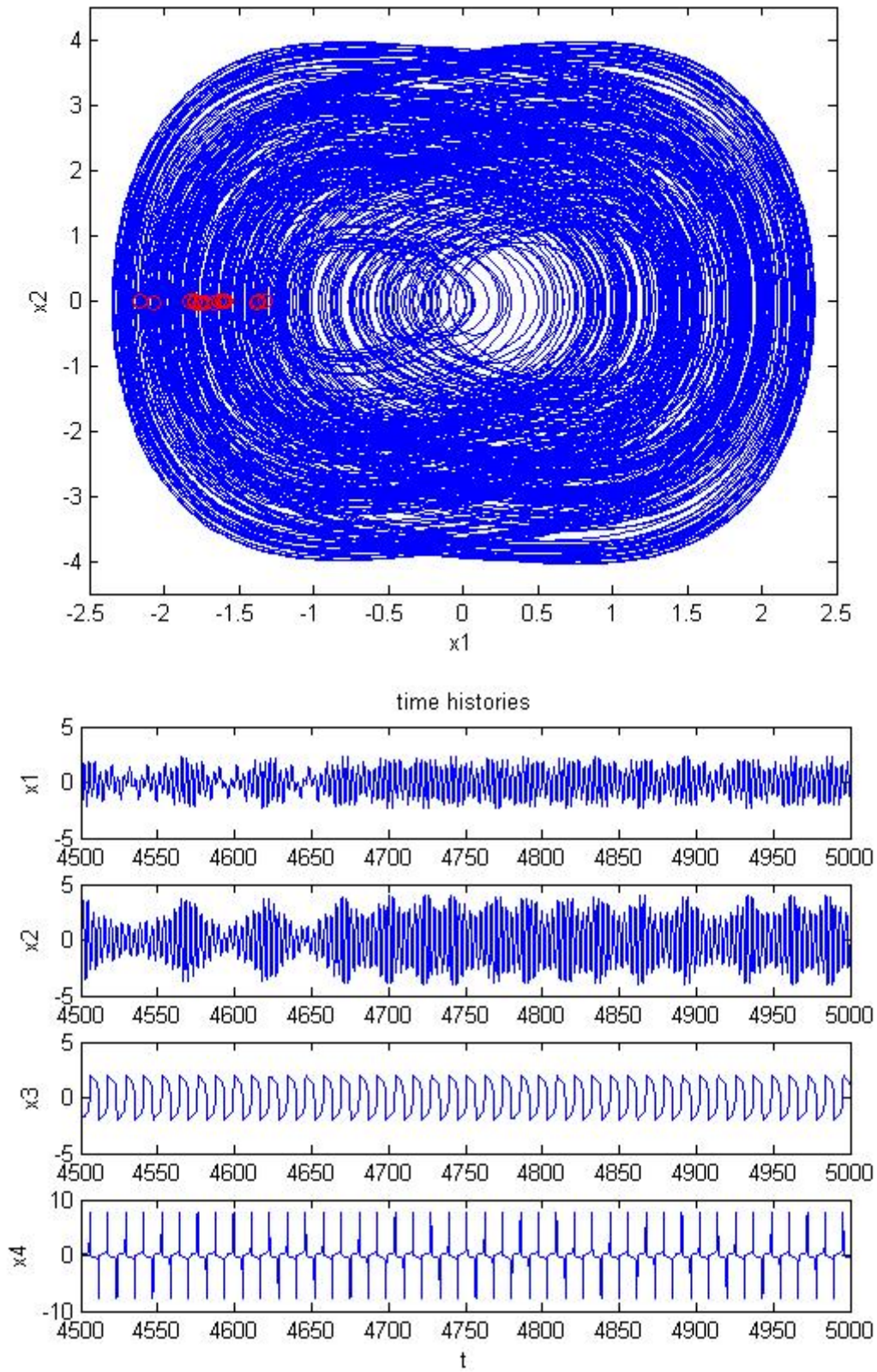


Fig. 2.5 Phase portrait, Poincaré maps, and time histories for new Duffing-Vander Pol system with $a=0.0006$ (chaos).

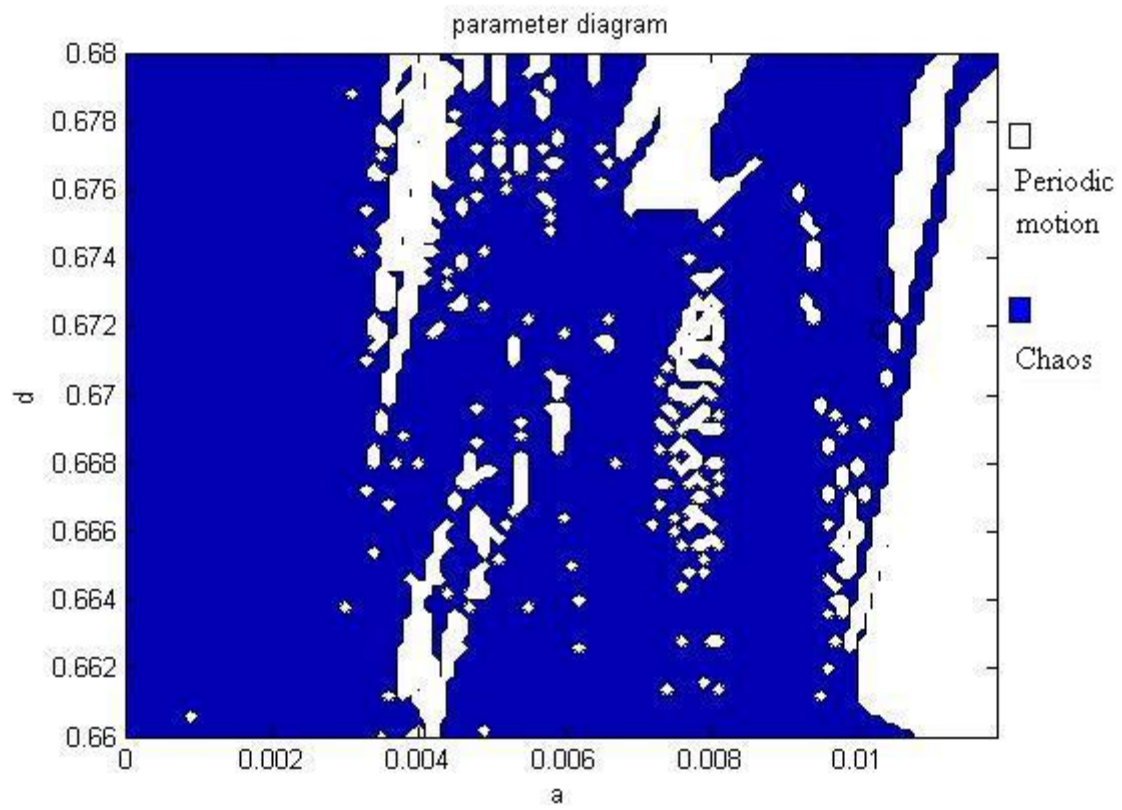


Fig. 2.6 The parametric diagram for new Duffing-Van der Pol system with $b=1$,
 $c=5, f=0.05$.

Chapter 3

Pragmatical Hybrid Projective Chaotic Generalized Synchronization of Chaotic System with Uncertain Parameters by Adaptive Control

A new kind of generalized synchronization, *pragmatical hybrid projective chaotic generalized synchronization* (PHPCGS) of two identical chaotic systems of which one has uncertain parameters, by pragmatical adaptive control, is achieved with the state vector of another hyperchaotic chaotic system as a constituent of the functional relation between master and slave. The PHPCGS is as follows:

$$y = G(x) = zHx \quad (3.1)$$

where $x = (x_1, x_2, \dots, x_n)^T, y = (y_1, y_2, \dots, y_n)^T \in \mathbb{R}^n$ are the n-dimensional state vectors of master system and slave system, respectively,

$H = \text{diag}[h_1, h_2, \dots, h_n] \in \mathbb{R}^{(n \times n)}$ is a constant scaling diagonal matrix where h_i are called scaling factors, which may either positive or negative to form the hybrid projective synchronization. $z = [z_1(t), z_2(t), \dots, z_n(t)]$ is a given state vector with

chaotic time function components. The existence of z causes so called chaotic synchronization. Based on the pragmatical asymptotical stability theorem, adaptive control law is used. Furthermore, the scheme can achieve not only projective synchronization, but also projective anti-synchronization. With all above consideration, PHPCGS is achieved. Numerical simulations are provided to verify the effectiveness of the proposed scheme.

3.1 The PHPCGS Scheme of Chaotic Systems by Adaptive Control

There are two identical nonlinear dynamical systems, and the master system

controls the slave system. The master system is given by

$$\dot{x} = Ax + f(x, B) \quad (3.2)$$

where $x = [x_1, x_2, \dots, x_n]^T \in R^n$ denotes a state vector, A is an $n \times n$ uncertain constant coefficient matrix, f is a nonlinear vector function, and B is a vector of uncertain constant coefficients in f . The slave system is given by

$$\dot{y} = \hat{A}y + f(y, \hat{B}) + u(t) \quad (3.3)$$

where $y = [y_1, y_2, \dots, y_n]^T \in R^n$ denotes a state vector, \hat{A} is an $n \times n$ estimated coefficient matrix, \hat{B} is a vector of estimated coefficients in f , and $u(t) = [u_1(t), u_2(t), \dots, u_n(t)]^T \in R^n$ is a control input vector. The chaotic system which affords chaotic z matrix, is called functional system because in Eq. (3.1), it is a constituent of function G . The functional system is given by

$$\dot{z} = Cz + g(z) \quad (3.4)$$

where $z = [z_1, z_2, \dots, z_n]^T \in R^n$ denotes a state vector, C is an $n \times n$ constant coefficient matrix, g is a nonlinear vector function. PHPCGS demands:

$$y = G(x, z) = zHx \quad (3.5)$$

Our goal is to accomplish Eq. (3.5) via controller $u(t)$ and parameter update dynamics.

Define the error vector e :

$$e = zHx - y \quad (3.6)$$

The synchronization is achieved when

$$\lim_{t \rightarrow \infty} e_i = 0 \quad (i = 1, 2, \dots, n) \quad (3.7)$$

By (3.2), (3.3), and (3.4), the error dynamics is

$$\begin{aligned} \dot{e} &= zH\dot{x} + \dot{z}Hx - \dot{y} \\ &= zHAx - \hat{A}y + zHf(x, B) - f(y, \hat{B}) + CzHx + g(z)Hx - u(t) \end{aligned} \quad (3.8)$$

A Lyapunov function $V(e, \tilde{A}_c, \tilde{B}_c)$ is chosen as a positive definite function of $e, \tilde{A}_c, \tilde{B}_c$:

$$V(e, \tilde{A}_c, \tilde{B}_c) = \frac{1}{2} e^T e + \frac{1}{2} \tilde{A}_c^T \tilde{A}_c + \frac{1}{2} \tilde{B}_c^T \tilde{B}_c \quad (3.9)$$

where $\tilde{A} = A - \hat{A}$, $\tilde{B} = B - \hat{B}$, \tilde{A}_c and \tilde{B}_c are two vectors whose elements are all the elements of matrix \tilde{A} and of matrix \tilde{B} , respectively. By properly choosing $u(t)$, $\dot{\tilde{A}}_c$, and $\dot{\tilde{B}}_c$, its time derivative \dot{V} along any solution of Eq. (3.8) and parameter update differential equations for \tilde{A}_c and \tilde{B}_c can be obtained as

$$\dot{V} = e^T C e \quad (3.10)$$

where C is a diagonal negative definite matrix. \dot{V} is a negative definite function of e but a negative semi-definite function of $e, \tilde{A}_c, \tilde{B}_c$. In the current scheme of adaptive synchronization [24-28], the traditional Lyapunov stability theorem and Babalat lemma are used to prove that the error vector approaches zero, as time approaches infinity. But the question that why the estimated parameters also approach uncertain parameters remains unanswered. By the GYC pragmatical asymptotical stability theorem, the question can be answered strictly. The equilibrium point $e = \tilde{A} = \tilde{B} = 0$ is pragmatically asymptotically stable. Under the assumption of equal probability, it is actually asymptotically stable, as shown in Appendix. Hence, PHPCGS can be achieved.

3.2 Description of Two New Chaotic 4D Systems, a New Duffing-Van der Pol System and a New Mathieu-Duffing System

This section introduces new Duffing-Van der Pol system and new Mathieu-Duffing system.

3.2.1 New Duffing-Van der Pol system

The master new Duffing-Van der Pol system:

$$\begin{cases} \frac{dx_1}{dt} = x_2 \\ \frac{dx_2}{dt} = -x_1 - x_1^3 - ax_2 + dx_3 \\ \frac{dx_3}{dt} = x_4 \\ \frac{dx_4}{dt} = -bx_3 + c(1 - x_3^2)x_4 + fx_1 \end{cases} \quad (3.11)$$

The slave system is

$$\begin{cases} \frac{dy_1}{dt} = y_2 + u_1 \\ \frac{dy_2}{dt} = -y_1 - y_1^3 - \hat{a}y_2 + \hat{d}y_3 + u_2 \\ \frac{dy_3}{dt} = y_4 + u_3 \\ \frac{dy_4}{dt} = -\hat{b}y_3 + \hat{c}(1 - y_3^2)y_4 + \hat{f}y_1 + u_4 \end{cases} \quad (3.12)$$

where u_1, u_2, u_3, u_4 are control inputs, a, b, c, d, f are uncertain parameters, $\hat{a}, \hat{b}, \hat{c}, \hat{d}$ and \hat{f} are estimated parameters. The master system exhibits chaos when the parameters are $a = 0.01, b = 1, c = 5, d = 0.67, f = 0.05$ and the initial states are $x_1(0) = 2, x_2(0) = 2.4, x_3(0) = 5, x_4(0) = 6$.

3.2.2 New Mathieu-Duffing system

The functional system is a new Mathieu-Duffing system. By coupling two nonautonomous nonlinear Mathieu system and Duffing system, a new Mathieu-Duffing system is obtained:

$$\begin{cases} \frac{dz_1}{dt} = z_2 \\ \frac{dz_2}{dt} = -(a_3 + b_3 z_3)z_1 - (a_3 + b_3 z_3)z_1^3 - c_3 z_2 + d_3 z_3 \\ \frac{dz_3}{dt} = z_4 \\ \frac{dz_4}{dt} = -z_3 - z_3^3 - f_3 z_4 + g_3 z_1 \end{cases} \quad (3.13)$$

This system exhibits chaos when the parameters of system are $a_3 = 20.3$,

$b_3=0.597, c_3=0.005, d_3=-24.44, f_3=0.002, g_3=14.63$ and the initial states of system are $z_1(0)=-2, z_2(0)=10, z_3(0)=-2, z_4(0)=10$, its phase portraits and time histories as shown in Fig. 3.1.

3.3 Numerical Results for PHPCGS of Two New Duffing-Van der Pol Systems

Since the master system, slave system, and functional system are described by Eq. (3.11), Eq. (3.12), and Eq. (3.13), respectively, the error dynamics Eq. (3.8) becomes:

$$\begin{cases} \dot{e}_1 = h_1(x_2z_1 + x_1z_2) - y_2 - u_1 \\ \dot{e}_2 = h_2 \left\{ z_2 \left[-x_1 - x_1^3 - ax_2 + dx_3 \right] + x_2 \left[-(a_3 + b_3z_3)(z_1 + z_1^3) - c_3z_2 + d_3z_3 \right] \right. \\ \quad \left. + y_1 + y_1^3 + \hat{a}y_2 - \hat{d}y_3 - u_2 \right\} \\ \dot{e}_3 = h_3(x_4z_3 + x_3z_4) - y_4 - u_3 \\ \dot{e}_4 = h_4 \left\{ z_4 \left[-bx_3 + c(1 - x_3^2)x_4 + \hat{f}x_1 \right] + x_4 \left[-z_3 - z_3^3 - f_3z_4 + g_3z_1 \right] \right. \\ \quad \left. + \hat{b}y_3 - \hat{c}(1 - y_3^2)y_4 - \hat{f}y_1 - u_4 \right\} \end{cases} \quad (3.14)$$

Choose a positive definite Lyapunov function for $e_1, e_2, e_3, e_4, \tilde{a}, \tilde{b}, \tilde{c}, \tilde{d}, \tilde{f}$:

$$V = \frac{1}{2}(e_1^2 + e_2^2 + e_3^2 + e_4^2 + \tilde{a}^2 + \tilde{b}^2 + \tilde{c}^2 + \tilde{d}^2 + \tilde{f}^2) \quad (3.15)$$

where $\tilde{a} = a - \hat{a}, \tilde{b} = b - \hat{b}, \tilde{c} = c - \hat{c}, \tilde{d} = d - \hat{d},$ and $\tilde{f} = f - \hat{f}$. Controllers and parameter update dynamics are selected as:

$$\begin{cases} u_1 = h_1(x_2z_1 + x_1z_2) - y_2 + e_1 \\ u_2 = h_2 \left\{ -z_2 \left[x_1 + x_1^3 + \hat{a}x_2 - \hat{d}x_3 \right] - x_2 \left[(a_3 + b_3z_3)(z_1 + z_1^3) + c_3z_2 - d_3z_3 \right] \right. \\ \quad \left. + y_1 + y_1^3 + \hat{a}y_2 - \hat{d}y_3 + e_2 \right\} \\ u_3 = h_3(x_4z_3 + x_3z_4) - y_4 + e_3 \\ u_4 = h_4 \left\{ z_4 \left[-bx_3 + c(1 - x_3^2)x_4 + \hat{f}x_1 \right] + x_4 \left[-z_3 - z_3^3 - f_3z_4 + g_3z_1 \right] \right. \\ \quad \left. + \hat{b}y_3 - \hat{c}(1 - y_3^2)y_4 - \hat{f}y_1 + e_4 \right\} \end{cases} \quad (3.16)$$

$$\begin{cases} \dot{\hat{a}} = -e_2 h_2 z_2 x_2 \\ \dot{\hat{b}} = -e_4 h_4 z_4 x_3 \\ \dot{\hat{c}} = e_4 h_4 z_4 (1 - x_3^2) x_4 \\ \dot{\hat{d}} = e_2 h_2 z_2 x_3 \\ \dot{\hat{f}} = e_4 h_4 z_4 x_1 \end{cases} \quad (3.17)$$

The time derivative of V is

$$\dot{V} = -e_1^2 - e_2^2 - e_3^2 - e_4^2 \leq 0 \quad (3.18)$$

which is negative semi-definite function for $e_1, e_2, e_3, e_4, \tilde{a}, \tilde{b}, \tilde{c}, \tilde{d}, \tilde{f}$. The Lyapunov asymptotical stability theorem cannot be satisfied in this case. The common origin of error dynamics and parameter update dynamics cannot be concluded to be asymptotically stable. By pragmatism asymptotical theorem, D is a 9-manifold, $n = 9$ and the number of error state variables $p = 4$. When $e_1 = e_2 = e_3 = e_4 = 0$ and $\tilde{a}, \tilde{b}, \tilde{c}, \tilde{d}, \tilde{f}$ take arbitrary values, $\dot{V} = 0$, so X is a 5-manifold, $m = n - p = 9 - 4 = 5$. $m + 1 < n$ are satisfied. By the pragmatism asymptotical stability theorem, the common origin of error dynamics (3.14) and parameter dynamics (3.17) is asymptotically stable. The equilibrium point $e_1 = e_2 = e_3 = e_4 = \tilde{a} = \tilde{b} = \tilde{c} = \tilde{d} = \tilde{f} = 0$ is pragmatically asymptotically stable. The PHPCGS is achieved under this scheme.

In this numerical simulation, we select the “unknown” parameter and initial states of the master system and of functional system the same as that in Section 3.2 to ensure the chaotic behavior. The initial states of slave system are $y_1(0) = y_2(0) = 5$ and $y_3(0) = y_4(0) = 10$, the estimated parameters have initial conditions $\hat{a}(0) = \hat{b}(0) = \hat{c}(0) = \hat{d}(0) = \hat{f}(0) = 0$ and the scaling matrix is $H = \text{diag}(2, \frac{-1}{2}, 2, \frac{-1}{2})$. The numerical results are shown in Fig. 3.2 and Fig. 3.3.

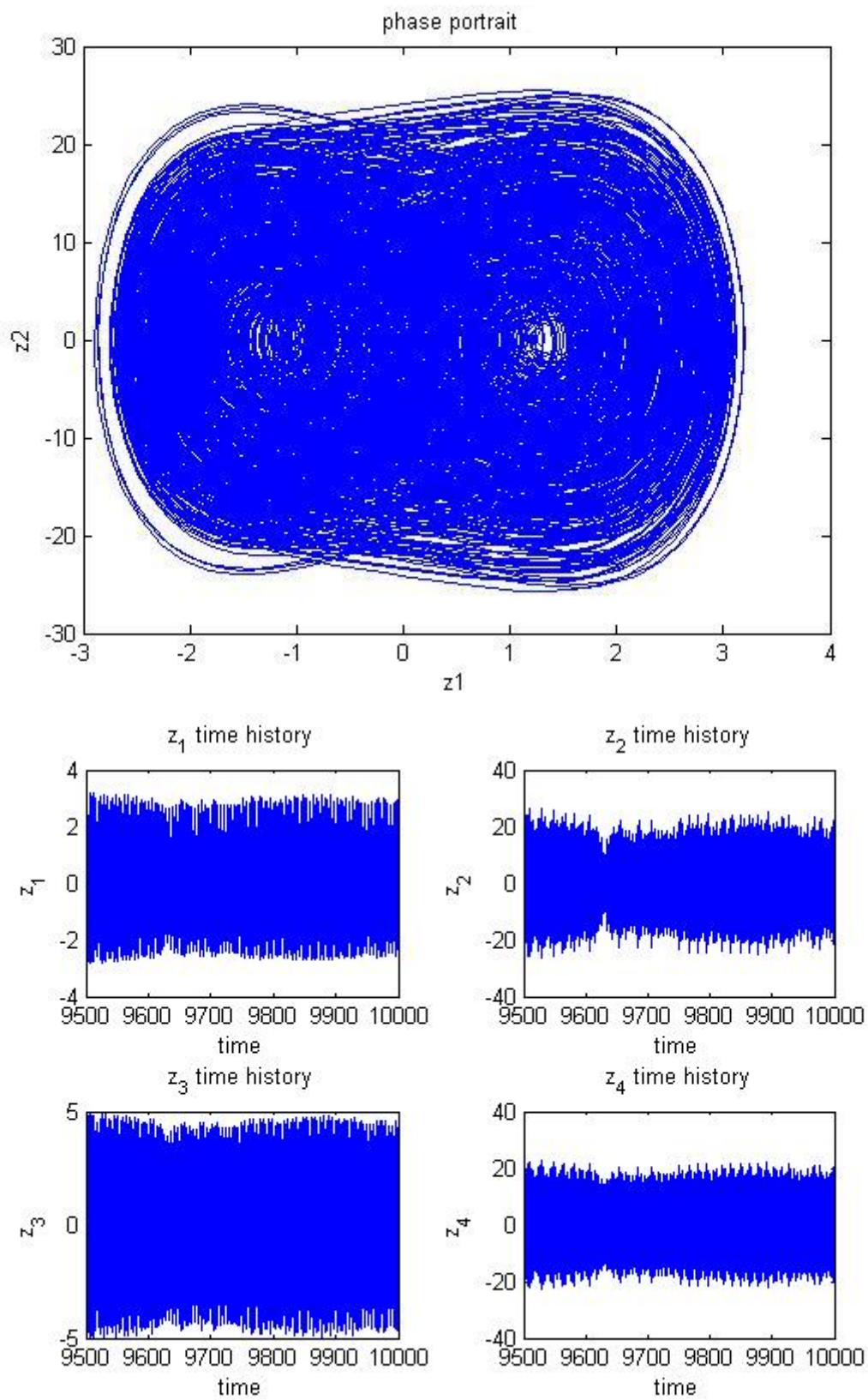


Fig. 3.1 Phase portrait and time histories of chaotic Mathieu-Duffing system.

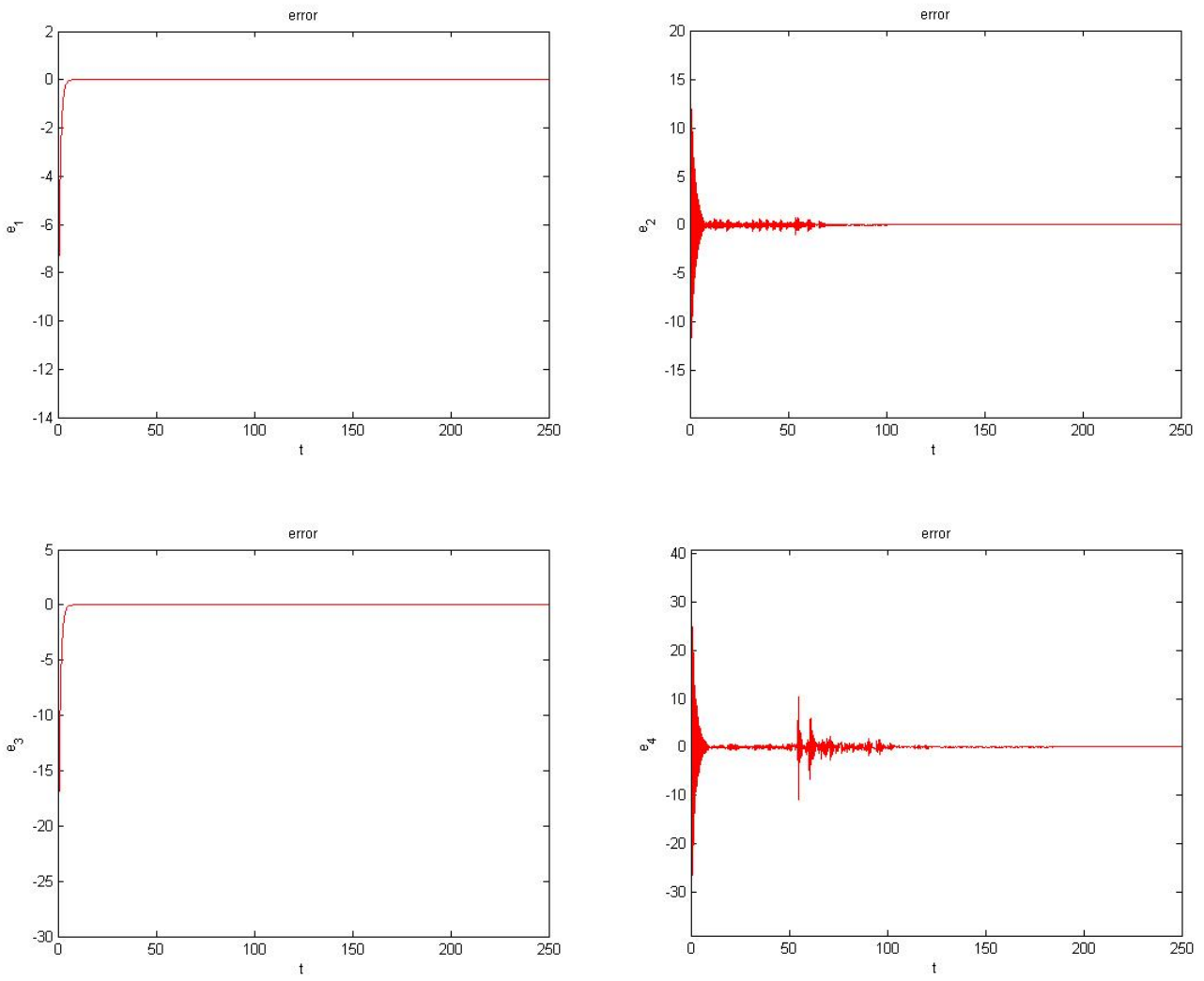


Fig. 3.2 Time histories of errors.

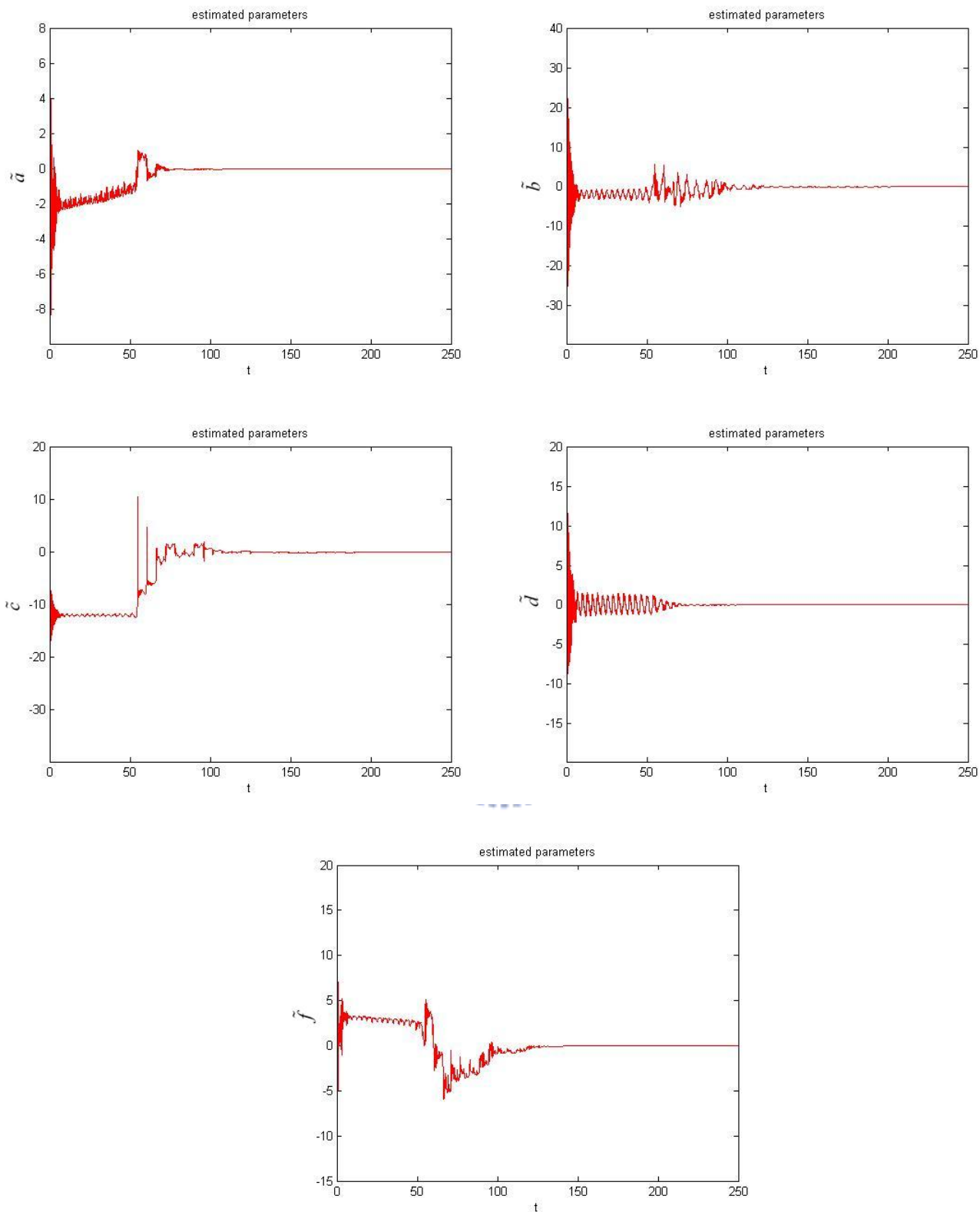


Fig. 3.3 Time histories of the differences of uncertain parameters and estimated parameters.

Chapter 4

Pragmatical Chaotic Symplectic Synchronization with Different Order System by New Dynamic Surface Control

A new type of chaotic synchronization, *pragmatical chaotic symplectic synchronization* (PCSS), is obtained with the state variables of another different order system as a constituent of the functional relation between “master” and “slave” . The PCSS as follows:

$$y = H(x, y, t) + F(t) \quad (4.1)$$

where x and y are the “master” and the “slave” system, respectively. The final state y of “slave” system not only depends upon the state x of “master” system but also depends upon itself. In other words, the “slave” system does not completely obey the “master” system but plays a role to determine the final state y of “slave” system. This kind of synchronization called “symplectic synchronization”*, and the “master” and “slave” system called partner A and partner B, respectively. When $H=H(x,t)$ symplectic synchronization becomes traditional generalized synchronization. Therefore the latter is a special case of the former.

* The term “**symplectic**” comes from the Greek for “intertwined”. H. Weyl first introduced the term in 1939 in his book “The Classical Groups”(P. 165 in both the first edition, 1939, and second edition, 1946, Princeton University Press)

$F(t)$ is a given chaotic vector of time from the states of another different order chaotic system. Based on the pragmatical asymptotical stability theorem, new dynamic surface control (NDSC) which makes the controllers more simple, and adaptive control, the synchronization is achieved. Numerical simulations are provided to verify the effectiveness of the proposed scheme.

4.1 Pragmatical Chaotic Symplectic Synchronization Scheme

There are two identical nonlinear chaotic dynamical systems, and the "master" system controls the "slave" system. In symplectic synchronization, the "master" system is called partner A:

$$\dot{x} = Ax + f(x, B) \quad (4.2)$$

where $x = [x_1, x_2, \dots, x_n]^T \in R^n$ denotes a state vector, A is an $n \times n$ uncertain constant coefficient matrix, f is a nonlinear vector function, and B is a vector of uncertain constant coefficients in f . The "slave" system is called partner B:

$$\dot{y} = \hat{A}y + f(y, \hat{B}) \quad (4.3)$$

where $y = [y_1, y_2, \dots, y_n]^T \in R^n$ denotes a state vector, \hat{A} is an $n \times n$ estimated coefficient matrix, \hat{B} is a vector of estimated coefficients in f . With controllers, partner B becomes

$$\dot{y}_u = \hat{A}y + f(y, \hat{B}) + u(t) \quad (4.4)$$

where $u(t) = [u_1(t), u_2(t), \dots, u_n(t)]^T \in R^n$ is a control input vector. The chaotic system which affords chaotic $F(t)$ vector, is called functional system. However, the PCSS also can be achieved even the order of functional system is different from that of partners A and B. Now we choose the order of the former is less than the latter. The augmented functional system can be easily obtained as shown in Section 4.3. The

augmented functional system becomes

$$\dot{F} = CF + g(F) \quad (4.5)$$

where $F = [F_1, F_2, \dots, F_n]^T \in R^n$ denotes a state vector, C is an $n \times n$ constant coefficient matrix, g is a nonlinear vector function. PCSS demands:

$$y = H(x, y, t) + F(t) \quad (4.6)$$

where $H(x, y, t)$ consists of state vector x of partner A and state vector y of partner B. Our goal is to accomplish Eq. (4.6) via controller $u(t)$ and parameter update dynamics. Define the error vector e :

$$e = H(x, y, t) - y_u + F(t) \quad (4.7)$$

The synchronization is achieved when

$$\lim_{t \rightarrow \infty} e_i = 0 \quad (i = 1, 2, \dots, n) \quad (4.8)$$

The error dynamics is

$$\dot{e} = \frac{\partial H}{\partial x} \dot{x} + \frac{\partial H}{\partial y} \dot{y} + \frac{\partial H}{\partial t} - \dot{y}_u + \dot{F}(t) \quad (4.9)$$

By Eq. (4.2) ~ Eq. (4.5), Eq. (4.9) becomes

$$\begin{aligned} \dot{e} = & \frac{\partial H}{\partial x} [Ax + f(x, B)] + \frac{\partial H}{\partial y} [\hat{A}y + f(y, \hat{B})] + \frac{\partial H}{\partial t} \\ & - \hat{A}y - f(y, \hat{B}) - u(t) + CF + g(F) \end{aligned} \quad (4.10)$$

In order to reduce terms of the $u(t)$, NDSC is used which makes $u(t)$ more simple. This method extends the traditional dynamic surface control [44]. A virtual controller W is chosen as follows

$$m\dot{W} + W = H(x, y, t) + F(t), \quad \lim_{t \rightarrow \infty} W(t) = H(x, y, t) + F(t) \quad (4.11)$$

The m is a time function to be determined. Define the boundary layer errors as

$$s = W - H(x, y, t) + F(t) \quad (4.12)$$

Its derivative is

$$\dot{s} = \frac{-s}{m} - \frac{d}{dt}(H(x, y, t) + F(t)) \quad (4.13)$$

Eq. (4.7) and Eq. (4.10) becomes

$$e = W - y_u \quad (4.14)$$

$$\dot{e} = \dot{W} - \hat{A}y - f(y, \hat{B}) - u(t) \quad (4.15)$$

A Lyapunov function $V(e, s, \tilde{A}_c, \tilde{B}_c)$ is chosen as a positive definite function of $e, s, \tilde{A}_c, \tilde{B}_c$:

$$V(e, s, \tilde{A}_c, \tilde{B}_c) = \frac{1}{2}e^T e + \frac{1}{2}s^T s + \frac{1}{2}\tilde{A}_c^T \tilde{A}_c + \frac{1}{2}\tilde{B}_c^T \tilde{B}_c \quad (4.16)$$

where $\tilde{A} = A - \hat{A}$, $\tilde{B} = B - \hat{B}$, \tilde{A}_c and \tilde{B}_c are two vectors whose elements are all the elements of matrix \tilde{A} and of matrix \tilde{B} , respectively. Its time derivative along any solution of Eq. (4.13) and Eq. (4.15) and parameter update differential equations for \tilde{A}_c and \tilde{B}_c is \dot{V} . Choose $u(t), m(t), \dot{\tilde{A}}_c$ and $\dot{\tilde{B}}_c$ so that

$$\dot{V} = e^T P e + s^T Q s \quad (4.17)$$

where P and Q are diagonal negative definite matrixes, and \dot{V} is a negative semi-definite function of $e, s, \tilde{A}_c, \tilde{B}_c$. In the current scheme of adaptive synchronization [24-28], the traditional Lyapunov stability theorem and Babalat lemma are used to prove that the error vector approaches zero, as time approaches infinity. But the question that why the estimated parameters also approach uncertain parameters remains unanswered. By the pragmatcal asymptotical stability theorem, the question can be answered strictly. The equilibrium point $e = s = \tilde{A} = \tilde{B} = 0$ is pragmatically asymptotically stable (see Appendix). Under the assumption of equal

probability, it is actually asymptotically stable. Hence, the PCSS can be achieved.

4.2 Numerical Results for the PCSS by New Dynamic

Surface Control

Since the partner A, new Duffing-Van der Pol system, is described as

$$\begin{cases} \frac{dx_1}{dt} = x_2 \\ \frac{dx_2}{dt} = -x_1 - x_1^3 - ax_2 + dx_3 \\ \frac{dx_3}{dt} = x_4 \\ \frac{dx_4}{dt} = -bx_3 + c(1 - x_3^2)x_4 + fx_1 \end{cases} \quad (4.18)$$

where a, b, c, d, f are uncertain parameters. The partner B is described as

$$\begin{cases} \frac{dy_1}{dt} = y_2 \\ \frac{dy_2}{dt} = -y_1 - y_1^3 - \hat{a}y_2 + \hat{d}y_3 \\ \frac{dy_3}{dt} = y_4 \\ \frac{dy_4}{dt} = -\hat{b}y_3 + \hat{c}(1 - y_3^2)y_4 + \hat{f}y_1 \end{cases} \quad (4.19)$$

where $\hat{a}, \hat{b}, \hat{c}, \hat{d}$ and \hat{f} are estimated parameters.

For this scheme, u_1, u_2, u_3 and u_4 are added to the partner B then becomes controlled partner B:

$$\begin{cases} \frac{dy_1}{dt} = y_2 + u_1 \\ \frac{dy_2}{dt} = -y_1 - y_1^3 - \hat{a}y_2 + \hat{d}y_3 + u_2 \\ \frac{dy_3}{dt} = y_4 + u_3 \\ \frac{dy_4}{dt} = -\hat{b}y_3 + \hat{c}(1 - y_3^2)y_4 + \hat{f}y_1 + u_4 \end{cases} \quad (4.20)$$

The chaotic Lü system is chosen as functional system [45] and the augmented state

variable is $z_4 = z_1^2$:

$$\begin{cases} \frac{dz_1}{dt} = g(z_2 - z_1) \\ \frac{dz_2}{dt} = -z_1 z_3 + h z_2 \\ \frac{dz_3}{dt} = z_1 z_2 - k z_3 \\ \frac{dz_4}{dt} = 2g z_1 (z_2 - z_1) \end{cases} \quad (4.21)$$

In the PCSS, we select the

$$H_i(x, y, t) = (-x_i)^j y_i + z_i^j \quad \begin{cases} i = 1, 2, \dots, n \\ j = \begin{cases} 2, & i = \text{even} \\ 3, & i = \text{odd} \end{cases} \end{cases} \quad (4.22)$$

Now $n=4$. By NDSC, the error dynamics Eq. (4.15) becomes:

$$\begin{cases} \dot{e}_1 = \dot{W}_1 - y_2 - u_1 \\ \dot{e}_2 = \dot{W}_2 + y_1 + y_1^3 + \hat{a}y_2 - \hat{d}y_3 - u_2 \\ \dot{e}_3 = \dot{W}_3 - y_4 - u_3 \\ \dot{e}_4 = \dot{W}_4 + \hat{b}y_3 - \hat{c}(1 - y_3^2)y_4 - \hat{f}y_1 - u_4 \end{cases} \quad (4.23)$$

and the boundary layer error dynamics Eq. (4.13) becomes:

$$\begin{cases} \dot{s}_1 = \frac{-s_1}{m_1} - [-3x_1^2 x_2 y_1 - x_1^3 y_2 + 3gz_1^2 (z_2 - z_1)] \\ \dot{s}_2 = \frac{-s_2}{m_2} - [-2x_2 y_2 (-x_1 - x_1^3 - ax_2 + dx_3) - x_2^2 (-y_1 - y_1^3 - \hat{a}y_2 + \hat{d}y_3) \\ + 2z_2 (-z_1 z_3 + h z_2)] \\ \dot{s}_3 = \frac{-s_3}{m_3} - [-3x_3^2 x_4 y_3 - x_3^3 y_4 + 3z_3^2 (z_1 z_2 - k z_3)] \\ \dot{s}_4 = \frac{-s_4}{m_4} - [-2x_4 y_4 (-bx_3 + c(1 - x_3^2)x_4 + fx_1) - x_4^2 (-\hat{b}y_3 + \hat{c}(1 - y_3^2)y_4 + \hat{f}y_1) \\ + 4gz_1 z_4 (z_2 - z_1)] \end{cases} \quad (4.24)$$

Choose a positive definite Lyapunov function for $e_1, e_2, e_3, e_4, s_1, s_2, s_3, s_4, \tilde{a}, \tilde{b}, \tilde{c}, \tilde{d}, \tilde{f}$:

$$V = \frac{1}{2}(e_1^2 + e_2^2 + e_3^2 + e_4^2 + s_1^2 + s_2^2 + s_3^2 + s_4^2 + \tilde{a}^2 + \tilde{b}^2 + \tilde{c}^2 + \tilde{d}^2 + \tilde{f}^2) \quad (4.25)$$

where $\tilde{a} = (a - \hat{a})$, $\tilde{b} = (b - \hat{b})$, $\tilde{c} = (c - \hat{c})$, $\tilde{d} = (d - \hat{d})$, and $\tilde{f} = (f - \hat{f})$. We

select controllers, estimated parameter dynamics, and the m as:

$$\begin{cases} u_1 = \dot{W}_1 - y_2 + e_1 \\ u_2 = \dot{W}_2 + y_1 + y_1^3 + \hat{a}y_2 - \hat{d}y_3 + e_2 \\ u_3 = \dot{W}_3 - y_4 + e_3 \\ u_4 = \dot{W}_4 + \hat{b}y_3 - \hat{c}(1 - y_3^2)y_4 - \hat{f}y_1 + e_4 \end{cases} \quad (4.26)$$

They are more simple.

$$\begin{cases} \dot{\hat{a}} = -2x_2^2 y_2 s_2 \\ \dot{\hat{b}} = -2x_3 x_4 y_4 s_4 \\ \dot{\hat{c}} = 2x_4^2 y_4 (1 - x_3^2) s_4 \\ \dot{\hat{d}} = 2x_2 x_3 y_2 s_2 \\ \dot{\hat{f}} = 2x_1 x_4 y_4 s_4 \end{cases} \quad (4.27)$$

$$\begin{cases} m_1 = \frac{-s_1}{-s_1 - 3x_1^2 x_2 y_1 - x_1^3 y_2 + 3gz_1^2 (z_2 - z_1)} \\ m_2 = \frac{-s_2}{-s_2 - 2x_2 y_2 (-x_1 - x_1^3 - \hat{a}x_2 + \hat{d}x_3) - x_2^2 (-y_1 - y_1^3 - \hat{a}y_2 + \hat{d}y_3) + 2z_2 (-z_1 z_3 + hz_2)} \\ m_3 = \frac{-s_3}{-s_3 - 3x_3^2 x_4 y_3 - x_3^3 y_4 + 3z_3^2 (z_1 z_2 - kz_3)} \\ m_4 = \frac{-s_4}{-s_4 - 2x_4 y_4 (-\hat{b}x_3 + \hat{c}(1 - x_3^2)x_4 + \hat{f}x_1) - x_4^2 (-\hat{b}y_3 + \hat{c}(1 - y_3^2)y_4 + \hat{f}y_1) + 4gz_1 z_4 (z_2 - z_1)} \end{cases} \quad (4.28)$$

The time derivative of V is

$$\dot{V} = -e_1^2 - e_2^2 - e_3^2 - e_4^2 - s_1^2 - s_2^2 - s_3^2 - s_4^2 \leq 0 \quad (4.29)$$

which is negative semi-definite function for $e_1, e_2, e_3, e_4, s_1, s_2, s_3, s_4, \tilde{a}, \tilde{b}, \tilde{c}, \tilde{d}, \tilde{f}$. The Lyapunov asymptotical stability theorem cannot be satisfied in this case. The common origin of error dynamics, parameter update dynamics, and boundary layer error dynamics cannot be concluded to be asymptotically stable. By pragmatcal asymptotical theorem, D is a 13-manifold, $n = 13$ and the number of error state variables $p = 8$. When $e_1 = e_2 = e_3 = e_4 = s_1 = s_2 = s_3 = s_4 = 0$ and $\tilde{a}, \tilde{b}, \tilde{c}, \tilde{d}, \tilde{f}$ take arbitrary values, $\dot{V} = 0$, so X is a 5-manifold, $m = n - p = 13 - 8 = 5$. $m + 1 < n$ are satisfied. By the pragmatcal asymptotical stability theorem, the common origin of error dynamics (4.23), boundary layer error dynamics (4.24), and parameter dynamics (4.27) are asymptotically stable. The equilibrium point $e_1 = e_2$

$= e_3 = e_4 = s_1 = s_2 = s_3 = s_4 = \tilde{a} = \tilde{b} = \tilde{c} = \tilde{d} = \tilde{f} = 0$ is pragmatically asymptotically stable. The PCSS is achieved under this scheme.

In this numerical simulation, we select the “unknown” parameter and initial states of the partner A and of functional system as $a=0.01, b=1, c=5, d=0.67, f=0.05, g=36, h=20, k=3$ to ensure the chaotic behavior. The initial states of those system are $x_1(0) = 2, x_2(0) = 2.4, x_3(0) = 5, x_4(0) = 6, y_1(0) = 5, y_2(0) = 5, y_3(0) = 10, y_4(0) = 10, z_1(0) = z_2(0) = z_3(0) = z_4(0) = 10$. The estimated parameters have initial conditions $\hat{a}(0) = \hat{b}(0) = \hat{c}(0) = \hat{d}(0) = \hat{f}(0) = 0$. The numerical results are shown in Fig. 4.1 ~ Fig. 4.4.



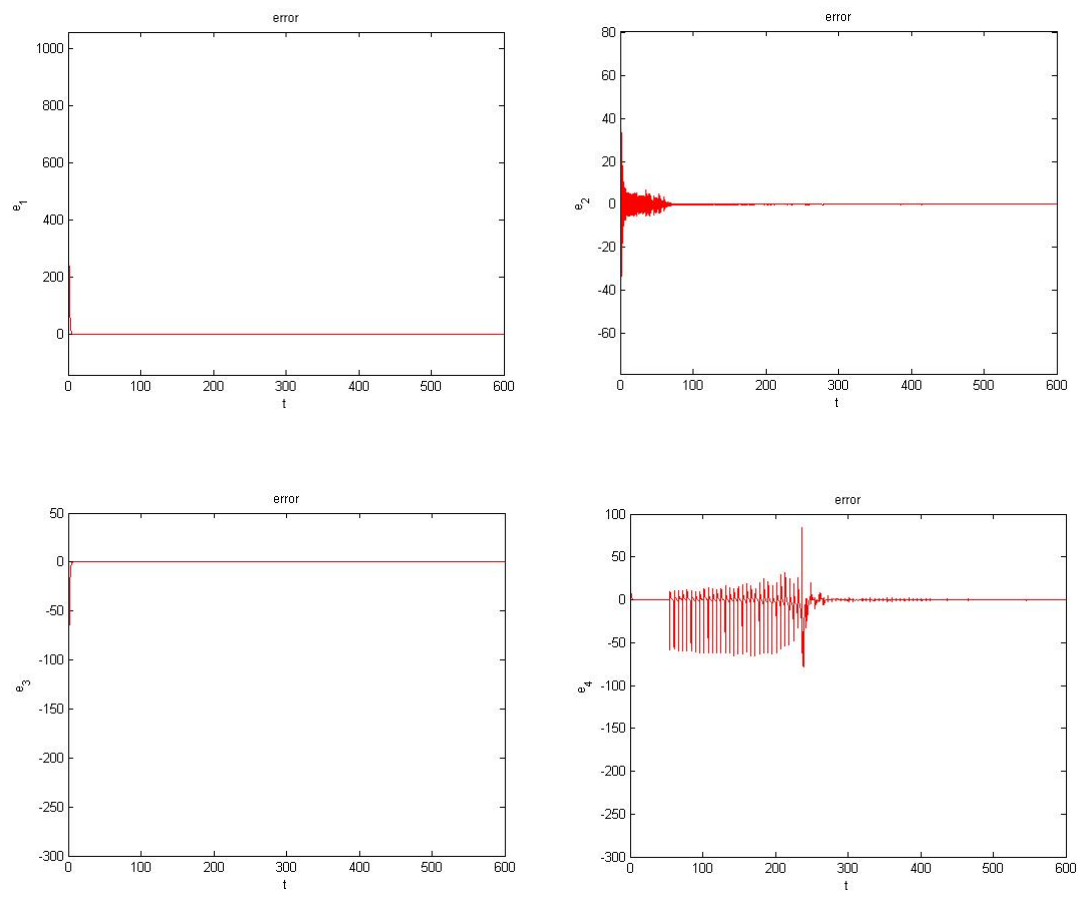


Fig. 4.1 Time histories of errors.

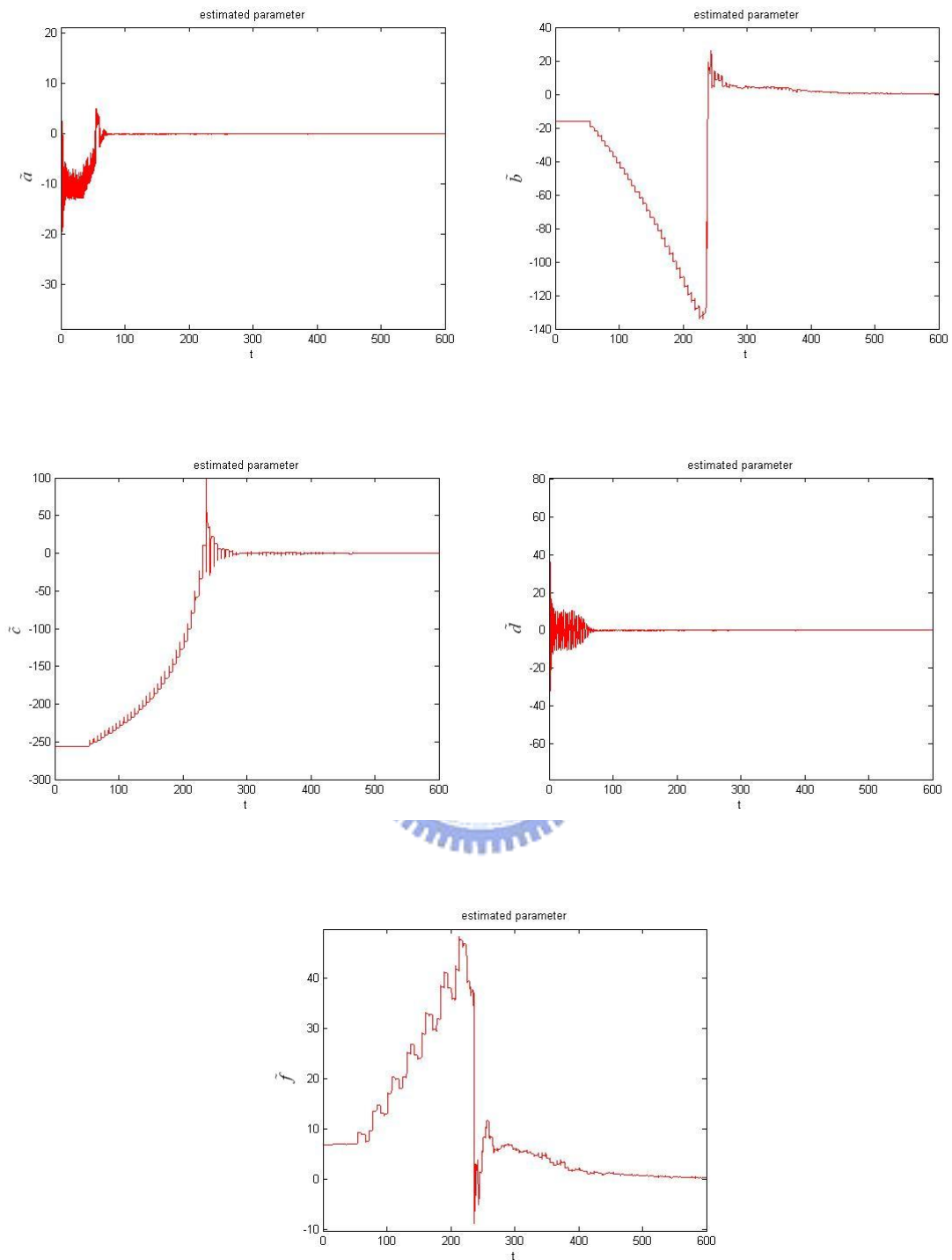


Fig. 4.2 Time histories of the differences of uncertain parameters and estimated parameters.

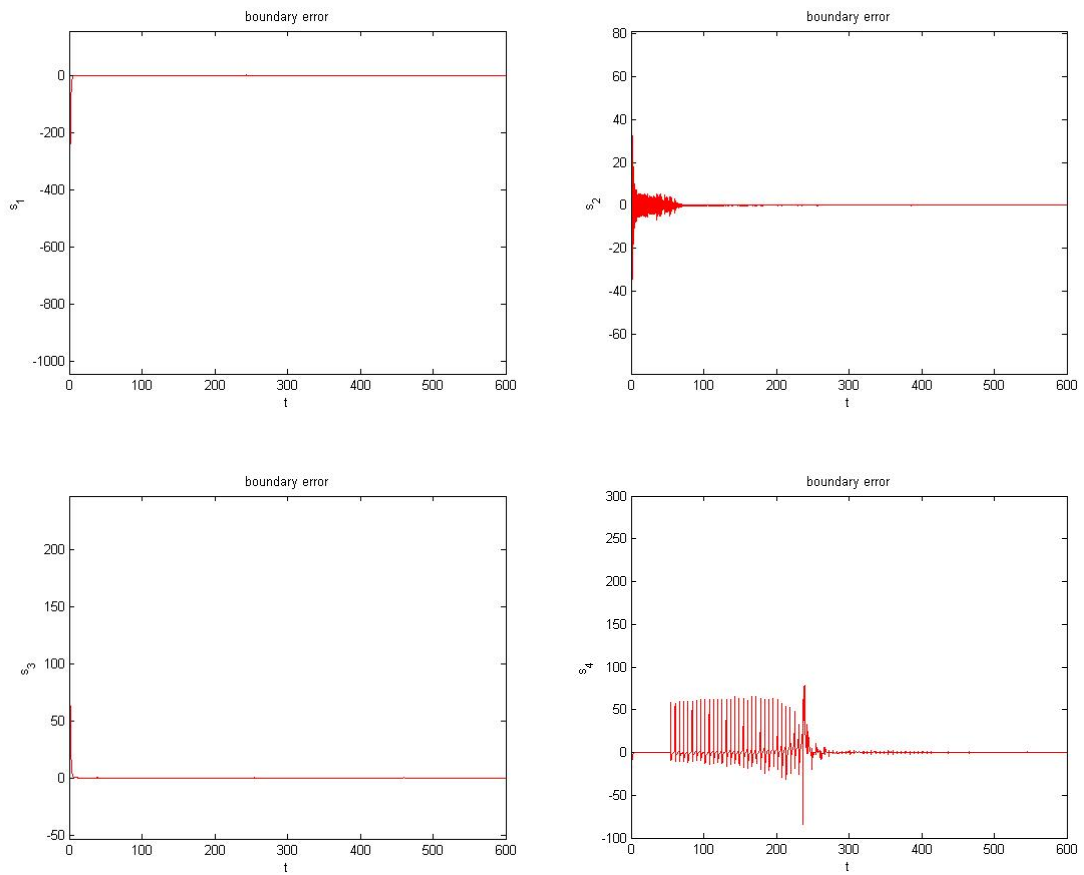


Fig. 4.3 Time histories of boundary layer errors.



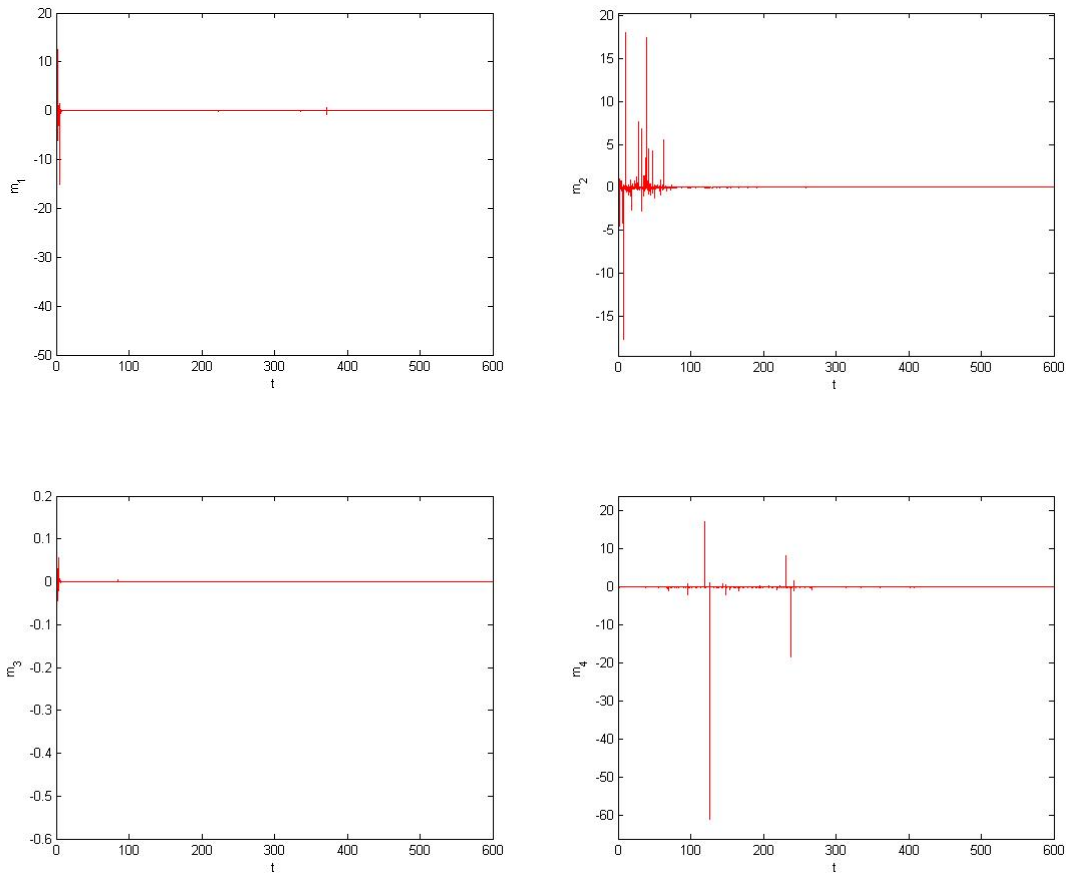


Fig. 4.4 Time histories of m which is a bounded function of time and approaches to zero.

Chapter 5

Chaos Generalized Synchronization of New Duffing-Van der Pol Systems by GYC Partial Region Stability Theory

A new chaos generalized synchronization strategy, using the GYC partial region stability theory, the controllers are of lower degree than that of controllers by using traditional Lyapunov asymptotical stability theorem. The simple linear homogeneous Lyapunov function of error states makes the controllers introducing less simulation error. A new Duffing-Van der Pol system and hyper-chaotic Lü system [46] are used as simulated examples.

5.1 Chaos Generalized Synchronization Strategy

Consider the following unidirectional coupled chaotic systems

$$\begin{aligned}\dot{\mathbf{x}} &= \mathbf{f}(t, \mathbf{x}) \\ \dot{\mathbf{y}} &= \mathbf{h}(t, \mathbf{y}) + \mathbf{u}\end{aligned}\tag{5.1}$$

where $\mathbf{x} = [x_1, x_2, \dots, x_n]^T \in R^n$, $\mathbf{y} = [y_1, y_2, \dots, y_n]^T \in R^n$ denote the master state vector and slave state vector respectively, \mathbf{f} and \mathbf{h} are nonlinear vector functions, and $\mathbf{u} = [u_1, u_2, \dots, u_n]^T \in R^n$ is a control input vector.

The generalized synchronization can be accomplished when $t \rightarrow \infty$, the limit of the error vector $\mathbf{e} = [e_1, e_2, \dots, e_n]^T$ approaches zero:

$$\lim_{t \rightarrow \infty} \mathbf{e} = 0\tag{5.2}$$

where

$$\mathbf{e} = \mathbf{G}(\mathbf{x}) - \mathbf{y}\tag{5.3}$$

$\mathbf{G}(\mathbf{x})$ is a given function of \mathbf{x} .

By using the partial region stability theory (see Appendix), the linear homogeneous terms of the entries of \mathbf{e} can be used to construct a positive definite Lyapunov function and the controllers can be designed in lower degree.

5.2 Numerical Simulations

Two new Duffing-Van der Pol systems with unidirectional coupling are given:

$$\begin{cases} \dot{x}_1 = x_2 \\ \dot{x}_2 = -x_1 - x_1^3 - ax_2 + dx_3 \\ \dot{x}_3 = x_4 \\ \dot{x}_4 = -bx_3 + c(1-x_3^2)x_4 + fx_1 \end{cases} \quad (5.4)$$

$$\begin{cases} \dot{y}_1 = y_2 + u_1 \\ \dot{y}_2 = -y_1 - y_1^3 - ay_2 + dy_3 + u_2 \\ \dot{y}_3 = y_4 + u_3 \\ \dot{y}_4 = -by_3 + c(1-y_3^2)y_4 + fy_1 + u_4 \end{cases}$$

CASE I. The generalized synchronization error function is

$$e_i = x_i - y_i + 30, \quad i = 1, 2, 3, 4 \quad (5.5)$$

The addition of the constant 30 makes the error dynamics always happens in the first quadrant. Our goal is $y_i = x_i + 30$, i.e.

$$\lim_{t \rightarrow \infty} e_i = \lim_{t \rightarrow \infty} (x_i - y_i + 30) = 0, \quad i = 1, 2, 3, 4 \quad (5.6)$$

The error dynamics becomes

$$\begin{cases} \dot{e}_1 = \dot{x}_1 - \dot{y}_1 = x_2 - y_2 + x_1^2 - x_1^2 - u_1 \\ \dot{e}_2 = \dot{x}_2 - \dot{y}_2 = -x_1 - x_1^3 - ax_2 + dx_3 - (-y_1 - y_1^3 - ay_2 + dy_3) + x_1^2 - x_1^2 - u_2 \\ \dot{e}_3 = \dot{x}_3 - \dot{y}_3 = x_4 - y_4 + x_3^2 - x_3^2 - u_3 \\ \dot{e}_4 = \dot{x}_4 - \dot{y}_4 = -bx_3 + c(1-x_3^2)x_4 + fx_1 - (-by_3 + c(1-y_3^2)y_4 + fy_1) + x_3^2 - x_3^2 - u_4 \end{cases} \quad (5.7)$$

Let initial states be $(x_1, x_2, x_3, x_4) = (2, 2.4, 5, 6)$, $(y_1, y_2, y_3, y_4) = (5, 5, 1, 1)$ and system parameters $a = 0.01$, $b = 1$, $c = 5$, $d = 0.67$, $f = 0.05$, we find that the error

dynamic always exists in first quadrant as shown in Fig. 5.1. By GYC partial region asymptotical stability theory, one can choose a Lyapunov function in the form of a positive definite function in first quadrant:

$$V = e_1 + e_2 + e_3 + e_4 \quad (5.8)$$

Its time derivative is

$$\begin{aligned} \dot{V} &= \dot{e}_1 + \dot{e}_2 + \dot{e}_3 + \dot{e}_4 \\ &= (x_2 - y_2 + x_1^2 - x_1^2 - u_1) \\ &\quad + (-x_1 - x_1^3 - ax_2 + dx_3 + y_1 + y_1^3 + ay_2 - dy_3 + x_1^2 - x_1^2 - u_2) \\ &\quad + (x_4 - y_4 + x_3^2 - x_3^2 - u_3) \\ &\quad + (-bx_3 + c(1 - x_3^2)x_4 + fx_1 + by_3 - c(1 - y_3^2)y_4 - fy_1 + x_3^2 - x_3^2 - u_4) \end{aligned} \quad (5.9)$$

Choose

$$\begin{cases} u_1 = x_2 - y_2 + x_1^2 + e_1 \\ u_2 = -x_1 - x_1^3 - ax_2 + dx_3 + y_1 + y_1^3 + ay_2 - dy_3 - x_1^2 + e_2 \\ u_3 = x_4 - y_4 + x_3^2 + e_3 \\ u_4 = -bx_3 + c(1 - x_3^2)x_4 + fx_1 + by_3 - c(1 - y_3^2)y_4 - fy_1 - x_3^2 + e_4 \end{cases} \quad (5.10)$$

We obtain

$$\dot{V} = -e_1 - e_2 - e_3 - e_4 < 0 \quad (5.11)$$

which is negative definite function in the first quadrant. Four state errors versus time and time histories of states are shown in Fig. 5.2 and Fig. 5.3.

CASE II. The generalized synchronization error function is

$$e_i = x_i - y_i + F \sin \omega t \cos \omega t + 50, \quad i = 1, 2, 3, 4 \quad (5.12)$$

Our goal is $y_i = x_i + F \sin \omega t \cos \omega t + 50$, i.e.

$$\lim_{t \rightarrow \infty} e_i = \lim_{t \rightarrow \infty} (x_i - y_i + F \sin \omega t \cos \omega t + 50) = 0, \quad i = 1, 2, 3, 4 \quad (5.13)$$

The error dynamics becomes

$$\dot{e}_i = \dot{x}_i - \dot{y}_i + F\omega \cos^2 \omega t - F\omega \sin^2 \omega t$$

$$\begin{cases} \dot{e}_1 = x_2 + F\omega \cos^2 \omega t - F\omega \sin^2 \omega t - y_2 + x_2^2 - x_2^2 - u_1 \\ \dot{e}_2 = -x_1 - x_1^3 - ax_2 + dx_3 + F\omega \cos^2 \omega t - F\omega \sin^2 \omega t \\ \quad - (-y_1 - y_1^3 - ay_2 + dy_3) + x_2^2 - x_2^2 - u_2 \\ \dot{e}_3 = x_4 + F\omega \cos^2 \omega t - F\omega \sin^2 \omega t - y_4 + x_4^2 - x_4^2 - u_3 \\ \dot{e}_4 = -bx_3 + c(1 - x_3^2)x_4 + fx_1 + F\omega \cos^2 \omega t - F\omega \sin^2 \omega t \\ \quad - (-by_3 + c(1 - y_3^2)y_4 + fy_1) + x_4^2 - x_4^2 - u_4 \end{cases} \quad (5.14)$$

Let initial states be $(x_1, x_2, x_3, x_4) = (2, 2.4, 5, 6)$, $(y_1, y_2, y_3, y_4) = (5, 5, 1, 1)$ and system parameters $a = 0.01$, $b = 1$, $c = 5$, $d = 0.67$, $f = 0.05$, $F = 5$ and $\omega = 0.2$, we find that the error dynamics always exists in first quadrant as shown in Fig. 5.4. By GYC partial region asymptotical stability theory, one can choose a Lyapunov function in the form of a positive definite function in first quadrant:

$$V = e_1 + e_2 + e_3 + e_4 \quad (5.15)$$

Its time derivative is

$$\begin{aligned} \dot{V} = & (x_2 + F\omega \cos^2 \omega t - F\omega \sin^2 \omega t - y_2 + x_2^2 - x_2^2 - u_1) + \\ & + (-x_1 - x_1^3 - ax_2 + dx_3 + F\omega \cos^2 \omega t - F\omega \sin^2 \omega t + y_1 + y_1^3 + ay_2 - dy_3 + x_2^2 - x_2^2 - u_2) \\ & + (x_4 + F\omega \cos^2 \omega t - F\omega \sin^2 \omega t - y_4 + x_4^2 - x_4^2 - u_3) \\ & + (-bx_3 + c(1 - x_3^2)x_4 + fx_1 + F\omega \cos^2 \omega t - F\omega \sin^2 \omega t + by_3 \\ & \quad - c(1 - y_3^2)y_4 - fy_1 + x_4^2 - x_4^2 - u_4) \end{aligned} \quad (5.16)$$

Choose

$$\begin{cases} u_1 = x_2 + F\omega \cos^2 \omega t - F\omega \sin^2 \omega t - y_2 + x_2^2 + e_1 \\ u_2 = -x_1 - x_1^3 - ax_2 + dx_3 + F\omega \cos^2 \omega t - F\omega \sin^2 \omega t + y_1 + y_1^3 + ay_2 - dy_3 - x_2^2 + e_2 \\ u_3 = x_4 + F\omega \cos^2 \omega t - F\omega \sin^2 \omega t - y_4 + x_4^2 + e_3 \\ u_4 = -bx_3 + c(1 - x_3^2)x_4 + fx_1 + F\omega \cos^2 \omega t - F\omega \sin^2 \omega t + by_3 \\ \quad - c(1 - y_3^2)y_4 - fy_1 - x_4^2 + e_4 \end{cases} \quad (5.17)$$

We obtain

$$\dot{V} = -e_1 - e_2 - e_3 - e_4 < 0 \quad (5.18)$$

which is negative definite function in first quadrant. Four state errors versus time and time histories of states are shown in Fig. 5.5 and Fig. 5.6.

CASE III. The generalized synchronization error function is

$$e_i = \frac{1}{10}x_i^3 - y_i + 80, \quad i = 1, 2, 3, 4 \quad (5.19)$$

Our goal is $y_i = \frac{1}{10}x_i^3 + 80$, i.e.

$$\lim_{t \rightarrow \infty} e_i = \lim_{t \rightarrow \infty} \left(\frac{1}{10}x_i^3 - y_i + 80 \right) = 0, \quad i = 1, 2, 3, 4 \quad (5.20)$$

The error dynamics become

$$\begin{cases} \dot{e}_i = \frac{3}{10}x_i^2\dot{x}_i - \dot{y}_i \\ \dot{e}_1 = \frac{3}{10}x_1^2x_2 - y_2 + x_1^2 - x_1^2 - u_1 \\ \dot{e}_2 = \frac{3}{10}x_2^2(-x_1 - x_1^3 - ax_2 + dx_3) - (-y_1 - y_1^3 - ay_2 + dy_3) + x_1^2 - x_1^2 - u_2 \\ \dot{e}_3 = \frac{3}{10}x_3^2x_4 - y_4 + x_3^2 - x_3^2 - u_3 \\ \dot{e}_4 = \frac{3}{10}x_4^2(-bx_3 + c(1 - x_3^2)x_4 + fx_1) - (-by_3 + c(1 - y_3^2)y_4 + fy_1) + x_3^2 - x_3^2 - u_4 \end{cases} \quad (5.21)$$

Let initial states be $(x_1, x_2, x_3, x_4) = (2, 2.4, 5, 6)$, $(y_1, y_2, y_3, y_4) = (5, 5, 1, 1)$ and system parameters $a = 0.01$, $b = 1$, $c = 5$, $d = 0.67$, $f = 0.05$, we find the error dynamics always exists in first quadrant as shown in Fig. 5.7. By GYC partial region asymptotical stability theory, one can choose a Lyapunov function in the form of a positive definite function in first quadrant:

$$V = e_1 + e_2 + e_3 + e_4 \quad (5.22)$$

Its time derivative is

$$\begin{aligned}
\dot{V} = & \left(\frac{3}{10} x_1^2 x_2 - y_2 + x_1^2 - x_1^2 - u_1 \right) \\
& + \left(\frac{3}{10} x_2^2 (-x_1 - x_1^3 - ax_2 + dx_3) + y_1 + y_1^3 + ay_2 - dy_3 + x_1^2 - x_1^2 - u_2 \right) \\
& + \left(\frac{3}{10} x_3^2 x_4 - y_4 + x_3^2 - x_3^2 - u_3 \right) \\
& + \left(\frac{3}{10} x_4^2 (-bx_3 + c(1-x_3^2)x_4 + fx_1) + by_3 - c(1-y_3^2)y_4 - fy_1 + x_3^2 - x_3^2 - u_4 \right)
\end{aligned} \tag{5.23}$$

Choose

$$\begin{cases}
u_1 = \frac{3}{10} x_1^2 x_2 - y_2 + x_1^2 + e_1 \\
u_2 = \frac{3}{10} x_2^2 (-x_1 - x_1^3 - ax_2 + dx_3) + y_1 + y_1^3 + ay_2 - dy_3 - x_1^2 + e_2 \\
u_3 = \frac{3}{10} x_3^2 x_4 - y_4 + x_3^2 + e_3 \\
u_4 = \frac{3}{10} x_4^2 (-bx_3 + c(1-x_3^2)x_4 + fx_1) + by_3 - c(1-y_3^2)y_4 - fy_1 - x_3^2 + e_4
\end{cases} \tag{5.24}$$

We obtain

$$\dot{V} = -e_1 - e_2 - e_3 - e_4 < 0 \tag{5.25}$$

which is negative definite function in first quadrant. Four state errors versus time and time histories of states are shown in Fig. 5.8 and Fig. 5.9.

CASE IV. The generalized synchronization error function is

$$e_i = x_i - y_i + \frac{1}{2} z_i + 150, \quad i = 1, 2, 3, 4 \tag{5.26}$$

$z = [z_1 \ z_2 \ z_3 \ z_4]^T$ is the state vector of hyperchaotic Lü system.

The goal system for synchronization is hyperchaotic Lü system and initial states is (1, 1, 1, 1), system parameters $a_1 = 36$, $b_1 = 20$, $c_1 = 3$, $d_1 = 1.3$.

$$\begin{cases} \dot{z}_1 = a_1(z_2 - z_1) + z_4 \\ \dot{z}_2 = b_1 z_2 - z_1 z_3 \\ \dot{z}_3 = -c_1 z_3 + z_1 z_2 \\ \dot{z}_4 = d_1 z_4 + z_1 z_3 \end{cases} \quad (5.27)$$

We have

$$\lim_{t \rightarrow \infty} e_i = \lim_{t \rightarrow \infty} (x_i - y_i + \frac{1}{2} z_i + 150) = 0 \quad i = 1, 2, 3, 4 \quad (5.28)$$

The error dynamics becomes

$$\begin{aligned} \dot{e}_i &= \dot{x}_i - \dot{y}_i + \frac{1}{2} \dot{z}_i \\ \begin{cases} \dot{e}_1 = x_2 + \frac{1}{2} [a_1(z_2 - z_1) + z_4] - y_2 + x_2^2 - x_2^2 - u_1 \\ \dot{e}_2 = -x_1 - x_1^3 - ax_2 + dx_3 + \frac{1}{2} (b_1 z_2 - z_1 z_3) - (-y_1 - y_1^3 - ay_2 + dy_3) + x_2^2 - x_2^2 - u_2 \\ \dot{e}_3 = x_4 + \frac{1}{2} (-c_1 z_3 + z_1 z_2) - y_4 + x_4^2 - x_4^2 - u_3 \\ \dot{e}_4 = -bx_3 + c(1 - x_3^2)x_4 + fx_1 + \frac{1}{2} (d_1 z_4 + z_1 z_3) - [-by_3 + c(1 - y_3^2)y_4 + fy_1] + x_4^2 - x_4^2 - u_4 \end{cases} \end{aligned} \quad (5.29)$$

Let initial states be $(x_1, x_2, x_3, x_4) = (2, 2.4, 5, 6)$, $(y_1, y_2, y_3, y_4) = (1, 1, 1, 1)$ and system parameters $a = 0.01$, $b = 1$, $c = 5$, $d = 0.67$, $f = 0.05$, we find the error dynamics always exists in first quadrant as shown in Fig. 5.10. By GYC partial region asymptotical stability theorem, one can choose a Lyapunov function in the form of a positive definite function in first quadrant:

$$V = e_1 + e_2 + e_3 + e_4 \quad (5.30)$$

Its time derivative is

$$\begin{aligned}
\dot{V} = & \left(x_2 + \frac{1}{2} [a_1(z_2 - z_1) + z_4] - y_2 + x_2^2 - x_2^2 - u_1 \right) \\
& + \left(-x_1 - x_1^3 - ax_2 + dx_3 + \frac{1}{2}(b_1z_2 - z_1z_3) + y_1 + y_1^3 + ay_2 - dy_3 + x_2^2 - x_2^2 - u_2 \right) \\
& + \left(x_4 + \frac{1}{2}(-c_1z_3 + z_1z_2) - y_4 + x_4^2 - x_4^2 - u_3 \right) \\
& + \left(-bx_3 + c(1 - x_3^2)x_4 + fx_1 + \frac{1}{2}(d_1z_4 + z_1z_3) + by_3 - c(1 - y_3^2)y_4 - fy_1 + x_4^2 - x_4^2 - u_4 \right)
\end{aligned} \tag{5.31}$$

Choose

$$\begin{cases}
u_1 = x_2 + \frac{1}{2} [a_1(z_2 - z_1) + z_4] - y_2 + x_2^2 + e_1 \\
u_2 = -x_1 - x_1^3 - ax_2 + dx_3 + \frac{1}{2}(b_1z_2 - z_1z_3) + y_1 + y_1^3 + ay_2 - dy_3 - x_2^2 + e_2 \\
u_3 = x_4 + \frac{1}{2}(-c_1z_3 + z_1z_2) - y_4 - u_3 + x_4^2 + e_3 \\
u_4 = -bx_3 + c(1 - x_3^2)x_4 + fx_1 + \frac{1}{2}(d_1z_4 + z_1z_3) + by_3 - c(1 - y_3^2)y_4 - fy_1 - x_4^2 + e_4
\end{cases} \tag{5.32}$$

We obtain

$$\dot{V} = -e_1 - e_2 - e_3 - e_4 < 0 \tag{5.33}$$

which is negative definite function in first quadrant. Four state errors versus time and time histories of states are shown in Fig. 5.11 and Fig. 5.12.

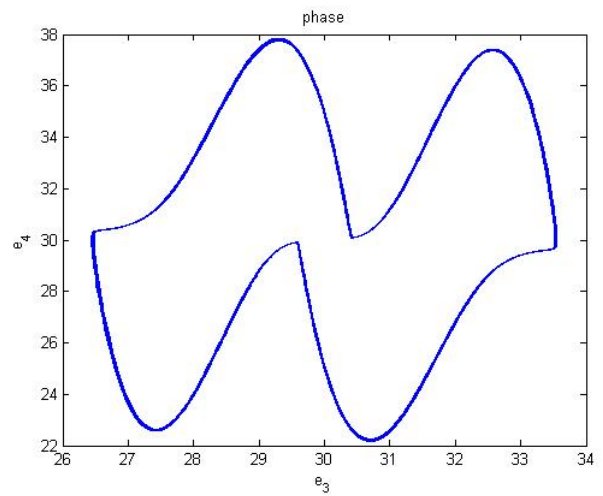
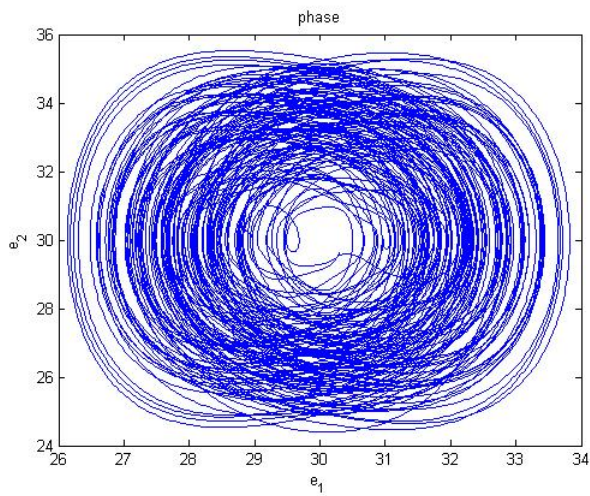


Fig. 5.1 Phase portraits of error dynamics for Case I.

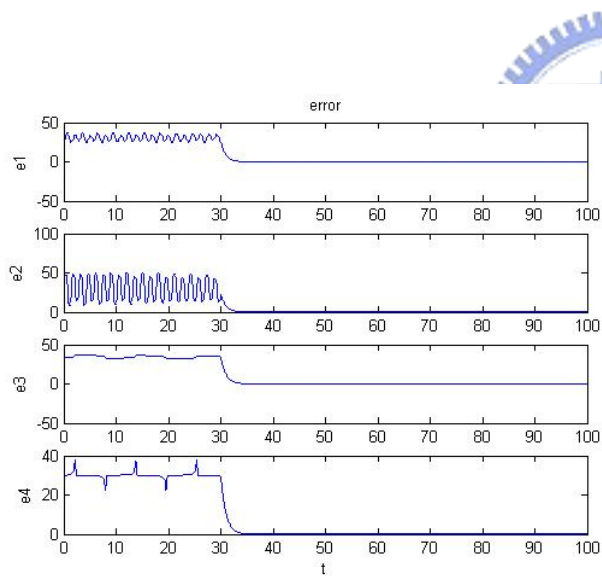


Fig. 5.2 Time histories of errors for Case I.

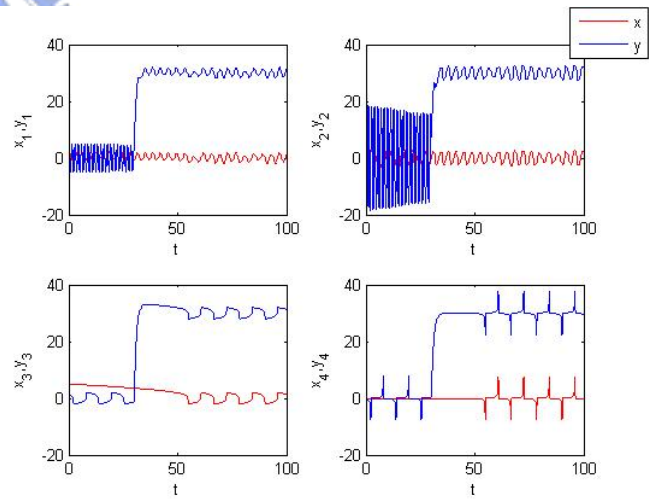


Fig. 5.3 Time histories of x_i, y_i

for Case I.

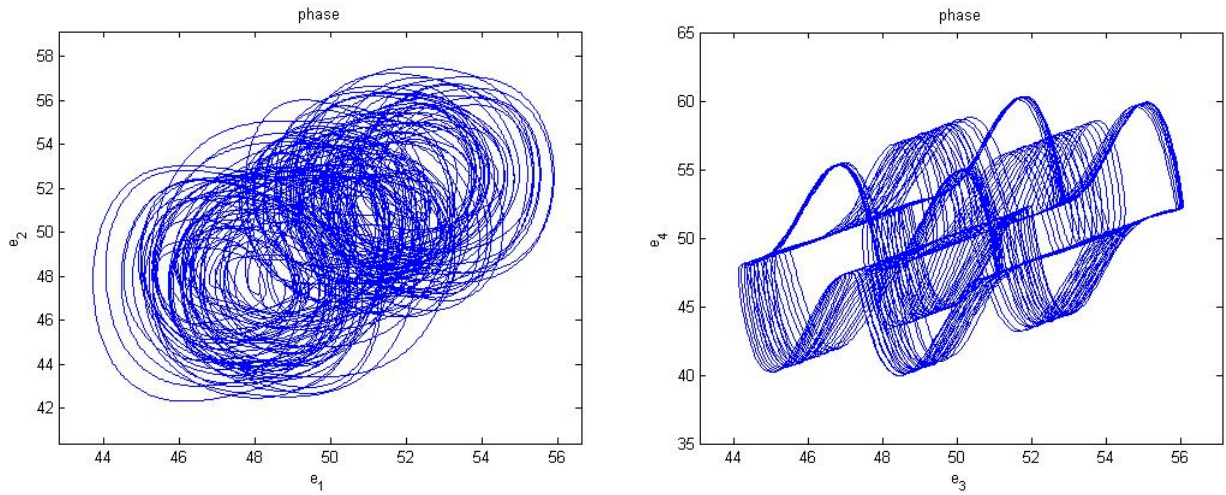


Fig. 5.4 Phase portrait of error dynamics for Case II.

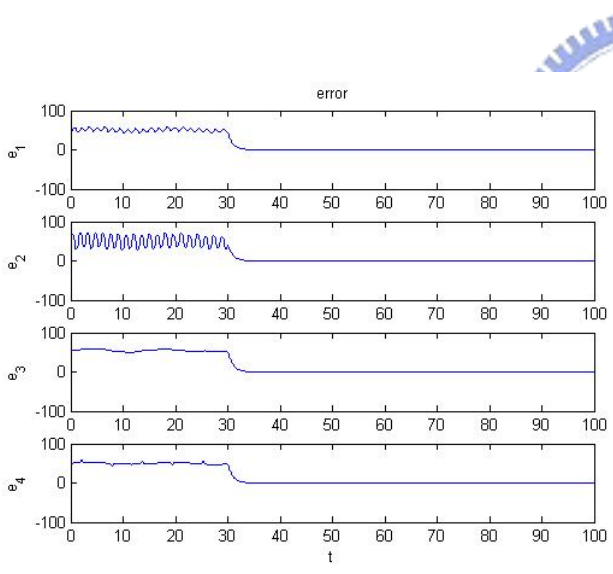


Fig. 5.5 Time histories of errors for Case II.

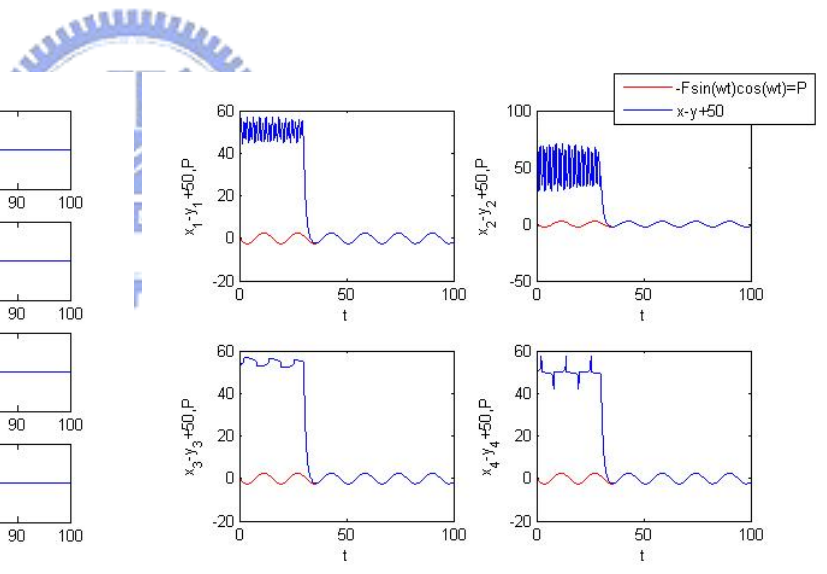


Fig. 5.6 Time histories of $x_i - y_i + 50$ and $-F \sin \omega t \cos \omega t$ for Case II.

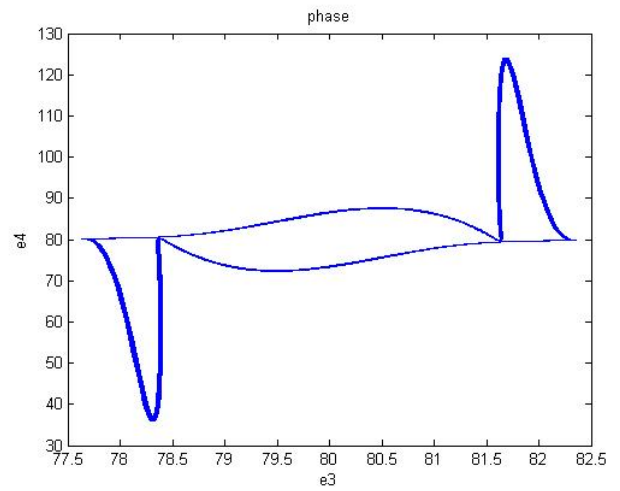
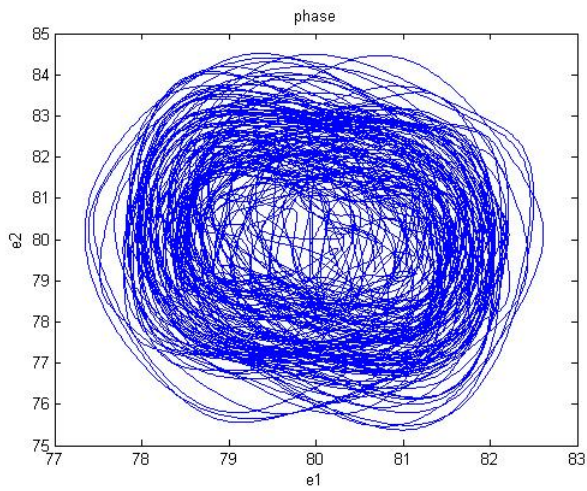


Fig. 5.7 Phase portraits of error dynamics for Case III.

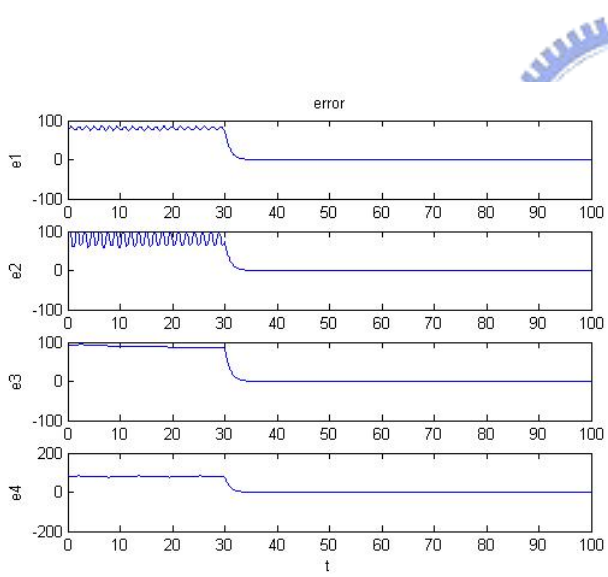


Fig. 5.8 Time histories of errors for Case III.

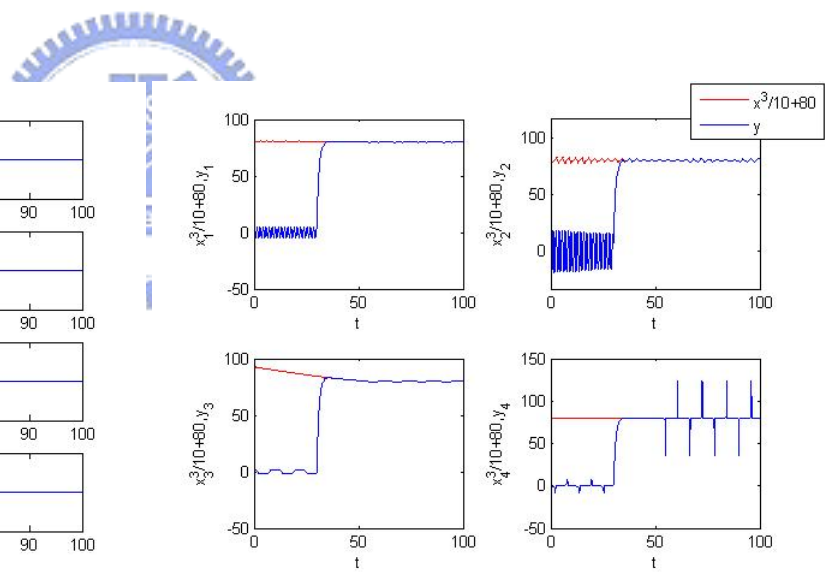


Fig. 5.9 Time histories of $\frac{x_i^3}{10} + 80$

and y_i for Case III.

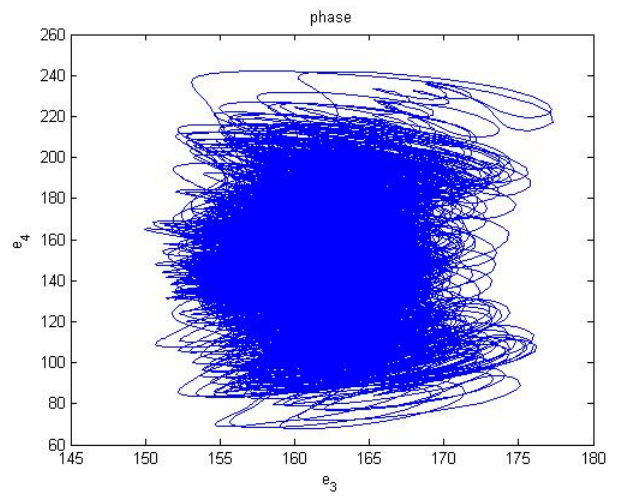
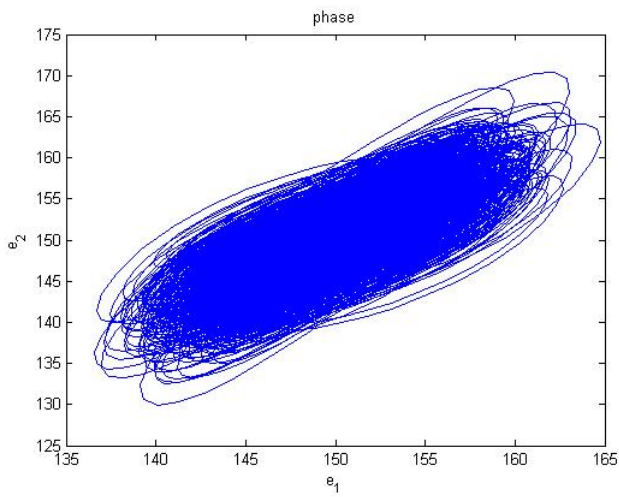


Fig. 5.10 Phase portrait of error dynamics for Case IV.

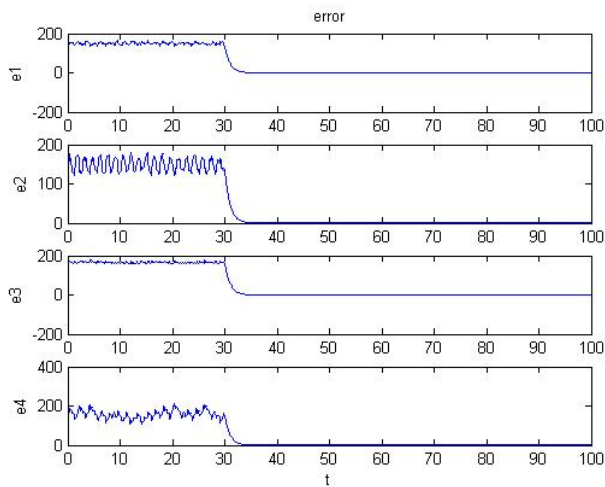


Fig. 5.11 Time histories of errors for

Case IV.

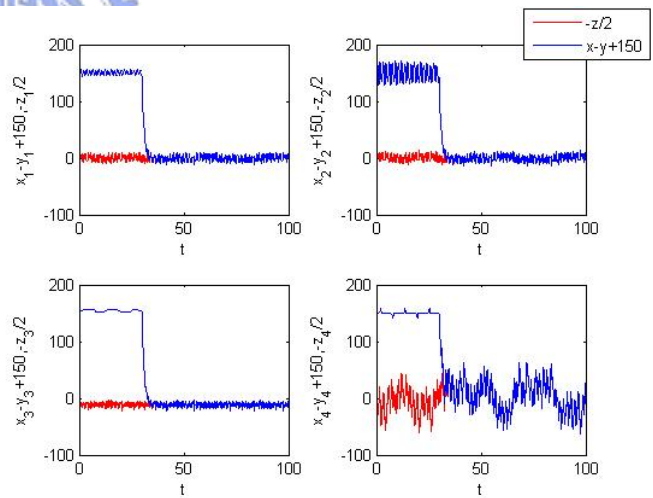


Fig. 5.12 Time histories of $x_i - y_i + 150$

and $-\frac{z_i}{2}$ for Case IV.

Chapter 6

Chaos Control and Anti-control of a New Duffing-Van der Pol System by GYC Partial Region Stability Theory

Using the GYC partial region stability theory, a new chaos control and anti-control strategy is proposed. The controllers are of lower degree than that of controllers by using traditional Lyapunov asymptotical stability theorem. The simple linear homogeneous Lyapunov function of error states makes the controllers introducing less simulation error. A new Duffing-Van der Pol system and hyper-chaotic Lü system are used as simulated examples.

6.1 Chaos Control Scheme

Consider the following chaotic systems

$$\dot{\mathbf{x}} = \mathbf{f}(t, \mathbf{x}) \quad (6.1)$$

where $\mathbf{x} = [x_1, x_2, \dots, x_n]^T \in R^n$ is a the state vector, $\mathbf{f}: R_+ \times R^n \rightarrow R^n$ is a vector function.

The goal system which can be either chaotic or regular, is

$$\dot{\mathbf{y}} = \mathbf{g}(t, \mathbf{y}) \quad (6.2)$$

where $\mathbf{y} = [y_1, y_2, \dots, y_n]^T \in R^n$ is a state vector, $\mathbf{g}: R_+ \times R^n \rightarrow R^n$ is a vector function.

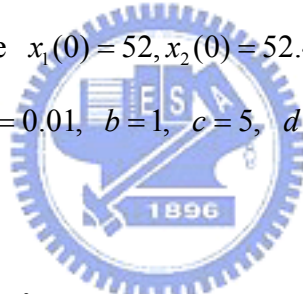
In order to make the chaos state vector \mathbf{x} approaching the goal state vector \mathbf{y} , define $\mathbf{e} = \mathbf{x} - \mathbf{y}$ as the state error. The chaos control is accomplished in the sense that [35-41]:

$$\lim_{t \rightarrow \infty} \mathbf{e} = \lim_{t \rightarrow \infty} (\mathbf{x} - \mathbf{y}) = 0 \quad (6.3)$$

In this Chapter, we will use examples in which the error dynamics is placed in the first quadrant of coordinate system and use the GYC partial region stability theory. The Lyapunov function is a simple linear homogeneous function of error states and the controllers are simpler because they are in lower degree than that of traditional controllers.

6.2 Numerical Simulations for Chaos Control

The following chaotic system is the new Duffing-Van der Pol system of which the old origin is translated to $(x_1, x_2, x_3, x_4) = (50, 50, 50, 50)$ and the chaotic motion always happens in the first quadrant of coordinate system (x_1, x_2, x_3, x_4) . This translated new Duffing-Van der Pol system is presented as simulated examples where the initial states of system are $x_1(0) = 52, x_2(0) = 52.4, x_3(0) = 55, x_4(0) = 56$ and the parameters of system are $a = 0.01, b = 1, c = 5, d = 0.67, f = 0.05$. The chaotic motion is shown in Fig. 6.1.



$$\begin{cases} \dot{x}_1 = (x_2 - 50) \\ \dot{x}_2 = -(x_1 - 50) - (x_1 - 50)^3 - a(x_2 - 50) + d(x_3 - 50) \\ \dot{x}_3 = (x_4 - 50) \\ \dot{x}_4 = -b(x_3 - 50) + c(1 - (x_3 - 50)^2)(x_4 - 50) + f(x_1 - 50) \end{cases} \quad (6.4)$$

In order to lead (x_1, x_2, x_3, x_4) to the goal, we add control terms u_1, u_2, u_3, u_4 to each equation of Eq. (6.4), respectively.

$$\begin{cases} \dot{x}_1 = (x_2 - 50) + u_1 \\ \dot{x}_2 = -(x_1 - 50) - (x_1 - 50)^3 - a(x_2 - 50) + d(x_3 - 50) + u_2 \\ \dot{x}_3 = (x_4 - 50) + u_3 \\ \dot{x}_4 = -b(x_3 - 50) + c(1 - (x_3 - 50)^2)(x_4 - 50) + f(x_1 - 50) + u_4 \end{cases} \quad (6.5)$$

CASE I. Control the chaotic motion to zero.

In this case we will control the chaotic motion of the new Duffing-Van der Pol system (6.4) to zero. The goal is $\mathbf{y} = 0$. The state error is $\mathbf{e} = \mathbf{x} - \mathbf{y} = \mathbf{x}$ and error dynamics becomes

$$\begin{cases} \dot{e}_1 = \dot{x}_1 = (x_2 - 50) + e_1^2 - e_1^2 + u_1 \\ \dot{e}_2 = \dot{x}_2 = -(x_1 - 50) - (x_1 - 50)^3 - a(x_2 - 50) + d(x_3 - 50) + e_1^2 - e_1^2 + u_2 \\ \dot{e}_3 = \dot{x}_3 = (x_4 - 50) + e_2^2 - e_2^2 + u_3 \\ \dot{e}_4 = \dot{x}_4 = -b(x_3 - 50) + c(1 - (x_3 - 50)^2)(x_4 - 50) + f(x_1 - 50) + e_2^2 - e_2^2 + u_4 \end{cases} \quad (6.6)$$

In Fig. 6.2, we see that the error dynamics always exists in first quadrant.

By GYC partial region stability theory, one can easily choose a Lyapunov function in the form of a positive definite function in first quadrant as:

$$V = e_1 + e_2 + e_3 + e_4 \quad (6.7)$$

Its time derivative through error dynamics (6.6) is

$$\begin{aligned} \dot{V} &= \dot{e}_1 + \dot{e}_2 + \dot{e}_3 + \dot{e}_4 \\ &= (x_2 - 50) + e_1^2 - e_1^2 + u_1 - (x_1 - 50) - (x_1 - 50)^3 - a(x_2 - 50) + d(x_3 - 50) + e_1^2 - e_1^2 + u_2 \\ &\quad + (x_4 - 50) + e_2^2 - e_2^2 + u_3 - b(x_3 - 50) + c(1 - (x_3 - 50)^2)(x_4 - 50) + f(x_1 - 50) + e_2^2 - e_2^2 + u_4 \end{aligned} \quad (6.8)$$

Choose

$$\begin{cases} u_1 = -(x_2 - 50) + e_1^2 - e_1 \\ u_2 = -(-(x_1 - 50) - (x_1 - 50)^3 - a(x_2 - 50) + d(x_3 - 50)) - e_1^2 - e_2 \\ u_3 = -(x_4 - 50) + e_2^2 - e_3 \\ u_4 = -(-b(x_3 - 50) + c(1 - (x_3 - 50)^2)(x_4 - 50) + f(x_1 - 50)) - e_2^2 - e_4 \end{cases} \quad (6.9)$$

We obtain

$$\dot{V} = -e_1 - e_2 - e_3 - e_4 < 0$$

which is negative definite function in first quadrant. The numerical results are shown in Fig.6.3. After 100 sec, the motion trajectories approach the origin.

CASE II. Control the chaotic motion to a product of sine and cosine functions.

In this case we will control the chaotic motion of the new Duffing-Van der Pol system (6.4) to a product of sine and cosine functions of time. The goal is $y = F \sin \omega t \cos \omega t$. The error equation

$$\mathbf{e} = \mathbf{x} - \mathbf{y} = \mathbf{x} - F \sin \omega t \cos \omega t \quad (6.10)$$

$$\lim_{t \rightarrow \infty} e_i = \lim_{t \rightarrow \infty} (x_i - F \sin \omega_i t \cos \omega_i t) = 0, \quad i = 1, 2, 3, 4$$

and $\dot{e}_i = \dot{x}_i - \omega_i F \cos^2 \omega_i t + \omega_i F \sin^2 \omega_i t$ ($i = 1, 2, 3, 4$) and $F = 5$, $\omega_1 = 0.2$, $\omega_2 = 0.4$, $\omega_3 = 0.6$, $\omega_4 = 0.8$. The error dynamics is

$$\begin{cases} \dot{e}_1 = \dot{x}_1 - \omega_1 F \cos^2 \omega_1 t + \omega_1 F \sin^2 \omega_1 t + e_3^2 - e_3^2 \\ \dot{e}_2 = \dot{x}_2 - \omega_2 F \cos^2 \omega_2 t + \omega_2 F \sin^2 \omega_2 t + e_3^2 - e_3^2 \\ \dot{e}_3 = \dot{x}_3 - \omega_3 F \cos^2 \omega_3 t + \omega_3 F \sin^2 \omega_3 t + e_4^2 - e_4^2 \\ \dot{e}_4 = \dot{x}_4 - \omega_4 F \cos^2 \omega_4 t + \omega_4 F \sin^2 \omega_4 t + e_4^2 - e_4^2 \end{cases} \quad (6.11)$$

In Fig. 6.4, the error dynamics always exists in first quadrant.

By GYC partial region stability theory, one can easily choose a Lyapunov function in the form of a positive definite function in first quadrant as:

$$V = e_1 + e_2 + e_3 + e_4$$

Its time derivative is

$$\begin{aligned} \dot{V} &= \dot{e}_1 + \dot{e}_2 + \dot{e}_3 + \dot{e}_4 \\ &= (x_2 - 50) - \omega_1 F \cos^2 \omega_1 t + \omega_1 F \sin^2 \omega_1 t + e_3^2 - e_3^2 + u_1 - (x_1 - 50) - (x_1 - 50)^3 \\ &\quad - a(x_2 - 50) + d(x_3 - 50) - \omega_2 F \cos^2 \omega_2 t + \omega_2 F \sin^2 \omega_2 t + e_3^2 - e_3^2 + u_2 + (x_4 - 50) \\ &\quad - \omega_3 F \cos^2 \omega_3 t + \omega_3 F \sin^2 \omega_3 t + e_4^2 - e_4^2 + u_3 - b(x_3 - 50) + c(1 - (x_3 - 50)^2)(x_4 - 50) \\ &\quad + f(x_1 - 50) - \omega_4 F \cos^2 \omega_4 t + \omega_4 F \sin^2 \omega_4 t + e_4^2 - e_4^2 + u_4 \end{aligned} \quad (6.12)$$

Choose

$$\begin{cases} u_1 = -((x_2 - 50) - \omega_1 F \cos^2 \omega_1 t + \omega_1 F \sin^2 \omega_1 t) + \dot{e}_1^2 - e_1 \\ u_2 = -((x_1 - 50) - (x_1 - 50)^3 - a(x_2 - 50) + d(x_3 - 50) - \omega_2 F \cos^2 \omega_2 t + \omega_2 F \sin^2 \omega_2 t) - \dot{e}_2^2 - e_2 \\ u_3 = -((x_4 - 50) - \omega_3 F \cos^2 \omega_3 t + \omega_3 F \sin^2 \omega_3 t) + \dot{e}_3^2 - e_3 \\ u_4 = -(-b(x_3 - 50) + c(1 - (x_3 - 50)^2)(x_4 - 50) + f(x_1 - 50) - \omega_4 F \cos^2 \omega_4 t + \omega_4 F \sin^2 \omega_4 t) - \dot{e}_4^2 - e_4 \end{cases} \quad (6.13)$$

We obtain

$$\dot{V} = -e_1 - e_2 - e_3 - e_4 < 0$$

which is negative definite function in first quadrant. The numerical results are shown in Fig.6.5 and Fig. 6.6. After 100 sec., the errors approach zero and the motion trajectories approach to sine and cosine functions.

CASE III. Control the chaotic motion to chaotic motion of hyper-chaotic Lü system.

In this case we will control chaotic motion of the new Duffing-Van der Pol system (6.4) to that of hyper-chaotic Lü system. The goal system is hyper-chaotic Lü system:

$$\begin{cases} \dot{z}_1 = a_1(z_2 - z_1) + z_4 \\ \dot{z}_2 = b_1 z_2 - z_1 z_3 \\ \dot{z}_3 = -c_1 z_3 + z_1 z_2 \\ \dot{z}_4 = d_1 z_4 + z_1 z_3 \end{cases} \quad (6.14)$$

The error equation is $\mathbf{e} = \mathbf{x} - \frac{1}{5}\mathbf{z}$. The goal is $\lim_{t \rightarrow \infty} \mathbf{e} = 0$. The error dynamics become

$$\begin{cases} \dot{e}_1 = \dot{x}_1 - \dot{z}_1 = (x_2 - 50) - \frac{1}{5}(a_1(z_2 - z_1) + z_4) + z_2^2 - z_2^2 + u_1 \\ \dot{e}_2 = \dot{x}_2 - \dot{z}_2 = -(x_1 - 50) - (x_1 - 50)^3 - a(x_2 - 50) + d(x_3 - 50) - \frac{1}{5}(b_1 z_2 - z_1 z_3) + z_2^2 - z_2^2 + u_2 \\ \dot{e}_3 = \dot{x}_3 - \dot{z}_3 = (x_4 - 50) - \frac{1}{5}(-c_1 z_3 + z_1 z_2) + z_4^2 - z_4^2 + u_3 \\ \dot{e}_4 = \dot{x}_4 - \dot{z}_4 = -b(x_3 - 50) + c(1 - (x_3 - 50)^2)(x_4 - 50) + f(x_1 - 50) - \frac{1}{5}(d_1 z_4 + z_1 z_3) + z_4^2 - z_4^2 + u_4 \end{cases} \quad (6.15)$$

By Fig. 6.7, we know that the error dynamics always exists in first quadrant.

By GYC partial region stability theory, one can easily choose a Lyapunov function in the form of a positive definite function in first quadrant as:

$$V = e_1 + e_2 + e_3 + e_4$$

Its time derivative is

$$\begin{aligned} \dot{V} &= \dot{e}_1 + \dot{e}_2 + \dot{e}_3 + \dot{e}_4 \\ &= (x_2 - 50) - \frac{1}{5}(a_1(z_2 - z_1) + z_4) + z_2^2 - z_2^2 + u_1 - (x_1 - 50) - (x_1 - 50)^3 \\ &\quad - a(x_2 - 50) + d(x_3 - 50) - \frac{1}{5}(b_1 z_2 - z_1 z_3) + z_2^2 - z_2^2 + u_2 + (x_4 - 50) \\ &\quad - \frac{1}{5}(-c_1 z_3 + z_1 z_2) + z_4^2 - z_4^2 + u_3 - b(x_3 - 50) + c(1 - (x_3 - 50)^2)(x_4 - 50) \\ &\quad + f(x_1 - 50) - \frac{1}{5}(d_1 z_4 + z_1 z_3) + z_4^2 - z_4^2 + u_4 \end{aligned} \quad (6.16)$$

Choose

$$\begin{cases} u_1 = -\left((x_2 - 50) - \frac{1}{5}(a_1(z_2 - z_1) + z_4)\right) + z_2^2 - e_1 \\ u_2 = -\left(- (x_1 - 50) - (x_1 - 50)^3 - a(x_2 - 50) + d(x_3 - 50) - \frac{1}{5}(b_1 z_2 - z_1 z_3)\right) - z_2^2 - e_2 \\ u_3 = -\left((x_4 - 50) - \frac{1}{5}(-c_1 z_3 + z_1 z_2)\right) + z_4^2 - e_3 \\ u_4 = -\left(-b(x_3 - 50) + c(1 - (x_3 - 50)^2)(x_4 - 50) + f(x_1 - 50) - \frac{1}{5}(d_1 z_4 + z_1 z_3)\right) - z_4^2 - e_4 \end{cases} \quad (6.17)$$

We obtain

$$\dot{V} = -e_1 - e_2 - e_3 - e_4 < 0$$

which is negative definite function in first quadrant. The numerical results are shown in Fig.6.8 and Fig. 6.9 where $a_1 = 36$, $b_1 = 20$, $c_1 = 3$, $d_1 = 1.3$. After 100 sec., the errors approach zero and the chaotic trajectories of the new Duffing-Van der Pol system approach to that of the hyper-chaotic Lü system.

6.3 Numerical Simulations for Chaos Anti-control

In this section, we will control periodic motion of the new Duffing-Van der Pol system to that of hyper-chaotic Lü system. The new Duffing-Van der Pol system exhibits periodic motion when the parameters of system are $a = 0.1$, $b = 1$, $c = 5$, $d = 0.67$, $f = 0.05$ and the initial states of system are $x_1(0) = 2, x_2(0) = 2.4, x_3(0) = 5, x_4(0) = 6$. The following periodic system

$$\begin{cases} \dot{x}_1 = (x_2 - 50) \\ \dot{x}_2 = -(x_1 - 50) - (x_1 - 50)^3 - a(x_2 - 50) + d(x_3 - 50) \\ \dot{x}_3 = (x_4 - 50) \\ \dot{x}_4 = -b(x_3 - 50) + c(1 - (x_3 - 50)^2)(x_4 - 50) + f(x_1 - 50) \end{cases} \quad (6.18)$$

is the new Duffing-Van der Pol system of which the old origin is translated to $(x_1, x_2, x_3, x_4) = (50, 50, 50, 50)$ and the periodic motion always happens in the first quadrant of coordinate system (x_1, x_2, x_3, x_4) . This translated new Duffing-Van der Pol system is presented as simulated examples where the initial states of system are $x_1(0) = 52, x_2(0) = 52.4, x_3(0) = 55, x_4(0) = 56$ and the parameters of system are $a = 0.1$, $b = 1$, $c = 5$, $d = 0.67$, $f = 0.05$. The periodic motion is shown in Fig. 6.10.

In order to lead (x_1, x_2, x_3, x_4) to the goal, we add control terms u_1, u_2, u_3, u_4 to each equation of Eq. (6.18), respectively.

$$\begin{cases} \dot{x}_1 = (x_2 - 50) + u_1 \\ \dot{x}_2 = -(x_1 - 50) - (x_1 - 50)^3 - a(x_2 - 50) + d(x_3 - 50) + u_2 \\ \dot{x}_3 = (x_4 - 50) + u_3 \\ \dot{x}_4 = -b(x_3 - 50) + c(1 - (x_3 - 50)^2)(x_4 - 50) + f(x_1 - 50) + u_4 \end{cases} \quad (6.19)$$

The goal system is hyper-chaotic Lü system:

$$\begin{cases} \dot{z}_1 = a_1(z_2 - z_1) + z_4 \\ \dot{z}_2 = b_1 z_2 - z_1 z_3 \\ \dot{z}_3 = -c_1 z_3 + z_1 z_2 \\ \dot{z}_4 = d_1 z_4 + z_1 z_3 \end{cases} \quad (6.20)$$

The error equation is $\mathbf{e} = \mathbf{x} - \frac{1}{5}\mathbf{z}$. The goal is $\lim_{t \rightarrow \infty} \mathbf{e} = 0$. The error dynamics becomes

$$\begin{cases} \dot{e}_1 = \dot{x}_1 - \dot{z}_1 = (x_2 - 50) - \frac{1}{5}(a_1(z_2 - z_1) + z_4) + z_1^2 - z_1^2 + u_1 \\ \dot{e}_2 = \dot{x}_2 - \dot{z}_2 = -(x_1 - 50) - (x_1 - 50)^3 - a(x_2 - 50) + d(x_3 - 50) - \frac{1}{5}(b_1 z_2 - z_1 z_3) + z_1^2 - z_1^2 + u_2 \\ \dot{e}_3 = \dot{x}_3 - \dot{z}_3 = (x_4 - 50) - \frac{1}{5}(-c_1 z_3 + z_1 z_2) + z_3^2 - z_3^2 + u_3 \\ \dot{e}_4 = \dot{x}_4 - \dot{z}_4 = -b(x_3 - 50) + c(1 - (x_3 - 50)^2)(x_4 - 50) + f(x_1 - 50) - \frac{1}{5}(d_1 z_4 + z_1 z_3) + z_3^2 - z_3^2 + u_4 \end{cases} \quad (6.21)$$

By Fig. 6.11, we know the error dynamics always exists in first quadrant.

By GYC partial region stability theory, one can easily choose a Lyapunov function in the form of a positive definite function in first quadrant as:

$$V = e_1 + e_2 + e_3 + e_4$$

Its time derivative is

$$\begin{aligned} \dot{V} &= \dot{e}_1 + \dot{e}_2 + \dot{e}_3 + \dot{e}_4 \\ &= (x_2 - 50) - \frac{1}{5}(a_1(z_2 - z_1) + z_4) + z_1^2 - z_1^2 + u_1 - (x_1 - 50) - (x_1 - 50)^3 \\ &\quad - a(x_2 - 50) + d(x_3 - 50) - \frac{1}{5}(b_1 z_2 - z_1 z_3) + z_1^2 - z_1^2 + u_2 + (x_4 - 50) \\ &\quad - \frac{1}{5}(-c_1 z_3 + z_1 z_2) + z_3^2 - z_3^2 + u_3 - b(x_3 - 50) + c(1 - (x_3 - 50)^2)(x_4 - 50) \\ &\quad + f(x_1 - 50) - \frac{1}{5}(d_1 z_4 + z_1 z_3) + z_3^2 - z_3^2 + u_4 \end{aligned} \quad (6.22)$$

Choose

$$\begin{cases} u_1 = -\left((x_2 - 50) - \frac{1}{5}(a_1(z_2 - z_1) + z_4)\right) + z_1^2 - e_1 \\ u_2 = -\left(-\left(x_1 - 50\right) - \left(x_1 - 50\right)^3 - a\left(x_2 - 50\right) + d\left(x_3 - 50\right) - \frac{1}{5}\left(b_1 z_2 - z_1 z_3\right)\right) - z_1^2 - e_2 \\ u_3 = -\left(\left(x_4 - 50\right) - \frac{1}{5}\left(-c_1 z_3 + z_1 z_2\right)\right) + z_3^2 - e_3 \\ u_4 = -\left(-b\left(x_3 - 50\right) + c\left(1 - \left(x_3 - 50\right)^2\right)\left(x_4 - 50\right) + f\left(x_1 - 50\right) - \frac{1}{5}\left(d_1 z_4 + z_1 z_3\right)\right) - z_3^2 - e_4 \end{cases} \quad (6.23)$$

We obtain

$$\dot{V} = -e_1 - e_2 - e_3 - e_4 < 0$$

which is negative definite function in first quadrant. The numerical results are shown in Fig.6.12 and Fig. 6.13 where $a_1 = 36$, $b_1 = 20$, $c_1 = 3$, $d_1 = 1.3$. After 200 sec., the errors approach zero and the periodic trajectories of the translated new Duffing-Van der Pol system approach to that of the hyper-chaotic Lü system.



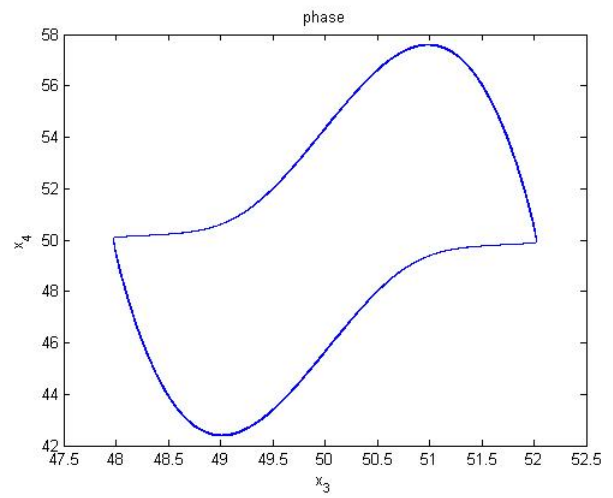
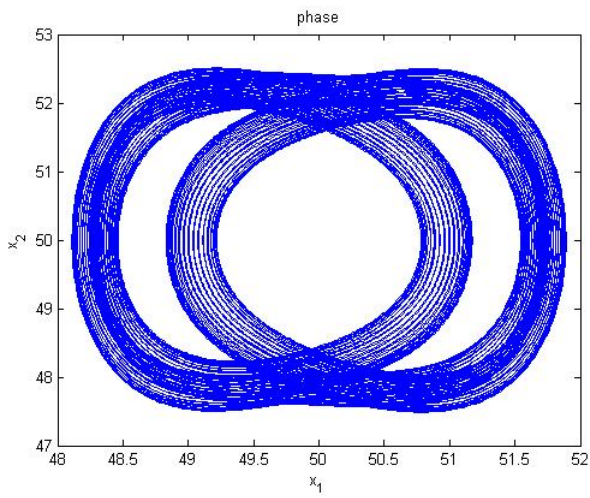


Fig. 6.1 Chaotic phase portraits for a new Duffing-Van der Pol system in the first quadrant.

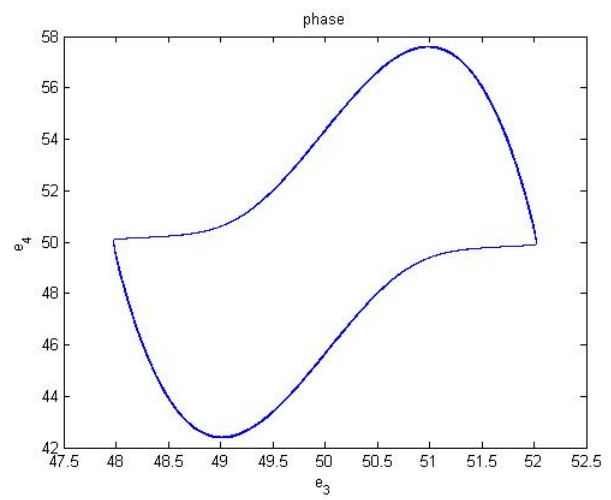
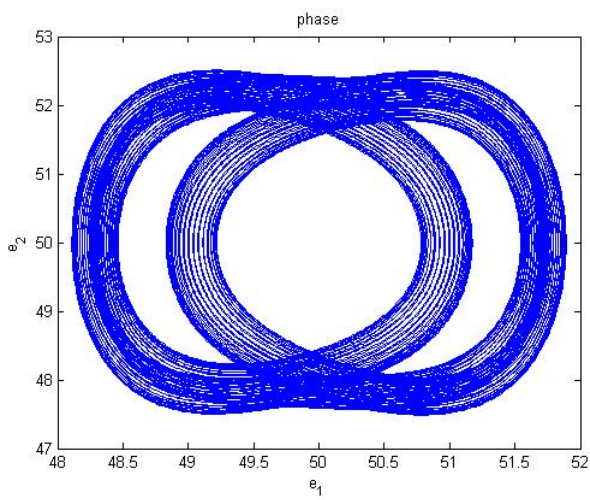


Fig. 6.2 Phase portrait of error dynamics for Case I.

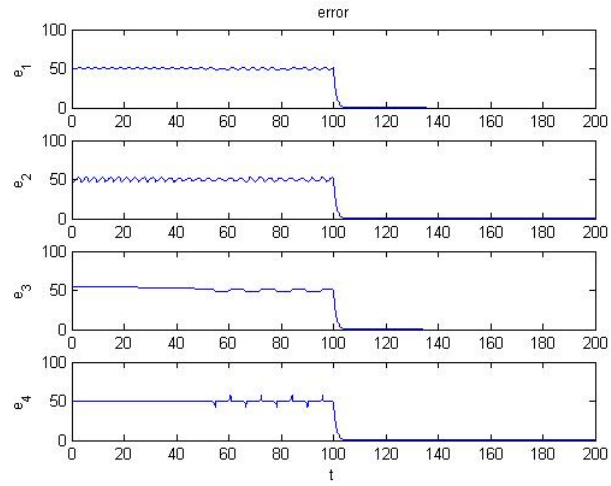


Fig.6.3 Time histories of errors for Case I.

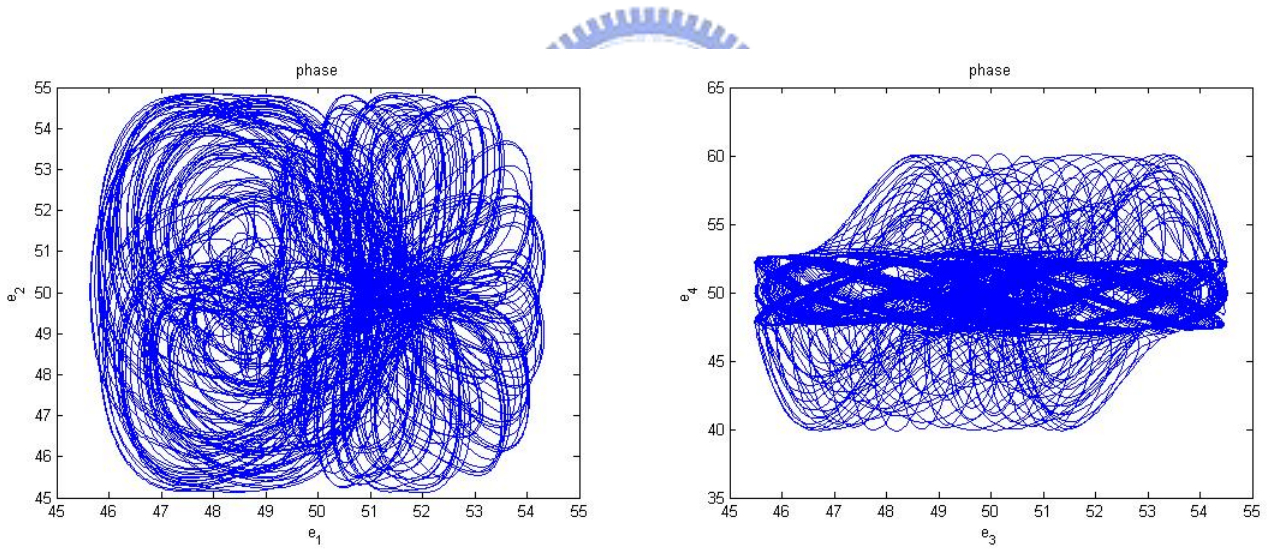


Fig. 6.4 Phase portrait of error dynamics for Case II.

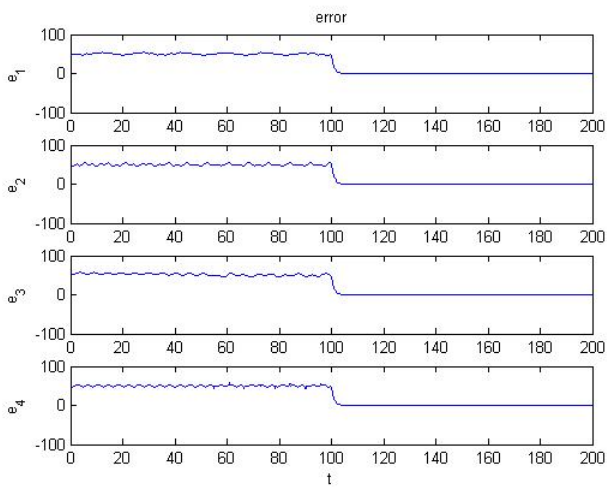


Fig. 6.5 Time histories of errors for

Case II.

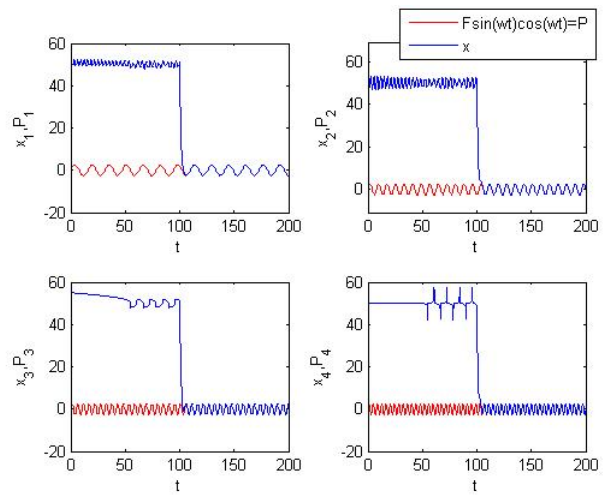


Fig. 6.6 Time histories of x_i for

Case II.

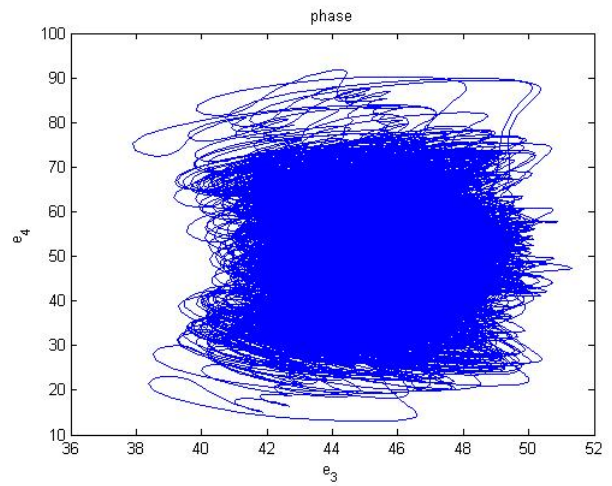
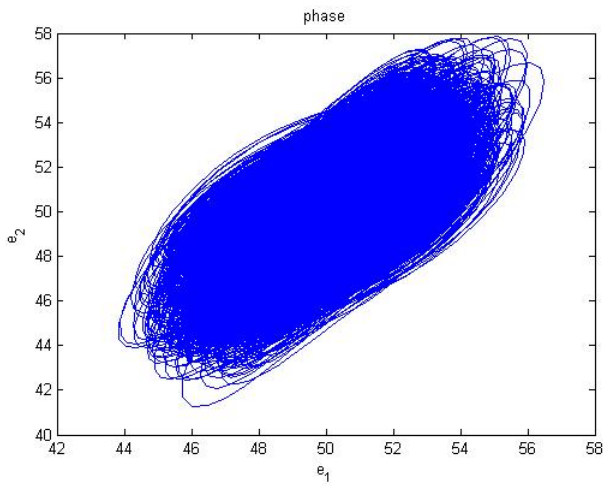


Fig. 6.7 Phase portrait of error dynamics for Case III.

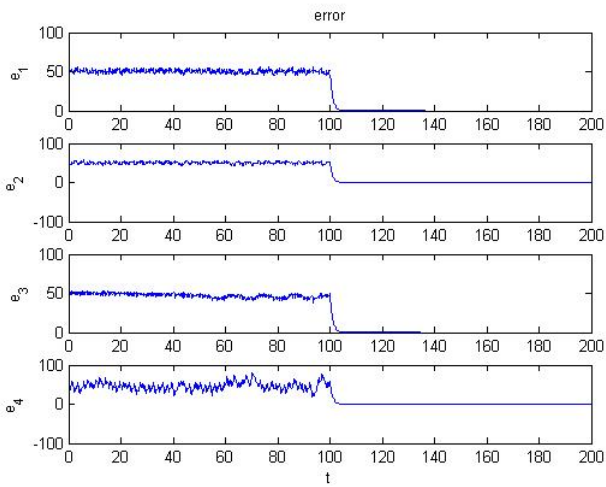


Fig. 6.8 Time histories of errors for

Case III.

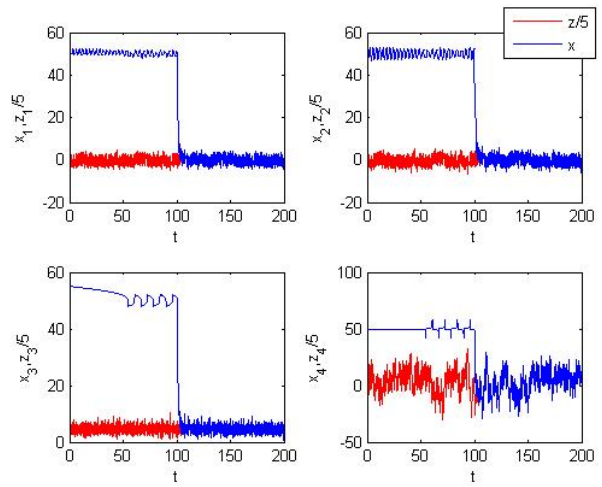


Fig. 6.9 Time histories of x_i for Case

III.

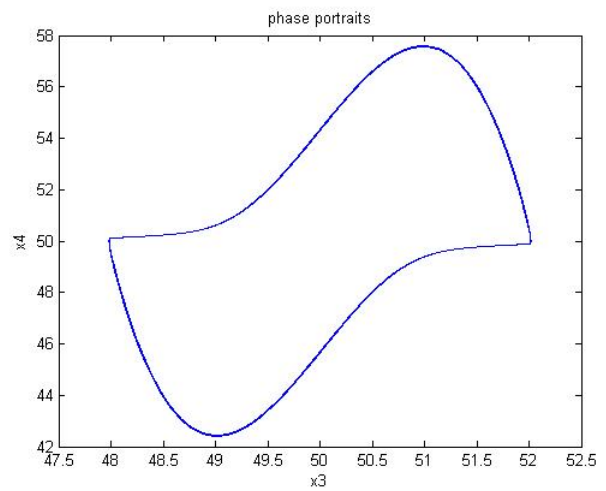
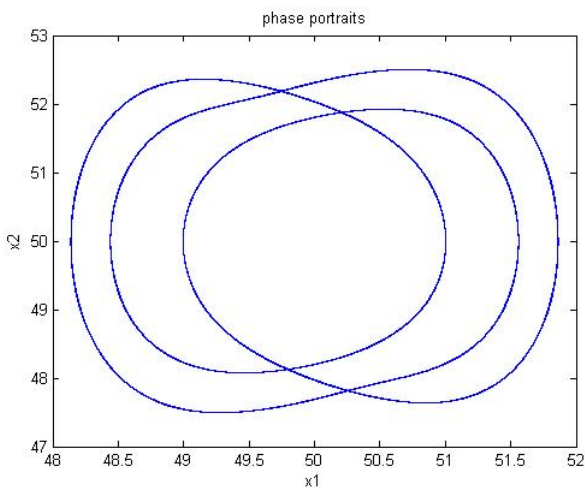


Fig. 6.10 Periodic phase portraits for a translated new Duffing-Van der Pol system in the first quadrant.

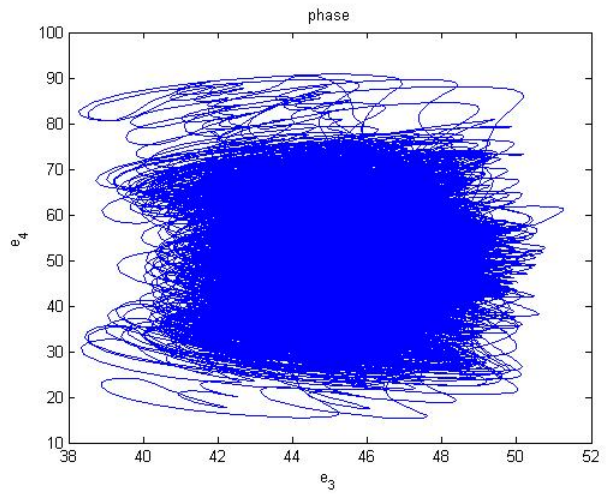
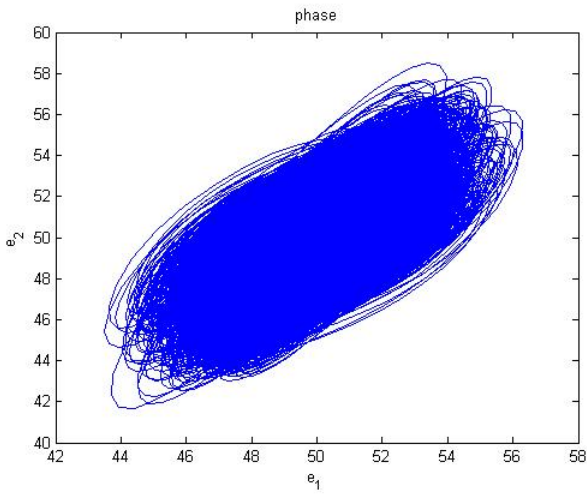


Fig. 6.11 Phase portraits of error dynamics.

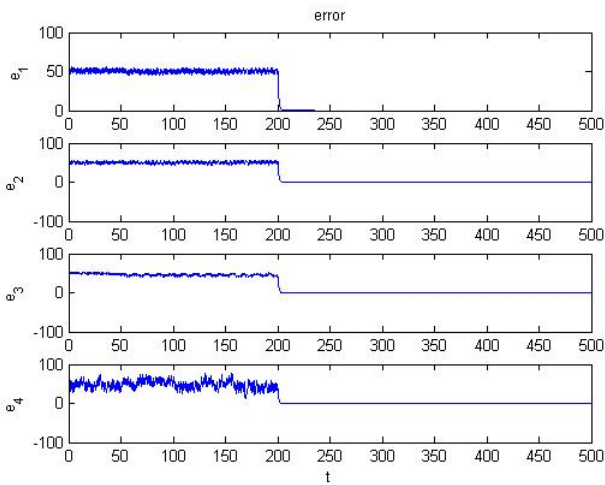


Fig. 6.12 Time histories of errors.

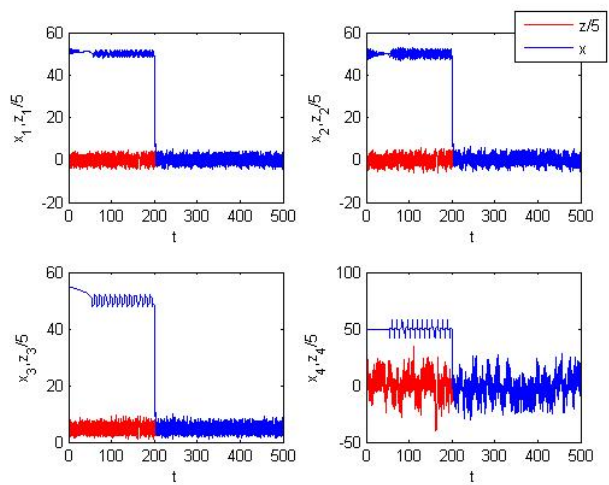


Fig. 6.13 Time histories of x_i .

Chapter 7

Hybrid Projective Symplectic Synchronization of a New Duffing-Van der Pol System with Legendre function Parameters by GYC Partial Region Stability Theory

A new type of chaotic synchronization, *hybrid projective symplectic synchronization* (HPSS), is obtained for a Duffing-Van der Pol system with constant parameter and a new Duffing-Van der Pol system with Legendre function parameters. The latter is used as “master” system and the former as “slave” system. Based on the GYC partial region stability theory, the scheme can be achieved not only for projective synchronization, but also for projective anti-synchronization. Numerical simulations are provided to verify the effectiveness of the proposed scheme.

7.1 Hybrid Projective Symplectic Synchronization Scheme

There are two nonlinear chaotic dynamical systems. The “master” system controls the “slave” system partly. In symplectic synchronization, the “master” system is called partner A:

$$\dot{x} = f(x) \quad (7.1)$$

where $x = [x_1, x_2, \dots, x_n]^T \in R^n$ is a state vector. The “slave” system is called partner

B:

$$\dot{y} = f(y) \quad (7.2)$$

where $y = [y_1, y_2, \dots, y_n]^T \in R^n$ is a state vector. With controllers, partner B becomes

$$\dot{y} = f(y) + u(t) \quad (7.3)$$

where $u(t) = [u_1(t), u_2(t), \dots, u_n(t)]^T \in R^n$ is a control input vector. HPSS demands:

$$y = H(x, y, t) = Gxy \quad (7.4)$$

where $H(x, y, t)$ consists of state vector x of partner A and state vector y of partner B, $G = \text{diag}(g_1, g_2, \dots, g_n) \in R^{(n \times n)}$ is a constant scaling matrix with positive and negative entries. Our goal is to accomplish Eq. (7.4) via controller $u(t)$. Define the error vector e :

$$e = H(x, y, t) - y \quad (7.5)$$

The synchronization is achieved when

$$\lim_{t \rightarrow \infty} e_i = 0 \quad (i = 1, 2, \dots, n) \quad (7.6)$$

The error dynamics is

$$\dot{e} = \frac{\partial H}{\partial x} \dot{x} + \frac{\partial H}{\partial y} \dot{y} + \frac{\partial H}{\partial t} - \dot{y} \quad (7.7)$$

By Eqs (7.2) ~ (7.4), Eq. (7.7) becomes

$$\dot{e} = \frac{\partial H}{\partial x} [f(x)] + \frac{\partial H}{\partial y} [f(y)] + \frac{\partial H}{\partial t} - f(y) - u(t) \quad (7.8)$$

By using the GYC partial region stability theory (see Appendix), the linear homogeneous terms of the entries of e can be used to construct a positive definite Lyapunov function in first quadrant and the controllers can be designed in lower degree. Hence, the HPSS can be achieved.

7.2 Chaos of a New Duffing-Van der Pol System with Legendre Function Parameters

This section introduces a new Duffing-Van der Pol system with Legendre function parameters.

$$\begin{cases} \frac{dx_1}{dt} = x_2 \\ \frac{dx_2}{dt} = -x_1 - x_1^3 - ax_2 + dx_3 \\ \frac{dx_3}{dt} = x_4 \\ \frac{dx_4}{dt} = -bx_3 + c(1-x_3^2)x_4 + fx_1 \end{cases} \quad (7.9)$$

where a, b, c, d, f are parameters. We select the Legendre functions [48] as parameters of the system. The Legendre functions are defined by

$$P_n^m(x) = (-1)^m (1-x^2)^{m/2} \frac{d^m}{dx^m} P_n(x) \quad (7.10)$$

where $P_n(x)$ is the Legendre polynomial of degree n .

$$P_n(x) = \frac{1}{2^n n!} \left[\frac{d^n}{dx^n} (x^2 - 1)^n \right] \quad (7.11)$$

Choosing $n=2$, we obtain

$$\begin{cases} L_1(x) = P_2^0(x) = P_2(x) \\ L_2(x) = P_2^1(x) = (-1)(1-x^2)^{1/2} \frac{d}{dx} P_2(x) \\ L_3(x) = P_2^2(x) = (-1)^2 (1-x^2) \frac{d^2}{dx^2} P_2(x) \\ P_2(x) = \frac{1}{2^2 \cdot 2!} \left[\frac{d^2}{dx^2} (x^2 - 1)^2 \right] \end{cases} \quad (7.12)$$

Changing the variable

$$x = \cos(t), \quad -1 \leq x \leq 1 \quad (7.13)$$

We have three periodic functions of time $L_1(x)$, $L_2(x)$, and $L_3(x)$ as shown in Fig. 7.1. When the parameters of system are $a=L_2+k$, $b=L_3$, $c=L_1+0.5$, $d=L_1+L_2$, $f=L_1$ and the initial states of system are $x_1(0)=2, x_2(0)=2.4, x_3(0)=5, x_4(0)=6$, the bifurcation diagram by changing constant parameter k is shown in Fig.

7.2. Its corresponding Lyapunov exponents are shown in Fig. 7.3. The phase portraits, time histories, and Poincaré maps of the systems are showed in Fig. 7.4 and Fig. 7.5. When $k=0.35$, period 1 phenomena are shown in Fig. 7.4. When $k=0$, the chaotic behaviors are given in Fig.7.5.

7.3 Numerical Results

Since the partner A is described by Eq. (7.9). The partner B is described as

$$\begin{cases} \frac{dy_1}{dt} = y_2 \\ \frac{dy_2}{dt} = -y_1 - y_1^3 - a_1 y_2 + d_1 y_3 \\ \frac{dy_3}{dt} = y_4 \\ \frac{dy_4}{dt} = -b_1 y_3 + c_1 (1 - y_3^2) y_4 + f_1 y_1 \end{cases} \quad (7.14)$$

where a_1 , b_1 , c_1 , d_1 and f_1 are constant parameters. For this scheme, u_1 , u_2 , u_3 and u_4 are added to the partner B then becomes controlled partner B:

$$\begin{cases} \frac{dy_1}{dt} = y_2 + u_1 \\ \frac{dy_2}{dt} = -y_1 - y_1^3 - a_1 y_2 + d_1 y_3 + u_2 \\ \frac{dy_3}{dt} = y_4 + u_3 \\ \frac{dy_4}{dt} = -b_1 y_3 + c_1 (1 - y_3^2) y_4 + f_1 y_1 + u_4 \end{cases} \quad (7.15)$$

In the HPSS, the error function is

$$e = Gxy - y + 100 \quad (7.16)$$

The addition of the constant 100 makes the error dynamics always happens in the first quadrant. Our goal is $y = Gxy + 100$, i.e.

$$\lim_{t \rightarrow \infty} e = \lim_{t \rightarrow \infty} (Gxy - y + 100) = 0 \quad (7.17)$$

The error dynamics Eq. (7.8) becomes:

$$\begin{cases} \dot{e}_1 = h_1(x_2 y_1 + x_1 y_2) - y_2 + y_1^2 - y_1^2 - u_1 \\ \dot{e}_2 = h_2 \left\{ y_2 \left[-x_1 - x_1^3 - a x_2 + d x_3 \right] + x_2 \left[-y_1 - y_1^3 - a_1 y_2 + d_1 y_3 \right] \right\} \\ \quad + y_1 + y_1^3 + a_1 y_2 - d_1 y_3 + y_1^2 - y_1^2 - u_2 \\ \dot{e}_3 = h_3(x_4 y_3 + x_3 y_4) - y_4 + y_4^2 - y_4^2 - u_3 \\ \dot{e}_4 = h_4 \left\{ y_4 \left[-b x_3 + c(1 - x_3^2) x_4 + f x_1 \right] + x_4 \left[-b_1 y_3 + c_1(1 - y_3^2) y_4 + f_1 y_1 \right] \right\} \\ \quad + b_1 y_3 - c_1(1 - y_3^2) y_4 - f_1 y_1 + y_4^2 - y_4^2 - u_4 \end{cases} \quad (7.18)$$

Let initial states be $(x_1, x_2, x_3, x_4) = (y_1, y_2, y_3, y_4) = (2, 2.4, 5, 6)$, system parameters $a = L_2, b = L_3, c = L_1 + 0.5, d = L_1 + L_2, f = L_1, a_l = 0.01, b_l = 1, c_l = 5, d_l = 0.67, f_l = 0.05$, and the scaling matrix is $G = \text{diag}(2, -1, 2, -1)$ we find the error dynamic always exists in first quadrant as shown in Fig. 7.6. By GYC partial region asymptotical stability theory, one can choose a Lyapunov function in the form of a positive definite function in first quadrant:

$$V = e_1 + e_2 + e_3 + e_4 \quad (7.19)$$

Its time derivative is

$$\begin{aligned} \dot{V} &= \dot{e}_1 + \dot{e}_2 + \dot{e}_3 + \dot{e}_4 \\ &= h_1(x_2 y_1 + x_1 y_2) - y_2 + y_1^2 - y_1^2 - u_1 \\ &\quad + h_2 \left\{ y_2 \left[-x_1 - x_1^3 - a x_2 + d x_3 \right] + x_2 \left[-y_1 - y_1^3 - a_1 y_2 + d_1 y_3 \right] \right\} \\ &\quad + y_1 + y_1^3 + a_1 y_2 - d_1 y_3 + y_1^2 - y_1^2 - u_2 + h_3(x_4 y_3 + x_3 y_4) - y_4 + y_4^2 - y_4^2 - u_3 \\ &\quad + h_4 \left\{ y_4 \left[-b x_3 + c(1 - x_3^2) x_4 + f x_1 \right] + x_4 \left[-b_1 y_3 + c_1(1 - y_3^2) y_4 + f_1 y_1 \right] \right\} \\ &\quad + b_1 y_3 - c_1(1 - y_3^2) y_4 - f_1 y_1 + y_4^2 - y_4^2 - u_4 \end{aligned} \quad (7.20)$$

Choose

$$\begin{cases} u_1 = h_1(x_2y_1 + x_1y_2) - y_2 + y_1^2 + e_1 \\ u_2 = h_2\{y_2[-x_1 - x_1^3 - ax_2 + dx_3] + x_2[-y_1 - y_1^3 - a_1y_2 + d_1y_3]\} \\ \quad + y_1 + y_1^3 + a_1y_2 - d_1y_3 - y_1^2 + e_2 \\ u_3 = h_3(x_4y_3 + x_3y_4) - y_4 + y_4^2 + e_3 \\ u_4 = h_4\{y_4[-bx_3 + c(1 - x_3^2)x_4 + fx_1] + x_4[-b_1y_3 + c_1(1 - y_3^2)y_4 + f_1y_1]\} \\ \quad + b_1y_3 - c_1(1 - y_3^2)y_4 - f_1y_1 - y_4^2 + e_4 \end{cases} \quad (7.21)$$

We obtain

$$\dot{V} = -e_1 - e_2 - e_3 - e_4 < 0 \quad (7.22)$$

which is negative definite function in the first quadrant. The numerical result is shown in Fig. 7.7.



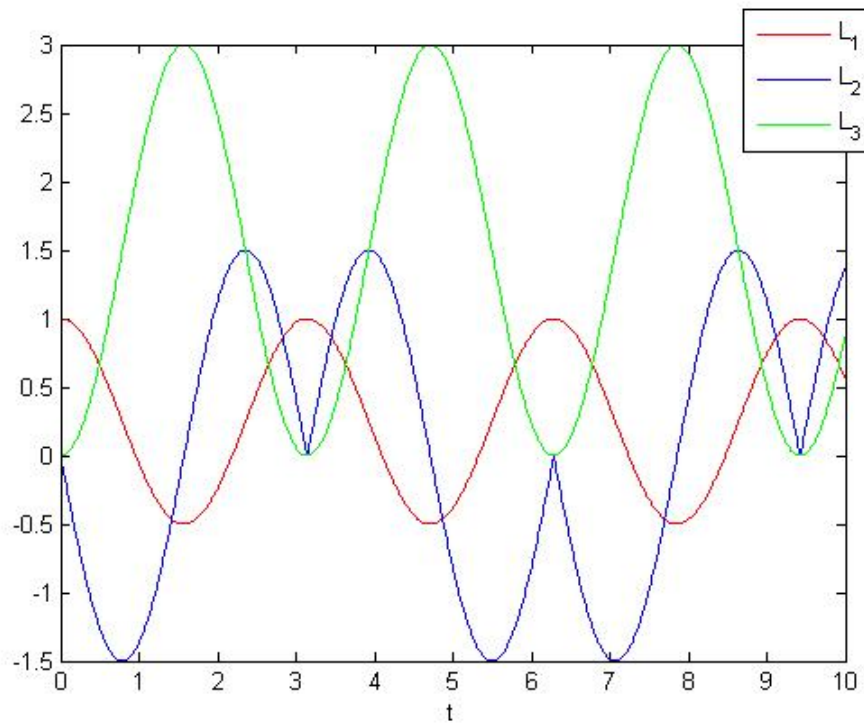


Fig. 7.1 Time histories of L_1 , L_2 , and L_3 .



bifurcation

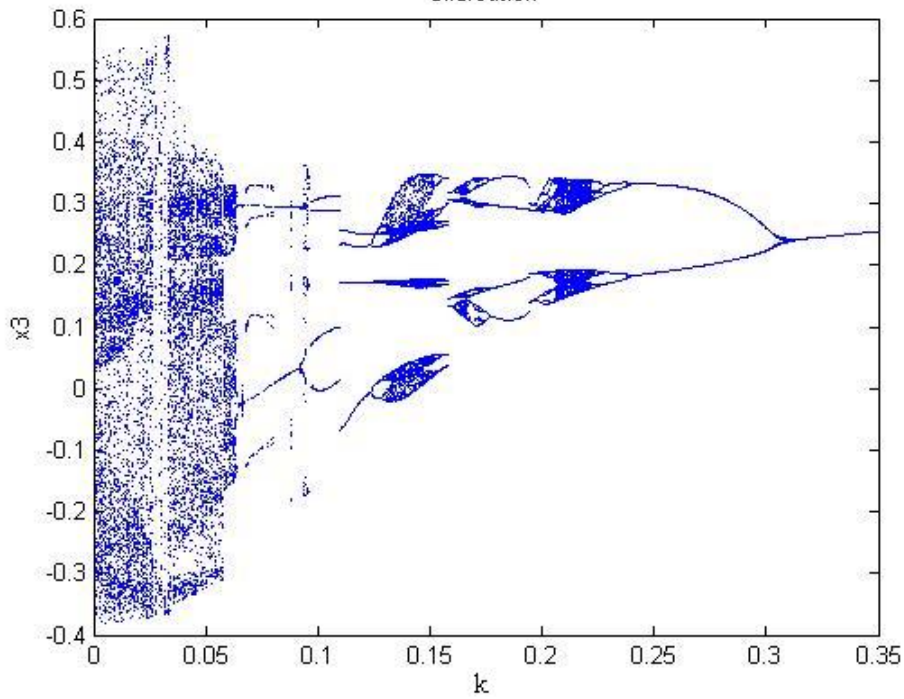


Fig. 7.2 The bifurcation diagram for new Duffing-Van der Pol system with Legendre function parameters.

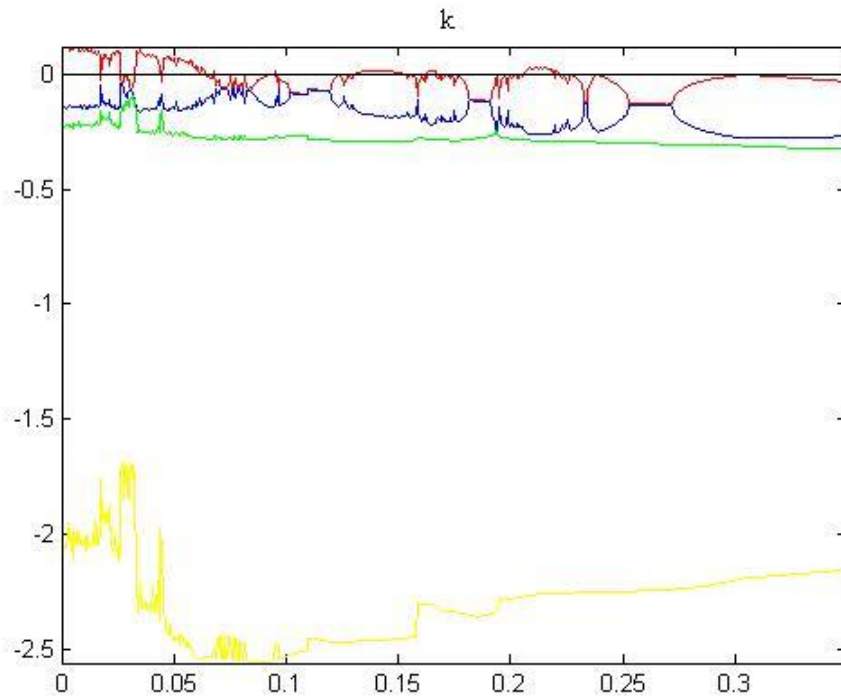


Fig. 7.3 The Lyapunov exponents for new Duffing-Van der Pol system with Legendre function parameters.

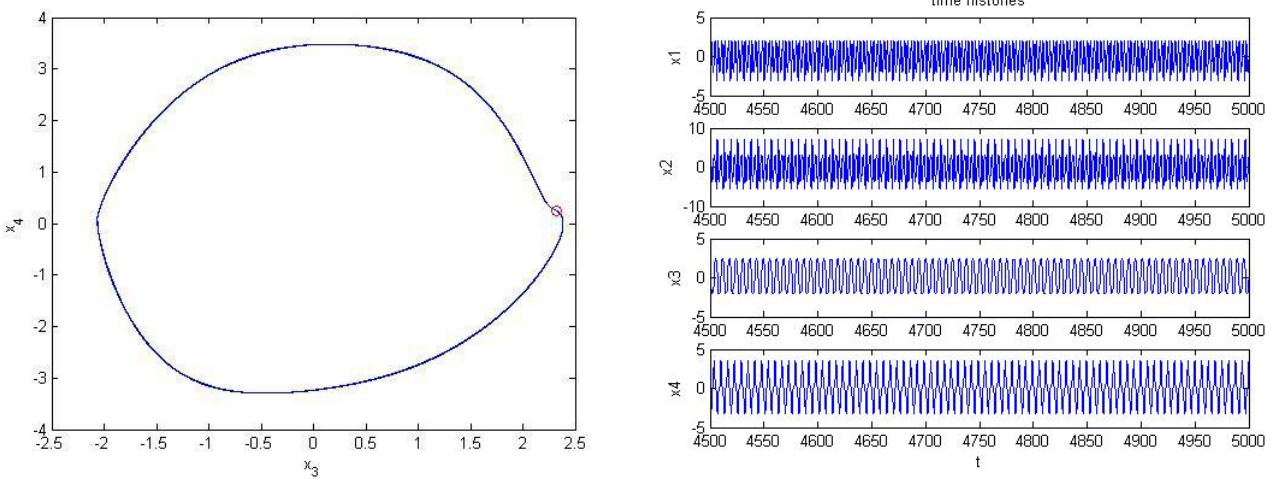


Fig. 7.4 Phase portrait, Poincaré maps, and time histories for new Duffing-Van der Pol system with Legendre function parameters when $k=0.35$ (period 1).

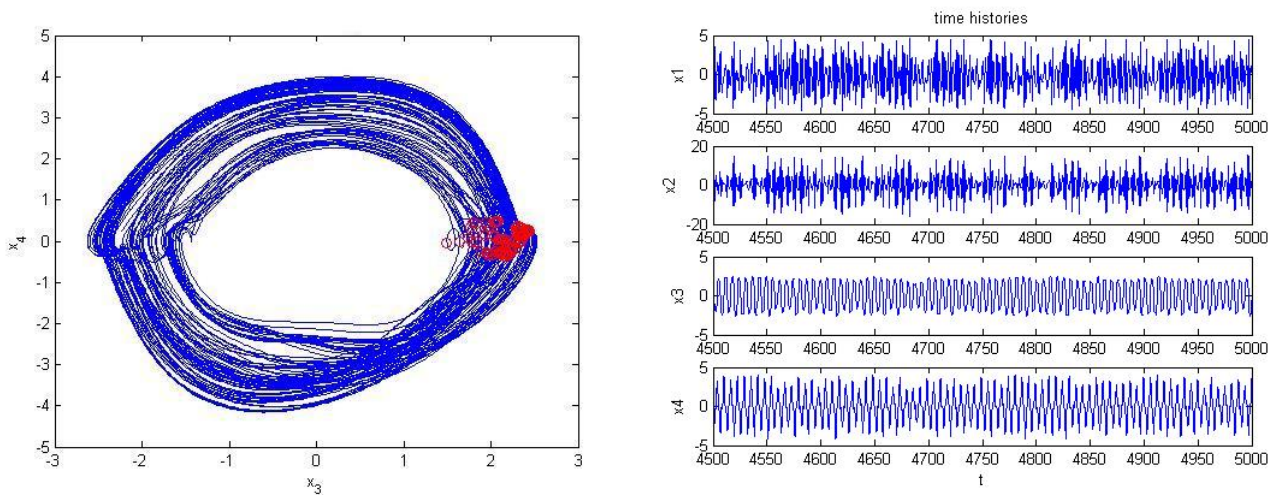


Fig. 7.5 Phase portrait, Poincaré maps, and time histories for new Duffing-Vander Pol system with Legendre function parameters when $k=0$ (chaos).

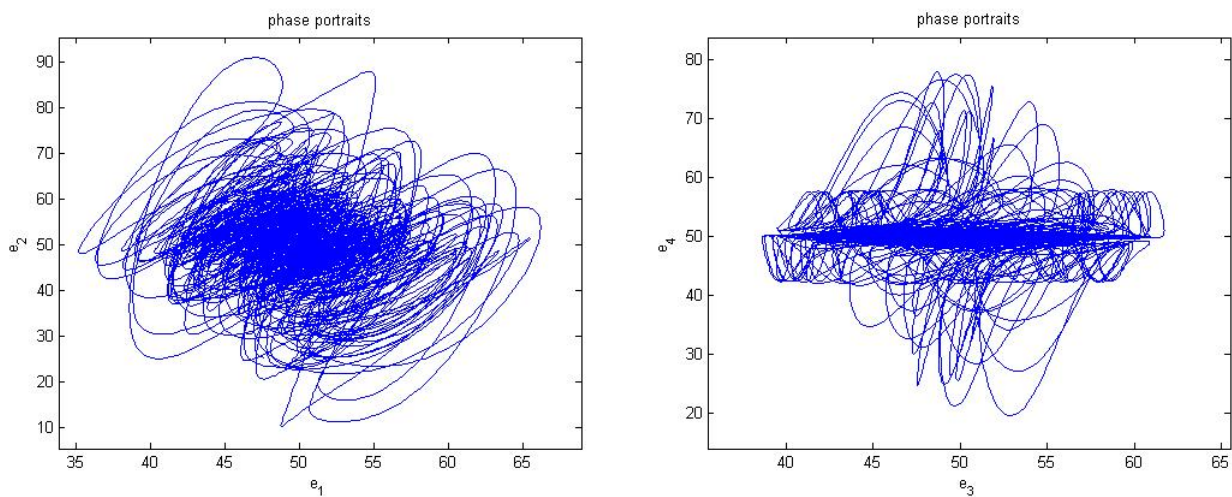


Fig. 7.6 Phase portraits of error dynamics.

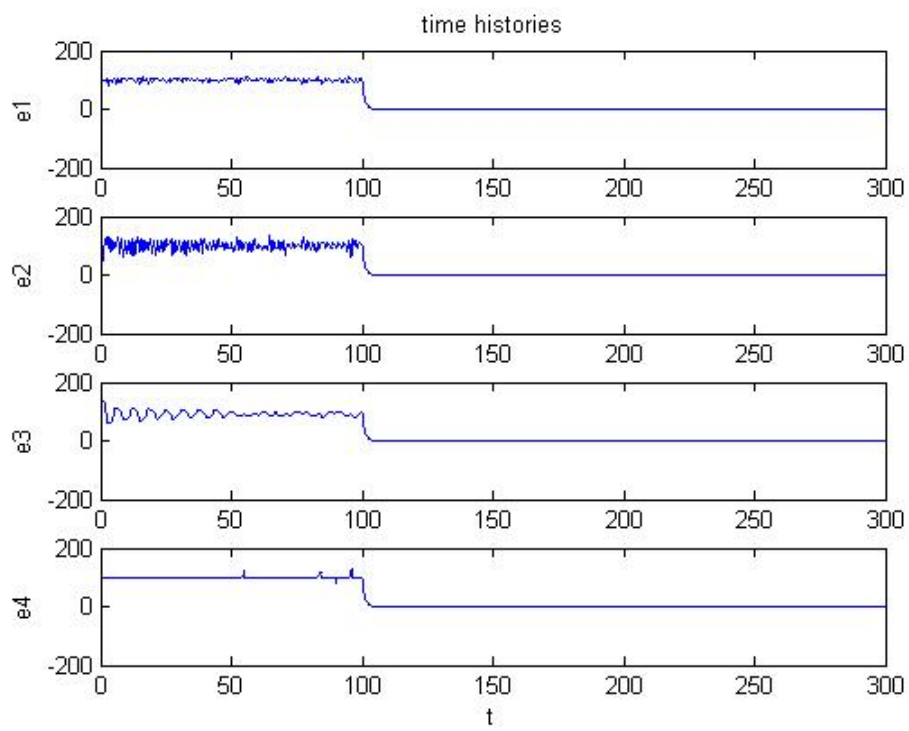


Fig. 7.7 Time histories of errors.



Chapter 8

Conclusions

In this thesis, the chaotic behavior in new Duffing-Van der Pol system is studied by phase portraits, time history, Poincaré maps, Lyapunov exponent, bifurcation diagrams, and parametric diagram.

Three kind of chaotic synchronization are presented. A new kind of generalized synchronization system in Chapter 3, *pragmatical hybrid projective chaotic generalized synchronization* (PHPCGS) of two chaotic systems with uncertain parameters, is obtained with the state variables of another hyperchaotic Mathieu-Duffing system as a constituent of the functional relation between master and slave. Based on the pragmatical asymptotical stability theorem, adaptive control law is used.

A new type for chaotic synchronization in Chapter 4, *pragmatical chaotic symplectic synchronization* (PCSS), is obtained with the state variables of another different order system as a constituent of the functional relation between “master” and “slave”. Traditional generalized synchronizations are special cases of the symplectic synchronization. The pragmatical asymptotical stability theorem is used. New dynamic surface control is also used for making the controllers more simple.

A new chaos generalized synchronization method, using GYC partial region stability theory, is proposed in Chapter 5. Moreover, we also study the chaos control and anti-control by using the GYC partial region stability theory in Chapter 6. By using this theory, the controllers are of lower degree than that of controllers by using traditional Lyapunov asymptotical stability theorem. The simple linear homogeneous Lyapunov function of error states makes that the controllers are simpler and introduce

less simulation error. In addition, by replacing the parameters of the system with Legendre function, the chaos synchronization can be successfully obtained in Section 7.



Appendix I GYC Pragmatical Asymptotical Theorem [29]

The stability for many problems in real dynamical systems is actual asymptotical stability, although may not be mathematical asymptotical stability. The mathematical asymptotical stability demands that trajectories from all initial states in the neighborhood of zero solution must approach the origin as $t \rightarrow \infty$. If there are only a small part or even one of initial states from which the trajectories or trajectory do not approach the origin as $t \rightarrow \infty$, the zero solution is not mathematically asymptotically stable. However, when the probability of occurrence of an event is zero, it means the event does not occur actually. If the probability of occurrence of the event that the trajectories from the initial states are that they do not approach zero when $t \rightarrow \infty$, is zero, the stability of zero solution is actual asymptotical stability though it is not mathematical asymptotical stability. In order to analyze the asymptotical stability of the equilibrium point of such systems, the pragmatical asymptotical stability theorem is used.

Let X and Y be two manifolds of dimensions m and n ($m < n$), respectively, and φ be a differentiable map from X to Y ; then $\varphi(X)$ is a subset of Lebesgue measure 0 of Y [47]. For an autonomous system

$$\frac{dx}{dt} = f(x_1, x_2, \dots, x_n) \quad (\text{A.1})$$

where $x = [x_1, x_2, \dots, x_n]^T$, the function $f = [f_1, f_2, \dots, f_n]^T$ is defined on $D \subset R^n$. Let $x = 0$ be an equilibrium point for the system (A.1). Then

$$f(0) = 0 \quad (\text{A.2})$$

For nonautonomous system,

$$\frac{dx}{dt} = f(x_1, x_2, \dots, x_{n+1}) \quad (\text{A.3})$$

where $t = x_{n+1} \in R_+$. The equilibrium point is

$$f(0, x_{n+1}) = 0 \quad (\text{A.4})$$

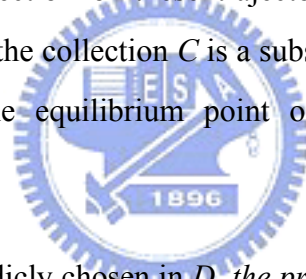
Definition: The equilibrium point for the dynamic system is pragmatically asymptotically stable provided that with initial points on C which is a subset of

Lebesgue measure 0 of D , the behaviors of the corresponding trajectories cannot be determined, while with initial points on $D - C$, the corresponding trajectories behave as that agree with traditional asymptotical stability[29,30].

Theorem: Let $V = [x_1, x_2, \dots, x_n]^T : D \rightarrow R_+$ positive definite, analytic on D , where x_1, \dots, x_n are all space coordinates such that the derivative of V through differential equation, \dot{V} , is negative semi-definite.

Let X be the m -manifold consisting of point set for which $\forall x \neq 0, \dot{V}(x) = 0$ and D is an n -manifold. If $m+1 < n$, then the equilibrium point of the system is pragmatically asymptotically stable.

Proof: Since every point of X can be passed by a trajectory of Eq. (A.1), which is one dimensional, the collection of these trajectories, C , is a $(m+1)$ -manifold [29,30]. If $(m+1) < n$, then the collection C is a subset of Lebesgue measure 0 of D . By the above definition, the equilibrium point of the system is pragmatically asymptotically stable. \square



If an initial point is ergodicly chosen in D , the probability of that the initial point falls on the collection C is zero. Here, equal probability is assumed for every point chosen as an initial point in the neighborhood of the equilibrium point. Hence, the event that the initial point is chosen from collection C does not occur actually. Therefore, under the equal probability assumption, pragmatical asymptotical stability becomes actual asymptotical stability. When the initial point falls on $D - C$, $\dot{V}(x) < 0$, the corresponding trajectories behave as if they agree with traditional asymptotical stability because by the existence and uniqueness of the solution of initial-value problem, these trajectories never meet C .

For Eq. (9) Lyapunov function V is a positive definite function of n variables, i.e. p error state variables and $n - p = m$ differences between unknown and estimated parameters, while $\dot{V} = e^T C e$ is a negative semi-definite function of n variables. Since the number of error state variables is always more than one, $p > 1$, $(m+1) < n$ is always satisfied. By pragmatical asymptotical stability theorem we have

$$\lim_{t \rightarrow \infty} e = 0 \quad (\text{A.5})$$

and the estimated parameters approach the uncertain parameters. The pragmatical generalized synchronizations is obtained. Therefore, *the equilibrium point of the system is pragmatically asymptotically stable. Under the equal probability assumption, it is actually asymptotically stable for both error state variables and parameter variables.*



Appendix II GYC Partial Region Stability Theory [42]

Consider the differential equations of disturbed motion of a nonautonomous system in the normal form

$$\frac{dx_s}{dt} = X_s(t, x_1, \dots, x_n), \quad (s = 1, \dots, n) \quad (\text{A2.1})$$

where the function X_s is defined on the intersection of the partial region Ω (shown in Fig. A2.1) and

$$\sum_s x_s^2 \leq H \quad (\text{A2.2})$$

and $t > t_0$, where t_0 and H are certain positive constants. X_s which vanishes when the variables x_s are all zero, is a real valued function of t, x_1, \dots, x_n . It is assumed that X_s is smooth enough to ensure the existence, uniqueness of the solution of the initial value problem. When X_s does not contain t explicitly, the system is autonomous.

Obviously, $x_s = 0$ ($s = 1, \dots, n$) is a solution of Eq.(A2.1). We are interested to the asymptotical stability of this zero solution on partial region Ω (including the boundary) of the neighborhood of the origin which in general may consist of several subregions (Fig. A2.1).

Definition 1:

For any given number $\varepsilon > 0$, if there exists a $\delta > 0$, such that on the closed given partial region Ω when

$$\sum_s x_{s0}^2 \leq \delta, \quad (s = 1, \dots, n) \quad (\text{A2.3})$$

for all $t \geq t_0$, the inequality

$$\sum_s x_s^2 < \varepsilon, \quad (s=1, \dots, n) \quad (\text{A2.4})$$

is satisfied for the solutions of Eq. (A2.1) on Ω , then the disturbed motion $x_s = 0 \quad (s=1, \dots, n)$ is stable on the partial region Ω .

Definition 2:

If the undisturbed motion is stable on the partial region Ω , and there exists a $\delta' > 0$, so that on the given partial region Ω when

$$\sum_s x_{s0}^2 \leq \delta', \quad (s=1, \dots, n) \quad (\text{A2.5})$$

The equality

$$\lim_{t \rightarrow \infty} \left(\sum_s x_s^2 \right) = 0 \quad (\text{A2.6})$$

is satisfied for the solutions of Eq.(A2.1) on Ω , then the undisturbed motion $x_s = 0 \quad (s=1, \dots, n)$ is asymptotically stable on the partial region Ω .

The intersection of Ω and region defined by Eq.(A2.5) is called the region of attraction.

Definition of Functions $V(t, x_1, \dots, x_n)$:

Let us consider the functions $V(t, x_1, \dots, x_n)$ given on the intersection Ω_1 of the partial region Ω and the region

$$\sum_s x_s^2 \leq h, \quad (s=1, \dots, n) \quad (\text{A2.7})$$

for $t \geq t_0 > 0$, where t_0 and h are positive constants. We suppose that the functions are single-valued and have continuous partial derivatives and become zero when $x_1 = \dots = x_n = 0$.

Definition 3:

If there exists $t_0 > 0$ and a sufficiently small $h > 0$, so that on partial region

Ω_1 and $t \geq t_0$, $V \geq 0$ (or ≤ 0), then V is a positive (or negative) semidefinite, in general semidefinite, function on the Ω_1 and $t \geq t_0$.

Definition 4:

If there exists a positive (negative) definite function $W(x_1 \dots x_n)$ on Ω_1 , so that on the partial region Ω_1 and $t \geq t_0$

$$V - W \geq 0 \text{ (or } -V - W \geq 0), \quad (\text{A2.8})$$

then $V(t, x_1, \dots, x_n)$ is a positive definite function on the partial region Ω_1 and $t \geq t_0$.

Definition 5:

If $V(t, x_1, \dots, x_n)$ is neither definite nor semidefinite on Ω_1 and $t \geq t_0$, then $V(t, x_1, \dots, x_n)$ is an indefinite function on partial region Ω_1 and $t \geq t_0$. That is, for any small $h > 0$ and any large $t_0 > 0$, $V(t, x_1, \dots, x_n)$ can take either positive or negative value on the partial region Ω_1 and $t \geq t_0$.

Definition 6: Bounded function V

If there exist $t_0 > 0$, $h > 0$, so that on the partial region Ω_1 , we have

$$|V(t, x_1, \dots, x_n)| < L$$

where L is a positive constant, then V is said to be bounded on Ω_1 .

Definition 7: Function with infinitesimal upper bound

If V is bounded, and for any $\lambda > 0$, there exists $\mu > 0$, so that on Ω_1 when

$$\sum_s x_s^2 \leq \mu, \text{ and } t \geq t_0, \text{ we have}$$

$$|V(t, x_1, \dots, x_n)| \leq \lambda$$

then V admits an infinitesimal upper bound on Ω_1 .

Theorem 1

If there can be found for the differential equations of the disturbed motion a definite function $V(t, x_1, \dots, x_n)$ on the partial region, and for which the derivative with respect to time based on these equations as given by the following:

$$\frac{dV}{dt} = \frac{\partial V}{\partial t} + \sum_{s=1}^n \frac{\partial V}{\partial x_s} X_s \quad (\text{A2.9})$$

is a semidefinite function on the partial region whose sense is opposite to that of V , or if it becomes zero identically, then the undisturbed motion is stable on the partial region.

Proof:

Let us assume for the sake of definiteness that V is a positive definite function. Consequently, there exists a sufficiently large number t_0 and a sufficiently small number $h < H$, such that on the intersection Ω_1 of partial region Ω and

$$\sum_s x_s^2 \leq h, \quad (s = 1, \dots, n)$$

and $t \geq t_0$, the following inequality is satisfied

$$V(t, x_1, \dots, x_n) \geq W(x_1, \dots, x_n),$$

where W is a certain positive definite function which does not depend on t . Besides that, Eq. (A2.9) may assume only negative or zero value in this region.

Let ε be an arbitrarily small positive number. We shall suppose that in any case $\varepsilon < h$. Let us consider the aggregation of all possible values of the quantities x_1, \dots, x_n , which are on the intersection ω_2 of Ω_1 and

$$\sum_s x_s^2 = \varepsilon, \quad (\text{A2.10})$$

and let us designate by $l > 0$ the precise lower limit of the function W under this condition. by virtue of Eq. (A2.5), we shall have

$$V(t, x_1, \dots, x_n) \geq l \quad \text{for } (x_1, \dots, x_n) \text{ on } \omega_2. \quad (\text{A2.11})$$

We shall now consider the quantities x_s as functions of time which satisfy the differential equations of disturbed motion. We shall assume that the initial values x_{s_0} of these functions for $t = t_0$ lie on the intersection Ω_2 of Ω_1 and the region

$$\sum_s x_s^2 \leq \delta, \quad (\text{A2.12})$$

where δ is so small that

$$V(t_0, x_{10}, \dots, x_{n0}) < l \quad (\text{A2.13})$$

By virtue of the fact that $V(t_0, 0, \dots, 0) = 0$, such a selection of the number δ is obviously possible. We shall suppose that in any case the number δ is smaller than ε . Then the inequality

$$\sum_s x_s^2 < \varepsilon, \quad (\text{A2.14})$$

being satisfied at the initial instant will be satisfied, in the very least, for a sufficiently small $t - t_0$, since the functions $x_s(t)$ vary continuously with time. We shall show that these inequalities will be satisfied for all values $t > t_0$. Indeed, if these inequalities were not satisfied at some time, there would have to exist such an instant $t = T$ for which this inequality would become an equality. In other words, we would have

$$\sum_s x_s^2(T) = \varepsilon,$$

and consequently, on the basis of Eq. (A2.11)

$$V(T, x_1(T), \dots, x_n(T)) \geq l \quad (\text{A2.15})$$

On the other hand, since $\varepsilon < h$, the inequality (Eq.(A2.4)) is satisfied in the entire interval of time $[t_0, T]$, and consequently, in this entire time interval $\frac{dV}{dt} \leq 0$.

This yields

$$V(T, x_1(T), \dots, x_n(T)) \leq V(t_0, x_{10}, \dots, x_{n0}),$$

which contradicts Eq. (A2.14) on the basis of Eq. (A2.13). Thus, the inequality (Eq. (A2.4)) must be satisfied for all values of $t > t_0$, hence follows that the motion is stable.

Finally, we must point out that from the view-point of mathematics, the stability on partial region in general does not be related logically to the stability on whole region. If an undisturbed solution is stable on a partial region, it may be either stable or unstable on the whole region and vice versa. From the viewpoint of dynamics, we are not interesting to the solution starting from Ω_2 and going out of Ω .

Theorem 2

If in satisfying the conditions of theorem 1, the derivative $\frac{dV}{dt}$ is a definite function on the partial region with opposite sign to that of V and the function V itself permits an infinitesimal upper limit, then the undisturbed motion is asymptotically stable on the partial region.

Proof:

Let us suppose that V is a positive definite function on the partial region and that consequently, $\frac{dV}{dt}$ is negative definite. Thus on the intersection Ω_1 of Ω and the region defined by Eq. (A2.7) and $t \geq t_0$ there will be satisfied not only the inequality (Eq. (A2.8)), but the following inequality as will:

$$\frac{dV}{dt} \leq -W_1(x_1, \dots, x_n), \quad (\text{A2.16})$$

where W_1 is a positive definite function on the partial region independent of t .

Let us consider the quantities x_s as functions of time which satisfy the differential equations of disturbed motion assuming that the initial values $x_{s0} = x_s(t_0)$ of these quantities satisfy the inequalities (Eq. (A2.12)). Since the undisturbed motion is stable in any case, the magnitude δ may be selected so small that for all values of $t \geq t_0$ the quantities x_s remain within Ω_1 . Then, on the basis of Eq. (A2.16) the derivative of function $V(t, x_1(t), \dots, x_n(t))$ will be negative at all times and, consequently, this function will approach a certain limit, as t increases without limit, remaining larger than this limit at all times. We shall show that this limit is equal to some positive quantity different from zero. Then for all values of $t \geq t_0$ the following inequality will be satisfied:

$$V(t, x_1(t), \dots, x_n(t)) > \alpha \quad (\text{A2.17})$$

where $\alpha > 0$.

Since V permits an infinitesimal upper limit, it follows from this inequality that

$$\sum_s x_s^2(t) \geq \lambda, \quad (s = 1, \dots, n), \quad (\text{A2.18})$$

where λ is a certain sufficiently small positive number. Indeed, if such a number λ did not exist, that is, if the quantity $\sum_s x_s(t)$ were smaller than any preassigned number no matter how small, then the magnitude $V(t, x_1(t), \dots, x_n(t))$, as follows from the definition of an infinitesimal upper limit, would also be arbitrarily small, which contradicts (A2.17).

If for all values of $t \geq t_0$ the inequality (Eq. (A2.18)) is satisfied, then Eq.

(A2.16) shows that the following inequality will be satisfied at all times:

$$\frac{dV}{dt} \leq -l_1,$$

where l_1 is positive number different from zero which constitutes the precise lower limit of the function $W_1(t, x_1(t), \dots, x_n(t))$ under condition (Eq. (A2.18)).

Consequently, for all values of $t \geq t_0$ we shall have:

$$V(t, x_1(t), \dots, x_n(t)) = V(t_0, x_{10}, \dots, x_{n0}) + \int_{t_0}^t \frac{dV}{dt} dt \leq V(t_0, x_{10}, \dots, x_{n0}) - l_1(t - t_0),$$

which is, obviously, in contradiction with Eq.(A2.17). The contradiction thus obtained shows that the function $V(t, x_1(t), \dots, x_n(t))$ approached zero as t increase without limit. Consequently, the same will be true for the function $W(x_1(t), \dots, x_n(t))$ as well,

from which it follows directly that

$$\lim_{t \rightarrow \infty} x_s(t) = 0, \quad (s = 1, \dots, n),$$

which proves the theorem.

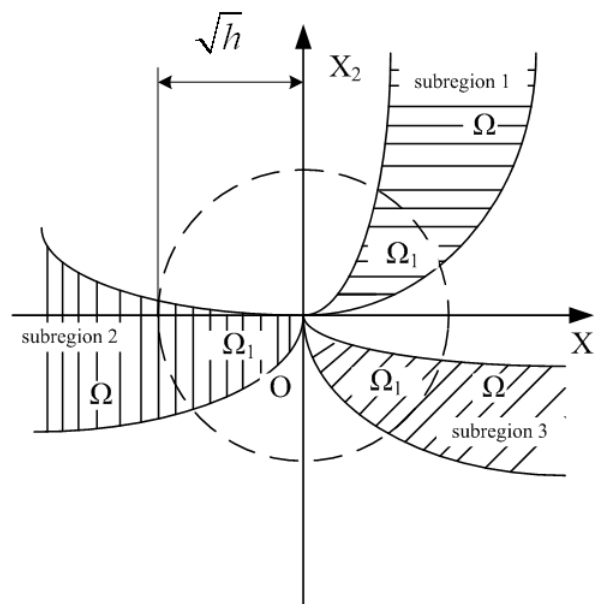
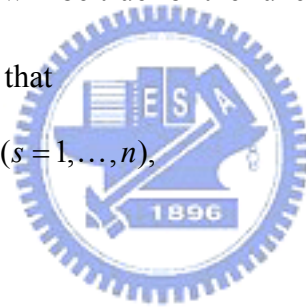


Fig. A2.1 Partial regions Ω and Ω_1 .

References

- [1]T.L. Carroll and L.M. Pecora, "Synchronizing chaotic circuits", IEEE Trans Circ Syst I 38 (1991) 453.
- [2]E. Ott, C. Grebogi and J.A. Yorke, "Controlling chaos", Phys Rev Lett 64 (1990) 1196.
- [3]D.P. Stoten and M. Di Bernardo, "Application of the minimal control synthesis algorithm to the control synchronization of chaotic systems", Int J Control 65 (1996) 925.
- [4]L.M. Pecora, T.L. Carroll, "Synchronization in chaotic systems", Phys. Rev. Lett. 64 (1990) 821.
- [5]T. Kapitaniak, "Continuous control and synchronization in chaotic systems", Chaos Solitons Fractals 6 (3) (1995) 237.
- [6]L. Kocarev, K.S. Halle, K. Eckert, L.O. Chua, U. Parlitz, "Experimental demonstration of secure communications via chaotic synchronization", Int. J. Bifur. Chaos 3 (1992) 709.
- [7]K.M. Cuomo, A.V. Oppenheim, "Circuit implementation of synchronized chaos with applications to communications", Phys. Rev. Lett. 71 (1993) 65.
- [8]L. Kocarev, U. Parlitz, "General approach for chaotic synchronization with applications to communication", Phys. Rev. Lett. 74 (1995) 5028.
- [9]S.K. Han, C. Kurrer, Y. Kuramoto, "Dephasing and bursting in coupled neural oscillators", Phys. Rev. Lett. 75 (1995) 3190.
- [10]B. Blasius, A. Huppert, L. Stone, "Complex dynamics and phase synchronization in spatially extended ecological systems", Nature 399 (1999) 354.
- [11]M. Lakshmanan, K. Murali, "Chaos in nonlinear oscillators: controlling and synchronization", Singapore: World Scientific (1996).
- [12]Y.G. Yu, S.C. Zhang, "The synchronization of linearly bidirectional coupled chaotic systems", Chaos Solitons Fractals 22 (2004) 189.
- [13]H.K. Chen, "Global chaos synchronization of new chaotic systems via nonlinear control", Chaos Solitons Fractals 23 (2005) 1245.
- [14]M.G. Rosenblum, A.S. Pikovsky, J. Kurths, "Phase synchronization of chaotic oscillators", Phys. Rev. Lett. 76 (1996) 1804.
- [15]E.R. Rosa, E. Ott, M.H. Hess, "Transition to phase synchronization of chaos",

- Phys. Rev. Lett. 80 (1998) 1642.
- [16]M.G. Rosenblum, A.S. Pikovsky, J. Kurths, “From phase to lag synchronization in coupled chaotic oscillators”, Phys. Rev. Lett. 78 (1997) 4193.
- [17]S. Sivaprakasam, E.M. Shahverdiev, P.S. spencer, K.A. Shore, “Experimental demonstration of anticipating synchronization in chaotic semiconductor lasers with optical feedback”, Phys. Rev. Lett. 87 (2001) 154101.
- [18]R. Mainieri, J. Rehacek, “Projective synchronization in three-dimensional chaotic systems”, Phys. Rev. Lett. 82 (1999) 3042.
- [19]G.L. Wen, D. Xu, “Observer-based control for full-state projective synchronization of a general class of chaotic maps in any dimension”, Phys. Lett. A 333 (2004) 420.
- [20]D. Xu, “Control of projective synchronization in chaotic systems”, Phys. Rev. E 63 (2001) 027201.
- [21]D. Xu, Z. Li, “Manipulating the scaling factor of projective synchronization in three-dimensional chaotic systems”, Chaos 11 (2001) 439.
- [22]D. Xu, C.Y. Chee, “Controlling the ultimate state of projective synchronization in chaotic systems of arbitrary dimension”, Phys. Rev. E 66 (2002) 046218.
- [23]L. Kocarev, U. Parlitz, “Generalized synchronization, predictability, and equivalence of unidirectionally coupled dynamical systems”, Phys. Rev. Lett. 76 (1996) 1816.
- [24]J.H. Park, “Adaptive synchronization of hyperchaotic chen system with uncertain parameters”, Chaos Solitons Fractals 26 (2005) 959.
- [25]J.H. Park, “Adaptive synchronization of rossler system with uncertain parameters”, Chaos Solitons Fractals 25 (2005) 333.
- [26]E.M. Elabbasy, H.N. Agiza, M.M. El-Desoky, “Adaptive synchronization of a hyperchaotic system with uncertain parameter”, Chaos Solitons Fractals 30 (2006) 1133.
- [27]X. Wu, Z.-H Guan, Z. Wu, T. Li, “Chaos synchronization between Chen system and Genesisio system”, Phys. Lett. A 364 (2007) 315.
- [28]M. Hu, Z. Xu, R. Zhang, A. Hu, “Adaptive full state hybrid projective synchronization of chaotic systems with the same and different order”, Phys. Lett. A 365 (2007) 315.
- [29]Z.-M. Ge, J.-K Yu, Y.-J. Chen, “Pragmatical asymptotical stability theorem with

- application to satellite system”, Japanese Journal of Applied Physics, 38 (1999) 6178.
- [30]Z.-M. Ge, J.-K. Yu, “Pragmatical asymptotical stability theorem on partial region and for partial variable with applications to gyroscopic systems”, Chin. J. Mech. 16 (4) (2000) 179.
- [31]Z.-M. Ge, C.-H. Yang, “Pragmatical generalized synchronization of chaotic systems with uncertain parameters by adaptive control”, Physica D, 231 (2007) 87.
- [32]Z.-M. Ge, C.-H. Yang, “Symplectic synchronization of different chaotic systems”, accepted by Chaos, Solitons and Fractals, (2007), doi:10.1016/j.chaos.2007.10.055
- [33]E.W. Bai, K.E. Lonngren, “Sequential synchronization of two Lorenz systems using active control”, Chaos, Solitons & Fractals, 11 (2000) 1041.
- [34]X.S. Yang, G. Chen, “Some observer-based criteria for discrete-time generalized chaos synchronization”, Chaos, Solitons & Fractals 13 (2002) 1303.
- [35]G. Chen, X. Dong, “On feedback control of chaotic continuous time systems”, IEEE Trans Circ Syst, 40 (1993) 591.
- [36]M.T. Yassen, “Chaos control of Chen chaotic dynamical system” Chaos, Solitons & Fractals, 15 (2003) 271.
- [37]M.T. Yassen, “Controlling chaos and synchronization for new chaotic system using linear feedback”, Chaos, Solitons & Fractals, 26 (2005) 913.
- [38]H.N. Agiza. Controlling chaos for the dynamical system of coupled dynamos. Chaos, Solitons & Fractals, 12 (2002) 341.
- [39]E.N. Sanchez, J.P. Perez, M. Martinez, G. Chen, “Chaos stabilization: an inverse optimal control approach”, Latin Am Appl Res: Int J, 32 (2002) 111.
- [40]M.T. Yassen, “Adaptive control and synchronization of a modified Chua’ s circuit system”, Appl Math Comput, 135 (2001) 113.
- [41]T.-L. Liao, S.-H. Lin, “Adaptive control and synchronization of Lorenz systems”, J Franklin Inst, 336 (1999) 925.
- [42]Z.-M. Ge, C.-W. Yao, H.-K. Chen, “Stability on Partial Region in Dynamics”, Journal of Chinese Society of Mechanical Engineer, 15 (1994) 140.
- [43]Z.-M. Ge, H.-K. Chen, “Three Asymptotical Stability Theorems on Partial Region with Applications”, Japanese Journal of Applied Physics, 37 (1998) 2762.

- [44]D. Swaroop, J. Hedrick, P. Yip, J. C. Gerdes, “Dynamic surface control for a class of nonlinear systems”, IEEE Trans. Automat. Control 45 (2000) 1893.
- [45]J. Lü, G. Chen, S. Zhang, “Dynamical analysis of a new chaotic attractor”, Int. J. Bifur. Chaos 12 (2002) 1001.
- [46]A.M. Chen, J.A. Lu, J.H. Lü, S.M. Yu, “Generating hyperchaotic Lü attractor via state feedback control”, Physica A, 364 (2006) 103.
- [47]Y. Matsushima, Differentiable manifolds, Marcel Dekker, City, 1972 pp.56-57.
- [48]S.-C. Chang, J.-M. Jin, Computation of special function.

